Arbeitsbericht NAB 20-08

TBO Bülach-1-1: Data Report

Dossier IV
Microfacies, Bio- and Chemo-stratigraphic Analysis

February 2021

National Cooperative
for the Disposal of
Radioactive Waste

Hardstrasse 73
P.O. Box 280
5430 Wettingen
Switzerland
Tel. +41 56 437 11 11

www.nagra.ch

nagra.

Arbeitsbericht NAB 20-08

TBO Bülach-1-1: Data Report

Dossier IV Microfacies, Bio- and Chemo-stratigraphic Analysis

February 2021

S. Wohlwend[1], H.R. Bläsi[2], S. Feist-Burkhardt[3,4], B. Hostettler[5], U. Menkveld-Gfeller[5], V. Dietze[6], G. Deplazes[7]

[1] Geological Institute, ETH Zurich
[2] Geo-Consulting, Wünnewil, Switzerland
[3] SFB Geological Consulting & Services, Ober-Ramstadt, Germany
[4] Département des Sciences de la Terre, Université de Genève
[5] Natural History Museum Bern
[6] Nördlingen, Germany
[7] Nagra

Keywords:
Bülach-1-1, Bülach-1-1B, BUL1-1, BUL1-1B, Nördlich Lägern, TBO, deep drilling campaign, microfacies, lithostratigraphy, biostratigraphy, ammonite stratigraphy, palynostratigraphy, chemostratigraphy, dinoflagellate cysts, stable carbon isotopes

National Cooperative for the Disposal of Radioactive Waste

Hardstrasse 73
P.O. Box 280
5430 Wettingen
Switzerland
Tel. +41 56 437 11 11

www.nagra.ch

Nagra Arbeitsberichte NAB ("Working Reports") present the results of work in progress that have not necessarily been subject to a comprehensive review. They are intended to provide rapid dissemination of current information.

This NAB aims at reporting drilling results at an early stage. Additional borehole-specific data will be published elsewhere.

In the event of inconsistencies between dossiers of this NAB, the dossier addressing the specific topic takes priority. In the event of discrepancies between Nagra reports, the chronologically later report is generally considered to be correct. Data sets and interpretations laid out in this NAB may be revised in subsequent reports. The reasoning leading to these revisions will be detailed there.

This Dossier was prepared by a project team consisting of:
S. Wohlwend (sampling, chemostratigraphy, conceptualisation and compilation)
H.R. Bläsi (microfacies)
S. Feist-Burkhardt (palynostratigraphy)
B. Hostettler, U. Menkveld-Gfeller, V. Dietze (ammonite stratigraphy)
G. Deplazes (project management and conceptualisation)

Editorial work: P. Blaser and M. Unger

The Dossier has greatly benefitted from technical discussions with, and reviews by, external and internal experts. Their input and work are very much appreciated!

"Copyright © 2021 by Nagra, Wettingen (Switzerland) / All rights reserved.
All parts of this work are protected by copyright. Any utilisation outwith the remit of the copyright law is unlawful and liable to prosecution. This applies in particular to translations, storage and processing in electronic systems and programs, microfilms, reproductions, etc."

Table of Contents

Table of Contents I

List of Tables II

List of Figures II

List of Appendices III

1 Introduction 1
1.1 Context 1
1.2 Location and specifications of the borehole 2
1.3 Documentation structure for the BUL1-1 borehole 5
1.4 Scope and objectives of this dossier 6

2 Methods 9
2.1 Microfacies 9
2.2 Ammonite preparation 11
2.3 Palynological sample preparation and quantitative analysis 11
2.4 Chemostratigraphy 12

3 Results 15
3.1 Microfacies 15
3.2 Ammonite stratigraphy 25
3.3 Palynostratigraphy 34
3.4 Chemostratigraphy 43

4 Correlation of BUL1-1 and BUL1-1B 57

5 Definition of specific lithostratigraphic boundaries 59

6 Conclusions 63

7 References 65

List of Tables

Tab. 1-1: General information about the BUL1-1 borehole 2
Tab. 1-2: List of dossiers included in NAB 20-08 5
Tab. 3-1: Microfacies analysis from BUL1-1 (536.16 – 1'034.81 m) and BUL1-1B (1'042.16 – 1'317.79 m); numbers in vol.-% 23
Tab. 3-2a: Ammonite and other macrofossil determination from BUL1-1 29
Tab. 3-2b: Ammonite determination from BUL1-1B 32
Tab. 3-3: List of analysed palynology samples from BUL1-1 42

List of Figures

Fig. 1-1: Tectonic overview map with the three siting regions under investigation 1
Fig. 1-2: Overview map of the investigation area in the Nördlich Lägern siting region with the location of the BUL1-1 borehole and the existing Weiach-1 borehole 3
Fig. 1-3: Lithostratigraphic profile and casing scheme for the BUL1-1 borehole 4
Fig. 1-4: Bülach-1-1 & Bülach-1-1B stratigraphy with core depth in metres 7
Fig. 1-5: Lithostratigraphy plot (1:5'000) from the Mesozoic succession with the individual sampling intervals for thin sections, macrofossils, palynological analysis and chemostratigraphy 8
Fig. 3-1a: Zones and subzones documented based on ammonites in BUL1-1 30
Fig. 3-1b: Zones and subzones documented based on ammonites in BUL1-1B 33
Fig. 3-2: Bulk rock (carbonate) isotopic data from the Lias Group (995.00 – 1'032.00 m) 44
Fig. 3-3: Organic isotopic data from the Lias Group (995.00 – 1'032.00 m) 45
Fig. 3-4: Bulk rock (carbonate) isotopic data from the lower Dogger Group – mainly Opalinus Clay (860.00 – 1'005.00 m) 48
Fig. 3-5: Organic isotopic data from the lower Dogger Group – mainly Opalinus Clay (860.00 – 1'005.00 m) 49
Fig. 3-6: Bulk rock (carbonate) isotopic data from the upper part of the Dogger Group (795.00 – 895.00 m) 52
Fig. 3-7: Organic isotopic data from the upper part of the Dogger Group (795.00 – 895.00 m) 53
Fig. 3-8: Whole bulk rock (carbonate) isotopic data from BUL1-1 (797.07 – 997.00 m) and BUL1-1B (995.85 – 1'031.20 m) 54
Fig. 3-9: Whole organic isotopic data from BUL1-1 (797.07 – 997.00 m) and BUL1-1B (995.85 – 1'031.20 m) 55
Fig. 4-1: Correlation of the double-cored interval of the Staffelegg Formation (BUL1-1 / BUL1-1B) 58
Fig. 5-1: 360° core photo (891.88 – 891.00 m) with the litho-boundary in red at 891.70 m and specific biostratigraphic datings (green: ammonite, yellow: palynomorphs) 60

List of Appendices

Appendix A: **List of all samples** **A-1**
Appendix A1a: List of all thin sections from BUL1-1 (536.16 – 1'034.81 m) A-2
Appendix A1b: List of all thin sections from BUL1-1B (1'042.16 – 1'317.79 m) A-3
Appendix A2a: List of all sampled macrofossils from BUL1-1 (801.65 – 1'030.44 m) A-4
Appendix A2b: List of all sampled macrofossils from BUL1-1B (996.65 – 1'005.06 m) A-5
Appendix A3a: List of other provisionally determined conspicuous macrofossils from BUL1-1 (785.50 – 1'028.74 m) A-6
Appendix A3b: List of other provisionally determined conspicuous macrofossils from BUL1-1B (996.66 – 1'029.60 m) A-7
Appendix A4: List of all palynological samples from BUL1-1 (804.49 – 996.31 m) A-8

Appendix B: **Photos microfacies** **B-1**

Appendix C: **Plates of ammonites** **C-1**
Plate I: BUL1-1 (1'016.77 – 997.17 m) C-3
Plate II: BUL1-1 (996.64 – 995.88 m) C-5
Plate III: BUL1-1 (995.53 – 812.03 m) C-7
Plate IV: BUL1-1 (810.58 – 801.65 m) C-9
Plate V: BUL1-1B (1'005.06 – 997.10 m) C-11

Appendix D: **Palynostratigraphy** *(in the digital version)* **D-1**
Appendix D1: Range Chart: Quantitative stratigraphic distribution of Middle Jurassic palynomorphs in the Bülach-1-1 borehole
Appendix D2: Depth/Age plot

Appendix E: **Chemostratigraphy** **E-1**
Appendix E1: List of all geochemical samples and results drilled mainly from specific calcareous beds in the Opalinus Clay and its upper confining unit E-2

1 Introduction

1.1 Context

To provide input for site selection and the safety case for deep geological repositories for radioactive waste, Nagra has drilled a series of deep boreholes in Northern Switzerland. The aim of the drilling campaign is to characterise the deep underground of the three remaining siting regions located at the edge of the Northern Alpine Molasse Basin (Fig. 1-1).

In this report, we present the results from the Bülach-1-1 borehole.

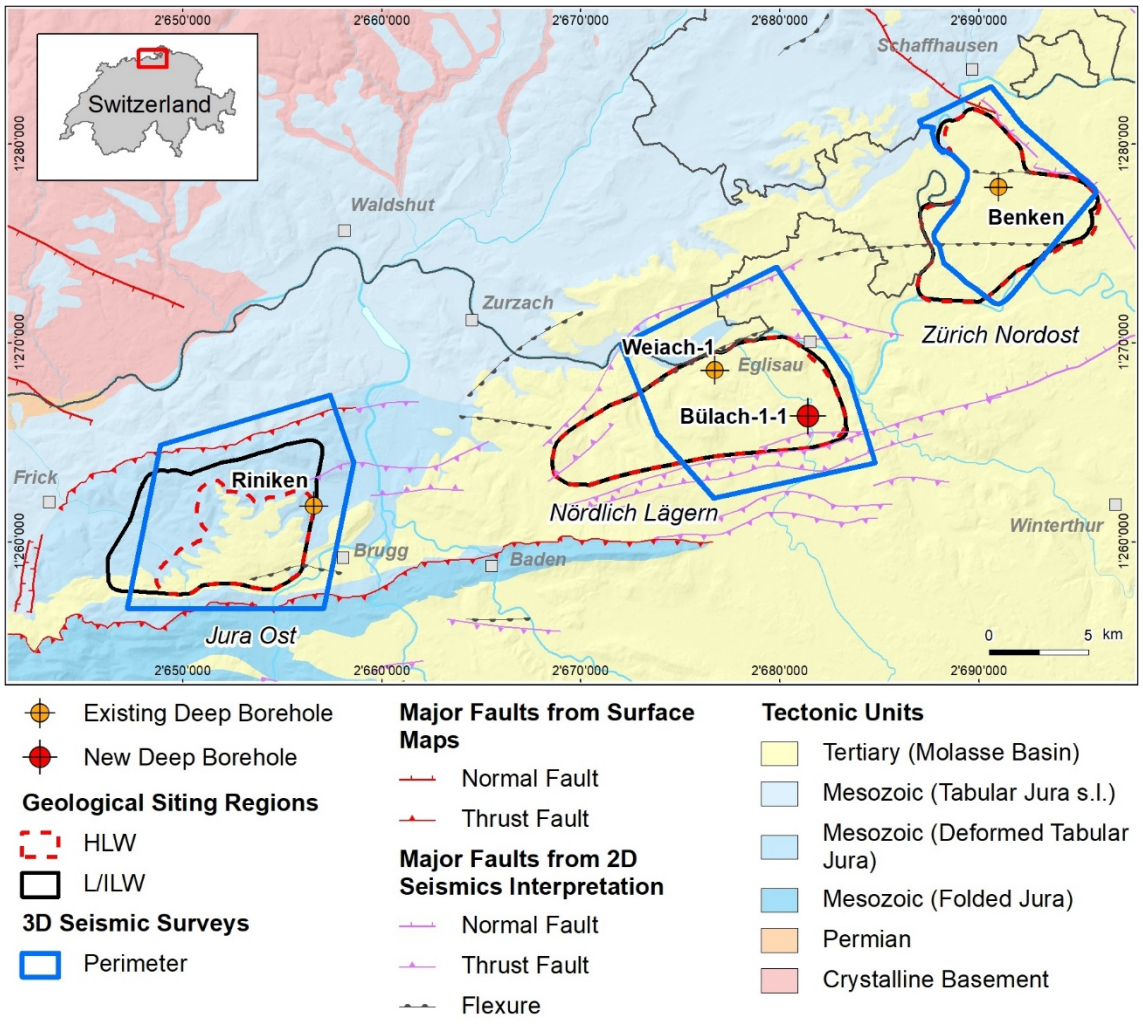

Fig. 1-1: Tectonic overview map with the three siting regions under investigation

1.2 Location and specifications of the borehole

The Bülach-1-1 (BUL1-1) exploratory borehole is the first deep borehole drilled within the framework of the TBO project. BUL1-1 is a vertical borehole. The drill site is located in the south-eastern part of the Nördlich Lägern siting region (Fig. 1-2). The borehole specifications are provided in Tab. 1-1. The lithostratigraphic profile and the casing scheme are shown in Fig. 1-3. Due to instabilities, the borehole was plugged back from 1'043.00 m to 918.70 m (*cf.* Dossier I). Resuming coring operations, a sidetrack was initiated with a kickoff point at 995.85 m. This sidetrack was labelled Bülach-1-1B (BUL1-1B). BUL1-1B reached the final depth of 1'370.19 m (measured depth MD core depth)[1]. For easier communication and labelling, the name BUL1-1 is generally used for the complete vertical borehole unless stated otherwise. Fig. 1-3 shows the combined lithostratigraphic profile of BUL1-1.

Tab. 1-1: General information about the BUL1-1 borehole

Location	Bülach (Canton Zurich / ZH), Switzerland
Siting region	Nördlich Lägern
Coordinates	2'681'446.028 / 1'266'298.472
Elevation	389.62 m asl (top of rig cellar)
Borehole depth	1'370.19 m MD core depth
Drilling period	15 April 2019 – 27 November 2019 (spud – rig release)
Drilling company	Daldrup & Söhne AG
Drilling rig	Wirth B 152t
Drilling fluid	Water-based mud with varying amounts of Pure-Bore®, Pure-Bore® ULV, soda ash, sodium bicarbonate, xanthan gum

[1] *Measured depth (MD)* below top rig cellar along borehole trajectory. In all dossiers, depth refers to MD unless stated otherwise.

MD core depth refers to the depth marked on the cores. Note that petrophysical logs have not been shifted to core depth, hence MD log depth differs from MD core depth. The depth shift between core depth and log depth is documented in Dossier V, Appendix E-1.

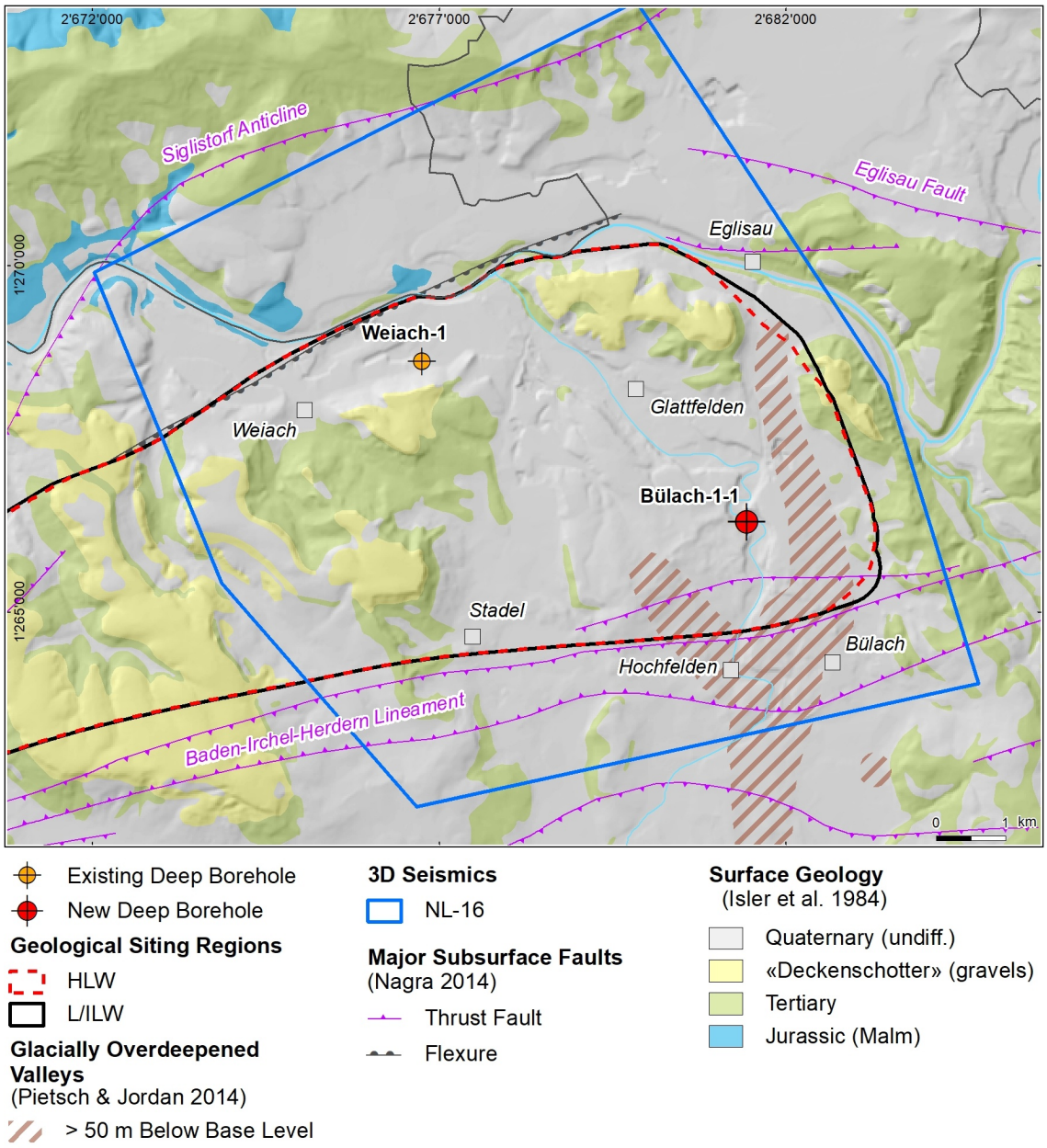

Fig. 1-2: Overview map of the investigation area in the Nördlich Lägern siting region with the location of the BUL1-1 borehole and the existing Weiach-1 borehole

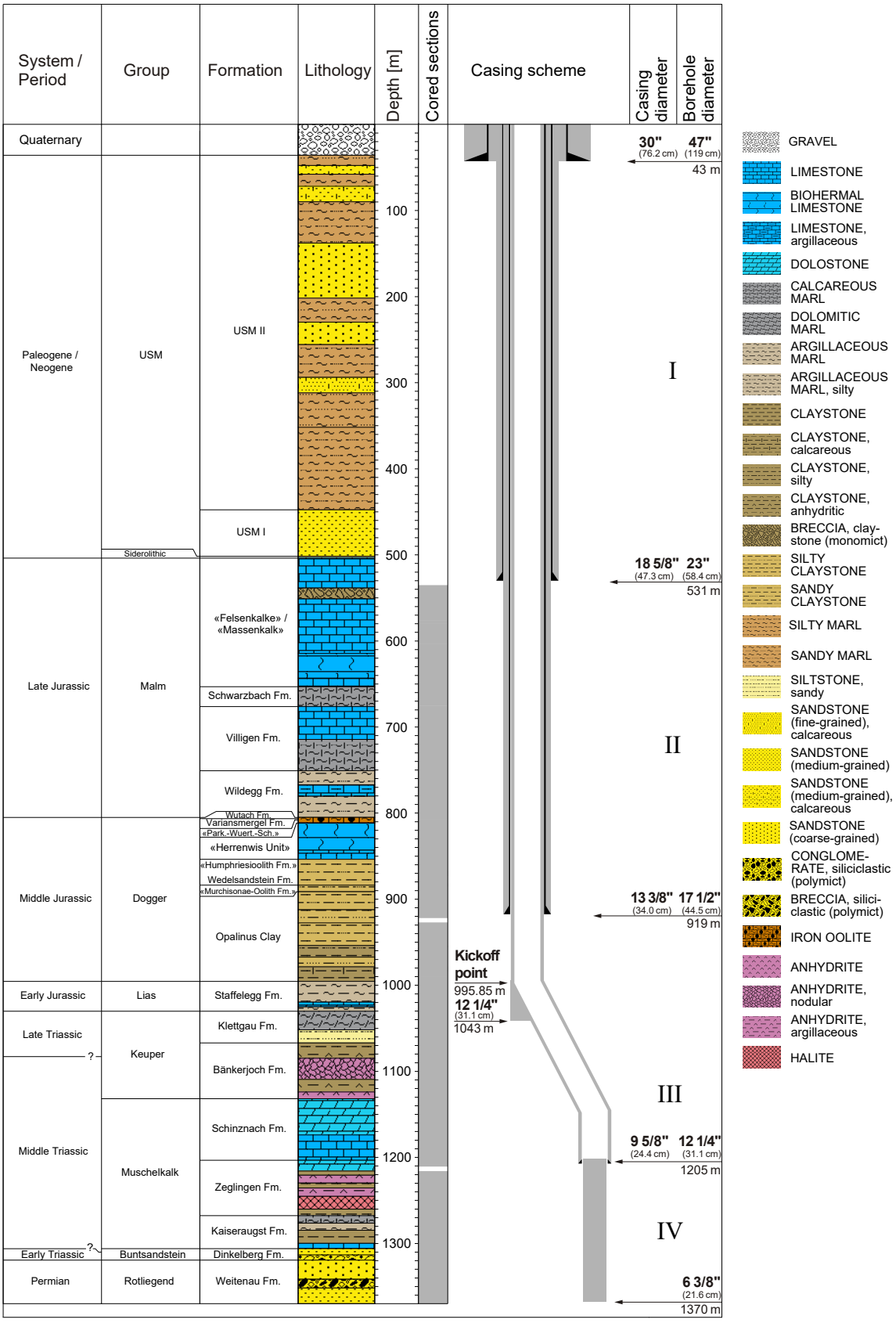

Fig. 1-3: Lithostratigraphic profile and casing scheme for the BUL1-1 borehole

1.3 Documentation structure for the BUL1-1 borehole

NAB 20-08 documents the majority of the investigations carried out in the BUL1-1 borehole, including laboratory investigations on core material. The NAB comprises a series of stand-alone dossiers addressing individual topics and a final dossier with a summary composite plot (Tab. 1-2).

This borehole documentation aims at early publication of the data collected in the BUL1-1 borehole. It includes the majority of the data available approximately one year after completion of the borehole. Some analyses are still ongoing (e.g. diffusion experiments, analysis of veins, hydrochemical interpretation of water samples) and will be published in separate reports.

The current borehole report will provide an important basis for the integration of datasets from different boreholes. The integration and interpretation of the results in the wider geological context will be documented later in separate geoscientific reports.

Tab. 1-2: List of dossiers included in NAB 20-08

Black marks the dossier at hand.

Dossier	Title	Authors
I	TBO Bülach-1-1: Drilling	M. Ammen & P.-J. Palten
II	TBO Bülach-1-1: Core Photography	D. Kaehr & M. Gysi
III	TBO Bülach-1-1: Lithostratigraphy	P. Jordan, H. Naef, P. Schürch, M. Schwarz, T. Ibele, R. Felber & M. Gysi
IV	TBO Bülach-1-1: Microfacies, Bio- and Chemostratigraphic Analysis	S. Wohlwend, H.R. Bläsi, S. Feist-Burkhardt, B. Hostettler, U. Menkveld-Gfeller, V. Dietze & G. Deplazes
V	TBO Bülach-1-1: Structural Geology	A. Ebert, L. Gregorczyk, E. Hägerstedt & M. Gysi
VI	TBO Bülach-1-1: Wireline Logging and Microhydraulic Fracturing	R. Garrard, J. Gonus, J. Desroches & E. Bailey
VII	TBO Bülach-1-1: Hydraulic Packer Testing	R. Schwarz, L. Schlickenrieder & T. Vogt
VIII	TBO Bülach-1-1: Rock Properties, Porewater Characterisation and Natural Tracer Profiles	M. Mazurek, L. Aschwanden, L. Camesi, T. Gimmi, A. Jenni, M. Kiczka, U. Mäder, D. Rufer, H.N. Waber, P. Wanner, P. Wersin & D. Traber
IX	TBO Bülach-1-1: Rock-mechanical and Geomechanical Laboratory Testing	E. Crisci, L. Laloui & S. Giger
X	TBO Bülach-1-1: Petrophysical Log Analysis	S. Marnat & J.K. Becker
	TBO Bülach-1-1: Summary Plot	Nagra

1.4 Scope and objectives of this dossier

The present data report complements the lithostratigraphic report (Dossier III) on the Bülach-1-1 borehole and its sidetrack Bülach-1-1B. The report documents data on microfacies analysis, ammonite- and palynostratigraphy as well as detailed geochemical (C, O and N isotopes) analyses. Preliminary results of these analyses already existed at data-freeze (31.01.2020) two months after the end of drilling operations and were integrated into the lithostratigraphic discussion and lithostratigraphic boundary definition (Dossier III).

The objectives of this report focusing on the Opalinus Clay and its confining units are:

- to specify the macroscopic description by a detailed microfacies analysis (components, matrix, cements),
- to allow a microfacies comparison of specific horizons, for example hardgrounds of the upper Opalinus Clay,
- to provide additional data on the diagenetic history of the sediment,
- to recover macrofossils from the stratigraphic interval of interest which are significant for facies changes and chronostratigraphic data,
- to compile an additional independent dataset of palynomorphs for chronostratigraphic data,
- to provide detailed geochemical (C, O and N isotopes) analyses with one metre spacing from the stratigraphic interval of interest,
- to allow a chemostratigraphic correlation (stable isotopes) with other deep boreholes in the three siting regions,
- to support the definition of the lithostratigraphic units.

The detailed stratigraphy of borehole Bülach-1-1 and its sidetrack Bülach-1-1B with core depth in metres can be found in Fig. 1-4. The stratigraphic intervals of interest for the different investigations (microfacies analysis, ammonite- and palynostratigraphy and geochemical analyses) and their specific sampling intervals are visualised in Fig. 1-5 with respect to the 1:5'000 lithostratigraphic profile.

All depths labelled with metres [m] in this report refer to "m MD core depth" if not stated otherwise.

TBO BÜLACH-1-1, BÜLACH-1-1B

System / Period		Group	Formation	Metres MD	Member / Sub-unit
Quaternary				36	
Paleogene / Neogene		Unt. Süss-wasser-molasse	USM II	448	
			USM I	502	
		Siderolithic		504	
Jurassic	Late	Malm	«Felsenkalke» / «Massenkalk»	653.57	
			Schwarzbach Fm.	676.58	
			Villigen Fm.	751.11	
			Wildegg Fm.	804.85	Effingen Mb.
				805.28	Birmenstorf Mb. and «Glaukonitsandmergel Bed»
	Middle	Dogger	Wutach Fm.	806.49	
			Variansmergel Fm.	808.00	
			«Parkinsoni-Württembergica-Sch.»	812.03	
			«Herrenwis Unit»	853.94	
			«Humphriesioolith Fm.»	855.53	
			Wedelsandstein Fm.	883.96	
			«Murchisonae-Oolith Fm.»	891.70	
			Opalinus Clay	912.55	«Sub-unit with silty calcareous beds»
				927.77	«Upper silty sub-unit»
				978.80	«Mixed clay-silt-carbonate sub-unit»
				995.85	«Clay-rich sub-unit»
	Early	Lias	Staffelegg Fm.	1'000.70	Gross Wolf Mb.
				1'006.81	Rietheim Mb.
				1'007.66	Breitenmatt Mb. / Rickenbach Mb.
				1'009.02	Grünschholz Mb.
				1'019.82	Frick Mb.
				1'025.42	Beggingen Mb.
				1'030.51	Schambelen Mb.
Triassic	Late	Keuper	Klettgau Fm.	1'041.70	Gruhalde Mb.
				1'044.42	Seebi Mb.
				1'050.82	Gruhalde Mb.
				1'052.03	Gansingen Mb.
	?1083			1'067.36	Ergolz Mb.
			Bänkerjoch Fm.	1'085.07	«Claystone with anhydrite nodules»
				1'109.60	«Cyclic sequence»
				1'124.14	«Thin-layered anhydrite claystone sequence»
				1'128.67	«Banded massive anhydrite»
				1'132.00	«Dolomite and anhydrite»
	Middle	Muschelkalk	Schinznach Fm.	1'135.77	Asp Mb.
				1'174.24	Stamberg Mb.
				1'176.19	Liedertswil Mb.
				1'204.73	Leutschenberg + Kienberg Mb.
			Zeglingen Fm.	1'214.0	«Dolomitzone»
				1'245.50	«Obere Sulfatzone»
				1'260.31	«Salzlager»
				1'267.94	«Untere Sulfatzone»
			Kaiseraugst Fm.	1'276.59	«Orbicularismergel»
				1'300.04	«Wellenmergel»
	?1310			1'306.17	«Wellendolomit»
	E.	Bsst.	Dinkelberg Fm.	1'319.63	
Permian		Rotlieg.	Weitenau Fm.	1'370.19	Final depth

Fig. 1-4: Bülach-1-1 & Bülach-1-1B stratigraphy with core depth in metres

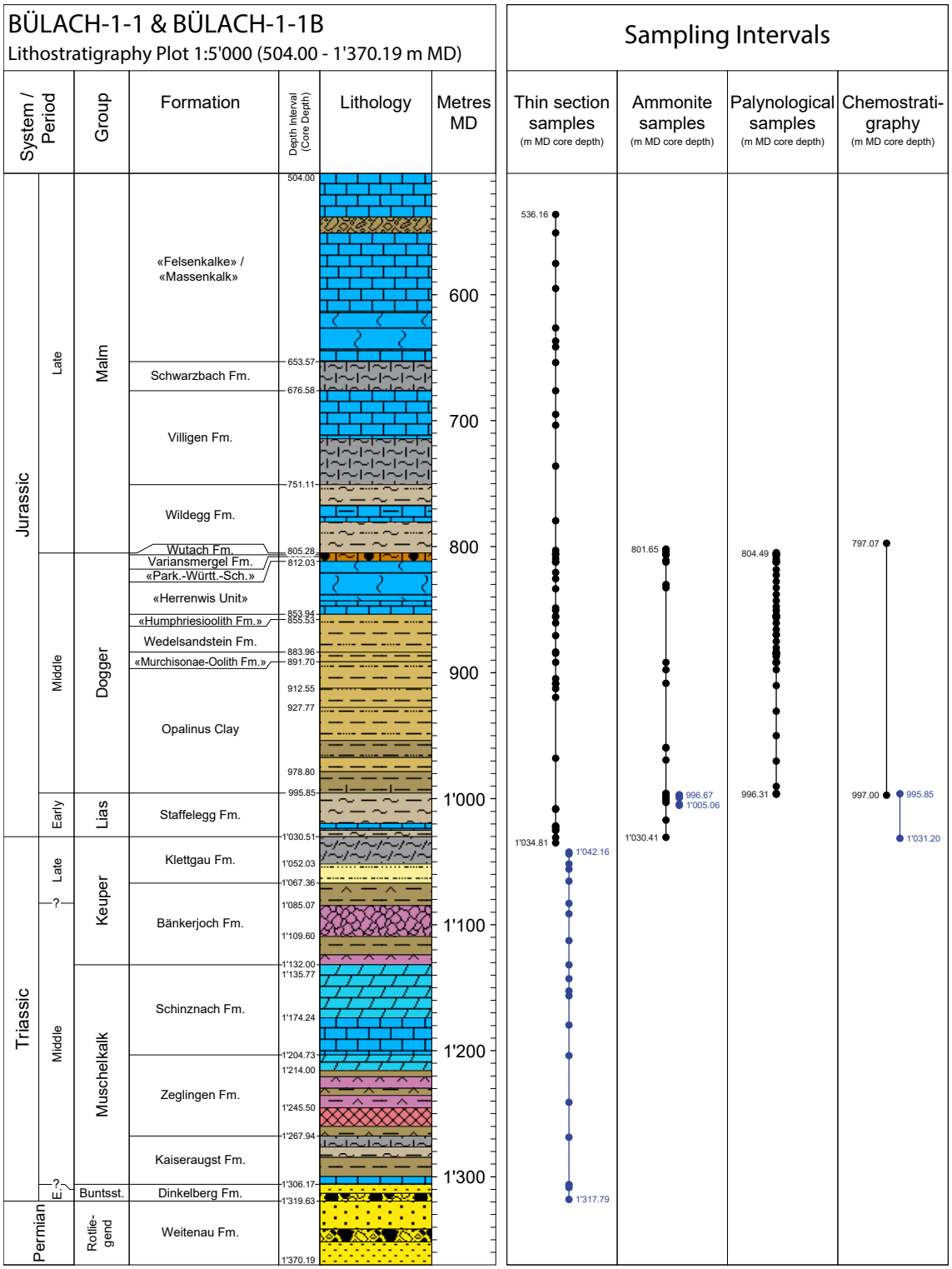

Fig. 1-5: Lithostratigraphy plot (1:5'000) from the Mesozoic succession with the individual sampling intervals for thin sections, macrofossils, palynological analysis and chemo-stratigraphy

1:5'000 stratigraphic plot modified from Dossier III. Samples in black are taken from BUL1-1, samples in blue from BUL1-1B.

2 Methods

2.1 Microfacies

Thin section preparation

All thin sections (TS) were cut edgewise from the core so that the long side is parallel to the coring direction and therefore covers as much of the stratigraphy as possible. The mean depth of the thin section corresponds to the Sample ID. Therefore, thin sections containing lithological boundaries may have Sample IDs that fall into only one of the two described intervals. However, the lower or upper range on the thin section still covers the interval. A list of all thin sections with their sampling range and Sample ID can be found in Appendices A1a and A1b of this report.

The thin sections from calcareous lithologies with a standard length of 4 cm were prepared at the University of Basel. Lithologies sensitive to water such as claystones and argillaceous sediments (swelling of clay minerals) or evaporates (dissolution of evaporitic minerals) were prepared by the Thin Section Lab (TSL) by using petroleum. Thin sections prepared by TSL are only 3 cm long. For better identification of the carbonate minerals calcite, Fe-calcite and Fe-dolomite, the left half of the thin sections was stained applying the technique of Dickson (1965). Thin sections with a macroscopic porosity were impregnated during preparation using a blue coloured epoxy resin to estimate the percentage of their porosity.

Thin section analyses

68 thin sections were analysed using a Zeiss polarisation microscope. First, all allochemical components, biogenic particles, siliciclastics, matrix and diagenetic alterations as neomorphic minerals, cements and replacements were studied. Then, to obtain the percentage of the components etc., 100 points were counted with a net micrometer ocular. For detrital quartz-bearing thin sections, the average grain size was evaluated in millimetres. To count inhomogeneous sediments, two different sections were looked at and averaged. A selection of 24 thin section photographs for microfacies analysis is documented in Appendix B (Figs. B-1 to B-24).

Components, matrix and cements (definitions)

To describe thin sections, several allochemical components (described below) were counted, and their numbers are documented in Section 3.1 (Microfacies). Some of the specific terms used for the components or matrix are explained as follows:

Clay matrix, micrite, microsparite (or pseudosparite): Sedimented mud consisting of clay minerals, other very small silicate grains, heavy minerals (i.e. clay matrix) and/or microcrystalline carbonate ooze (i.e. micrite). Microsparite is defined as a mosaic of small calcite crystals formed by aggrading neomorphism; originally, it was micrite and not a diagenetic pore-filling cement. Alternatively, microsparite could also be the product of dedolomitisation as seen in the «Felsenkalke» / «Massenkalk».

Dolomitic matrix: primary microcrystalline dolostone ooze

Limonitic matrix: Calcite micrite mixed with microcrystalline limonitic grains grown during diagenesis.

Limonitic echinoderms, limonitic bivalves: Fragments, parts of echinoderms and bivalves, with limonite filling the skeletal structure of the fossil.

Fe-stromatolites and stromatolitic clasts: Iron-mineralised microbial mats or and microbial clasts.

Fe-ooids or iron-ooids: Limonitic/goethitic or chamositic ooids, with a visible concentric structure; some iron-ooids are replaced by calcite (calcitic iron-ooids), a few show relicts of iron mineral layers (BUL1-1B-908.33).

Intraclasts: Rock fragments of early diagenetic cemented sediment, reworked and sedimented in the same sedimentary environment.

Calcite cement (sparite): "Normal" cement, calcite crystals grown – filled in – within the primary pore space or in leached components. In this column, the amount of calcite crystal pseudomorphs after gypsum (BUL1-1B-1123.99) was also noted.

"Stellate cement": Calcite "cement" grown within the matrix and not filling primary or secondary pore space. The calcite crystals form small "stellates", i.e. a habitus typical for "hiatus beds" (firm-, hardgrounds) (Wetzel & Allia 2000).

Cone-in-cone calcite: Rows of piled calcite cones grown during diagenesis which were named "Tutenmergel" in the Swabian realm.

(Fe)-Dolomite: Normally dolomite rhombohedrons that originated during diagenesis; in special cases, the dolomite replaces gypsum crystals that were sedimented as detritical gypsum crystals (e.g. BUL1-1B-1091.12). In some cases, the rhombohedrons consist of iron-dolostone, which are stained blue after the thin section staining.

Dedolomite: Calcite replacement of dolomite: each single dolomite rhombohedron is replaced by a few smaller calcite crystals. When it was a total dolostone and the calcitic replacement has been completed, the result is a thoroughly crystalline, sparitic/ microsparitic limestone (e.g. BUL1-1-626.22, 594.92 or 575.05). In addition, another dedolomite type exists with larger calcite crystals jointly replacing a few dolomite crystals, thus forming a calcite mosaic similar to marble.

Anhydrite: Present in various forms: as a rock-forming mineral, as a vein mineral, mainly replacing "Fasergips", and as cement in sandstones (e.g. Dinkelberg Formation, BUL1-1B-1308.34 or in the Ergolz Member of the Klettgau Formation).

Quartz cement: Authigenic quartz rims grown during diagenesis around detrital quartz grains (e.g. BUL1-1B-1308.34); also quartz/chalcedony in silicified bivalves.

Porosity: Thin sections with a macroscopic porosity were impregnated during preparation using a blue coloured epoxy resin to estimate the volume percentage (vol.-%) of their porosity.

Hardground: Thin sections from hardgrounds document synsedimentarily cemented and lithified carbonate layers which have been exposed on the seafloor. During that time period the hardgrounds are therefore mostly encrusted and bored by organisms and may consist of early marine calcite cements and are in parts mineralised by iron and manganese oxides or calcium phosphates.

2.2 Ammonite preparation

The BUL1-1 and BUL1-1B cores were carefully examined for macrofossils at the Würenlingen (Aargau) core storage facility. In the two cores (Lias Group of BUL1-1 and sidetrack BUL1-1B), "doubles" of "simultaneous" ammonites were reduced to one sample in the sample list (Appendix A2a) and recovered in BUL1-1 and not in the sidetrack when possible. The cores were examined for ammonites and other macrofossils in the bedding and fractured surfaces as well as on the outer surface of the core; the core itself was not broken open. A list of all samples with their sampling range and Sample ID can be found in Appendices A2a and A2b of this report. In addition to ammonites, other conspicuous fossils were identified to the extent possible and entered in the list (Appendices A3a & A3b), even when they were not subsequently, or only occasionally, recovered. The ammonites were then secured from the core and brought to the Natural History Museum in Bern, where they were prepared, documented and afterwards archived in the earth sciences collection.

For the preparation, we used mechanical methods such as air tools and fine sandblasting equipment as well as a chemical etching method using potassium hydroxide (KOH). Sodium hydrogen carbonate was mainly used as an abrasive. In one case (at 852.11 m), some biloxite (white corundum) was used. Residual material from preparing five ammonite samples (marked in grey in Appendix A4) was used as material for palynological samples. Before being photographed, we applied ammonium chloride steam to the fossils to make their fine structure more visible. A selection of ammonites is documented on five plates (Plates I – V) in Appendix C.

The names of several ammonite taxa are followed by a question mark, for example in *Pleydellia*? sp. The question mark after the genus name was used to indicate a question regarding the correct taxonomical assignment of the specimen to the genus.

2.3 Palynological sample preparation and quantitative analysis

Palynolgical processing of the rock samples was carried out by PLS Palynological Laboratory Services Ltd. (Holyhead, Anglesey, UK). Processing follows the standard protocol (Wood et al. 1996) using concentrated HCl and concentrated HF, followed by a short oxidation with HNO_3 and, if necessary, treatment with ultrasound. The residues are sieved at a mesh size of 15 µm. Residues are mounted on microscope slides and analysed using transmitted light microscopy. A list of all samples with their sampling range and Sample ID can be found in Appendix A4 of this report.

Two consecutive counts were carried out in the quantitative microscopic analysis. In the first count, 200 grains of all palynomorphs were counted and the number of dinoflagellate cysts noted (column 'DA *Dinocysts (count 1)*' in Appendix D1). In a second count, only dinoflagellate cysts were counted until a total of 100 cysts was reached. The reminder of the slide was checked for additional, out-of-count species. Taxa recorded out of count are marked with a '+' in the range chart. Taxa only questionably identified are marked with a '?' in the range chart. Occurrences of fungal remains are recorded semi-quantitatively (R = Rare, O = Occasional, C = Common, A = Abundant, S = Superabundant).

Results are illustrated using the StrataBugs v2.1 software package (Appendices D1 and D2). Numerical age dates used for the Composite Standard and the Depth/Age plot are in line with those of the *Geologic Time Scale 2016* (OGG et al. 2016). On the range chart Appendix D1, several abbreviations are used (AC = Acritarchs, ALBO = Algae, *Botryococcus* and *Pediastrum*, ALPR = Algae, Prasinophytes, ALZY = Algae, Zygnematophyceae, DA = Dinocyst abundance,

DC = Dinoflagellate cysts, FT = Foraminiferal test linings, FU = Fungi, MP = Miscellaneous palynomorphs, SP = Spores and pollen). Several dinoflagellate cyst taxa contain a question mark in their name, for example in *Evansia*? *eschachensis*. The question mark after the genus name indicates uncertainty regarding the taxonomical assignment of the species to the genus.

2.4 Chemostratigraphy

Sampling

The sampling of the BUL1-1 and BUL1-1B cores focused primarily on the Dogger and Lias Groups and therefore primarily on the clay mineral-rich layers of the Opalinus Clay. The sampling resolution was one metre, except for some intervals with denser sampling density (mainly Rietheim and Schambelen Members of the Staffelegg Formation). All 419 samples (BUL1-1: n = 245 and BUL1-1B: n = 174) were drilled with a micro-drill. In general clay mineral-rich lithologies were sampled. Diagenetic calcite and siderite veins and nodules were avoided. The drilled powder amounted to around 1 g of material. A list of specific samples with results from calcareous beds, septarian nodules and a macrofossil (belemnite) can be found in Appendix E1 of this report.

Inorganic (carbonate) analysis

The 419 samples were analysed for stable carbon ($\boldsymbol{\delta^{13}C_{carb}}$) and oxygen isotope ($\boldsymbol{\delta^{18}O_{carb}}$) of bulk carbonate; 401 continuous samples (roughly in metre resolution) and additional 18 samples from specific calcareous beds in the Opalinus Clay and its upper confining unit (Appendix E1). Varying amounts of powder to reach approximately 120 µg of carbonate in the vial were weighed using a Mettler Toledo MT5 Fact microbalance in 12 ml vacutainers. The headspace was flushed with pure He and then the samples were reacted with 100 % phosphoric acid at 72 °C in a ThermoFisher GasBench II carbonate device connected to a ThermoFisher Delta V PLUS mass spectrometer. The instrument is calibrated with international carbonate standards NBS19 and NBS18 distributed by the International Atomic Energy Agency (IAEA), Vienna and internal standards (MS2 "Carrara marble"; $\delta^{13}C_{carb}$ = 2.16 ‰, $\delta^{18}O_{carb}$ = -1.85 ‰). The reproducibility of the measurements based on replicated standards was ± 0.05 ‰ for $\delta^{13}C_{carb}$ and ± 0.06 ‰ for $\delta^{18}O_{carb}$. All isotope measurements were performed at the Stable Isotope Laboratory of the ETH Zurich (Geological Institute). The isotope values are reported in the conventional delta notation with respect to the Vienna Pee Dee Belemnite (VPDB).

The **Total Carbonate content** (TCarb) was calculated based on a calibration using extracted CO_2 from the known weight of the internal standard material (MS2), which is composed to 100 % of carbonate (calcite). The mean area of the m/z 44 peak (corresponding to the most abundant isotopologue $^{12}C^{16}O_2$) in the mass spectrometer allows the carbonate content to be estimated from the individual bulk rock samples. The individual uncertainty for TCarb, represents the average from all standard deviations from the MS2 and is ± 5.73 %. However, the TCarb values calculated from the reaction of the phosphoric acid with the bulk rock, only reflect the carbonate that was able to react during the reaction time (~ 60 min). However, ankerite and especially siderite, for example, roughly require a 60 h reaction time for full dissolution at 70 °C (Fernandez et al. 2016). Therefore, the calculated carbonate content (TCarb) does not completely represent the total amount of all different carbonates. The data reflect a mixed signal composed mostly of calcite and dolomite with a smaller component of the other more resistant carbonates (see also Wohlwend et al. 2019b).

Organic analyses

The powders remaining after inorganic analysis from 322 samples (BUL1-1: n = 150 and BUL1-1B: n = 172) were decarbonated in quantities of less than 1 g in 10 ml of 3 M HCl for 12 h in 15 ml centrifuge tubes, to ensure the complete removal of carbonate. For neutralisation purposes, the residue was subsequently washed three times with deionised water, and then centrifuged and decanted. After drying at 70 °C in an oven for at least 72 h the samples were homogenised with a mortar and pestle. Depending on the organic carbon content of each specific sample, a different amount was weighed in a tin capsule using a Mettler Toledo MT5 Fact microbalance so that, approximately the same amount of organic carbon was always measured.

$\delta^{13}C_{org}$ and **$\delta^{15}N_{org}$** were measured by flash combustion on a ThermoFisher Scientific FlashEA elemental analyser connected to a Delta V isotope ratio mass spectrometer (IRMS) operated in continuous flow mode. The samples were combusted in an O_2 atmosphere in a quartz reactor at 1'020 °C packed with $(Co_3O_4)Ag$ and Cr_2O_3 to form CO_2, N_2, NO_X and H_2O. These gases were then transferred through a reduction reactor containing elemental Cu at 600 °C to remove excess O_2 and to reduce NO_X to N_2. H_2O and SO_X were subsequently removed using anhydrous $Mg(ClO_4)_2$ and elemental Ag. Then, N_2 and CO_2 were separated in a packed gas chromatographic column and analysed for their isotopic composition using the IRMS. Isotope ratios are reported in conventional delta notation with respect to atmospheric N_2 (AIR) and VPDB standards, respectively. The methods were calibrated with the International Atomic Energy Agency (IAEA)-N1 ($\delta^{15}N$ = 0.45 ‰), IAEA-N2 ($\delta^{15}N$ = +20.41 ‰) and IAEA-N3 ($\delta^{15}N$ = +4.72 ‰) reference materials for nitrogen, and NBS22 ($\delta^{13}C$ = -30.03 ‰) and IAEA-CH-6 ($\delta^{13}C$ = -10.46 ‰) for carbon. Reproducibility of the measurements is better than ± 0.2 ‰ for both nitrogen and carbon. Reproducibility and accuracy of the measurements are based on replicate analyses of the internal laboratory standards atropine, peptone and nicotinamide. All geochemical measurements were performed at the Stable Isotope Laboratory of the ETH Zurich (Geological Institute).

The Total Organic Carbon (**TOC_{decarb}**) and Total Nitrogen (**TN_{decarb}**) contents of the decarbonised samples were calculated based on the known carbon and nitrogen contents of atropine (70.56 wt.-% C, 4.84 wt.-% N). The individual uncertainty for TOC_{decarb}, represents the average from all standard deviations from atropine during that calculation and is ± 0.50 %, respective ± 0.04 % for the TN_{decarb}. The calculated TN_{decarb} reflects a mixture of bound inorganic and organic nitrogen and therefore also contains ammonium, which substitutes for K^+ in the interlayer exchange sites of illite (Scheffer & Schachtschnabel 1984).

The **carbon-to-nitrogen ratio** (C/N ratio) is a ratio of the mass of carbon to the mass of nitrogen. In this study, the ratio was calculated using the TOC_{decarb} and the TN_{decarb}. As mentioned above, the C/N ratios can also be influenced by inorganic nitrogen in the form of soil-derived ammonium (Scheffer & Schachtschnabel 1984). Due to this inorganic nitrogen, the C/N ratios of sediments containing additional inorganic nitrogen will decrease. Therefore, C/N ratios are referred to as organic carbon/total nitrogen (TOC_{decarb}/TN_{decarb}) giving the ratio of the C and N masses of the decarbonised samples (C_{org}/N_{org}). The calculated ratios allow to distinguish between marine (C/N ≤ 10; Parsons 1975) *versus* terrigenous matter (C/N ≥ 12; Kukal 1971) in marine sediments.

$$\frac{C_{org}}{N_{org}} = \frac{TOC_{decarb}}{TN_{decarb}} * \frac{atomic\ mass\ (C)}{atomic\ mass\ (N)} = \frac{TOC_{decarb}}{TN_{decarb}} * \frac{14.007}{12.011}$$

The Total Organic Carbon (**TOC)** of the whole/bulk sample was calculated using the semi-quantitative carbonate content (TCarb) and semi-quantitative TOC_{decarb} content based on the following equation:

$$TOC = (1 - TCarb) * TOC_{decarb}$$

3 Results

3.1 Microfacies

Dinkelberg Formation (BUL1-1B-1317.79, 1308.34 & 1306.32)

The two thin sections BUL1-1B-1317.79 and BUL1-1B-1308.34 are quite similar: both are quartz sandstones with a quartz content (grains and cement) of 71 vol.-% and 75 vol.-%, respectively (Tab. 3-1), anhydrite cement (15 and 12 vol.-%, resp.) and porosity (6 and 13 vol.-%, resp.). However, BUL1-1B-1308.34 consists more of monomineralic quartz grains, BUL1-1B-1317.79 on the other hand more of polymineralic quartz rock fragments. This has influenced diagenesis, where the quartz grains served as nuclei for authigenic quartz overgrowth cements (Fig. B-1, Appendix B); BUL1-1B-1308.34 thus has more quartz cement.

The BUL1-1B-1306.32 sample is a matrix-rich (45 vol.-%, Tab. 3-1), poorly sorted sandstone, with grain sizes ranging from 0.03 to 0.70 mm (average 0.12 mm). Nearly all of the detrital silicate grains (55 vol.-%, Tab. 3-1, column "detrital quartz + silicate rock fragments") are monomineralic quartz grains. Only few feldspar, mica and polymineralic quartz rock fragments are present.

Kaiseraugst Formation (BUL1-1B-1306.01 & 1268.42) and Zeglingen Formation (BUL1-1B-1'240.72)

The BUL1-1B-1306.01 sample, taken from the border zone of the Dinkelberg to the Kaiseraugst Formation, is composed of thin dolomicritic microbial mat laminae and thin sandstone layers. It contains two different sandstones: one poorly sorted, coarse-grained sandstone with rock fragments and a dolomicritic matrix and a second, fine-grained sandstone with a clay matrix and iron dolomite.

The two thin sections BUL1-1B-1268.42 and BUL1-1B-1240.72, the former from the Kaiseraugst Formation and the latter from the Zeglingen Formation, are both laminated anhydrites (92 and 85 vol.-% anhydrite, resp., Tab. 3-1). The anhydrite crystals in BUL1-1B-1240.72 are very small (0.01 – 0.05 mm, rarely up to 0.30 mm). The 0.10 mm dolomite rhombohedrons (15 vol.-%, Tab. 3-1) are concentrated in darker, probably primary argillaceous layers. In contrast, BUL1-1-1268.42 consists of clusters of columnar, up to 0.50 mm long anhydrite crystals and very small, 0.01 mm long dolomite crystals (8 vol.-%).

Schinznach Formation (BUL1-1B-1203.66, 1179.39, 1156.20, 1152.47 & 1142.62)

The BUL1-1B-1203.66 sample comes from a section with dolomitic microbial mats: The thin section shows close-fitting, small (0.10 – 0.20 mm) calcite ooids (53 vol.-%, Tab. 3-1), calcite cement (16 vol.-%) and up to 4 mm long anhydrite crystals (22 vol.-%) replacing the ooids and cement (Fig. B-2).

The BUL1-1B-1179.39 thin section is one of the echinoderm-bivalve beds sedimented in the lower part of the Schinznach Formation. It is composed of 31 vol.-% bivalves, 16 vol.-% echinoderm particles, intraclasts (11 vol.-%) and sparitic calcite cement (26 vol.-%, Tab. 3-1).

The three BUL1-1B-1156.20, BUL1-1B-1152.47 and BUL1-1B-1142.62 samples (Stamberg Member) are, from a mineralogical point of view, dolomites. The thin sections show the primary composition: TS BUL1-1B-1156.20 and BUL1-1B-1152.47 are oolitic sediments: the first consists of ooids and bivalves and the second is a pure oosparite. Ooids and bivalves are now composed of dolomite rhombohedrons (Fig. B-3) but are counted as ooids (55 and 73 vol.-%, resp., Tab. 3-1) and bivalves (10 vol.-%). Both have a remarkable porosity (30 and 27 vol.-%, resp.), but it is not clear if some of the pores were caused by the preparation.

Thin section BUL1-1B-1142.62 is a micritic sediment composed of 0.05 – 0.15 mm-sized micritic pellets (37 vol.-%, Tab. 3-1) in a micritic matrix. Some of the pellets are probably micritised ooids. Small dolomite rhombohedrons (24 vol.-%) and porosity (17 vol.-%) are also present.

Bänkerjoch Formation (BUL1-1B-1131.60, 1123.99, 1112.37, 1091.12 & 1082.87)

The BUL1-1B-1131.60 sample, a black-dotted dolomite layer, which seems to have black components, is a dolomicrite (78 vol.-%, Tab. 3-1) with roundish anhydrite crystals and crystal aggregates up to 5 mm long (22 vol.-%).

A very special example of a gypsum sediment being replaced by a carbonate is TS BUL1-1B-1123.99: a thin layer with a "sandy" appearance, consisting of calcite crystals that replace gypsum twin rosettes (Fig. B-4).

The sample of the fine-layered anhydrite section, BUL1-1B-1112.37, consists of clusters of columnar anhydrite (78 vol.-%, Tab. 3-1) with floating, 0.1 – 0.7 mm-sized, zoned dolomite crystals (18 vol.-%).

When analysing the anhydritic, argillaceous and dolomitic beds of the Bänkerjoch Formation, a frequently asked question is whether these arenitic-looking brownish thin layers really contain quartz grains or not? The answer is that the investigated layers do not. BUL1-1B-1091.12, the analysed sample (Tab. 3-1) for this lithology, is full of dolomite crystals (52 vol.-%, Tab. 3-1), pseudomorph after gypsum crystals (Fig. B-5). As seen in the old boreholes of e.g. Weiach and Benken, this means that these former gypsum crystals have grown in an early sediment, then eroded, sedimented again as gypsum sand, and have then been replaced by dolomite during later diagenesis. The significant anhydrite content of the sample (40 vol.-%) originates from anhydrite veins (formerly "Fasergips") and anhydrite cement in the dolomite layer.

Nonetheless, sediments with quartz grains exist: BUL1-1B-1082.87 consists of 18 vol.-% silt-sized quartz grains (Tab. 3-1) in a dolomicrite (74 vol.-%).

Klettgau Formation (BUL1-1B-1065.22, 1055.72, 1051.53, 1043.65, 1042.16 & 1034.81)

The analysis focused on the dolomite beds/members and the sandy/silty members interstratified in the argillaceous, dolomitic marly succession (as for example BUL1-1-1'034.81) of the Klettgau Formation.

The two thin sections, BUL1-1B-1065.22 and BUL1-1B-1055.72 of the Ergolz Member, show similar composition: small ripples with alternating fine-grained sandstone laminae, anhydrite-cemented, (Fig. B-6) and argillaceous siltstone laminae. BUL1-1B-1055.72, the sample containing red laminae, has thicker sandstone laminae than BUL1-1B-1065.22 (grey coloured), where the argillaceous siltstone laminae dominate. Consequently, BUL1-1B-1055.72 has a higher content of quartz/silicate rock fragments (68 *vs.* 50 vol.-%, Tab. 3-1), a higher proportion of anhydrite cement (17 *vs.* 6 vol.-%), but a lower clay matrix (15 *vs.* 40 vol.-%).

The BUL1-1B-1051.53 sample of the Gansingen Member is a stromatolite, a laminated dolomicrite with a few small, dispersed 0.10 – 0.60 mm-long anhydrite crystals (13 vol.-%, Tab. 3-1).

The BUL1-1B-1043.65 and BUL1-1B-1042.16 thin sections represent the Seebi Member: BUL1-1B-1043.65 is a coarse-grained sandstone typical for this member: 70 vol.-% quartz/rock fragments (Tab. 3-1) with a grain size up to 3 mm, partly embedded in a dolomitic matrix (17 vol.-%) and partly cemented by anhydrite (8 vol.-%) (Fig. B-7). The sample also contains a number of dolomicritic intraclasts (5 vol.-%). BUL1-1B-1042.16, from the upper dolomitic part of the member, is a dolomicrite (94 vol.-%, Tab. 3-1) containing some quartz grains (3 vol.-%, Tab. 3-1) and small dolomite veins, which come from the pedogenic origin of the bed.

Staffelegg Formation (BUL1-1-1030.57, 1025.00, 1024.54, 1022.64, 1022.08, 1021.30, 1008.20 & 1007.70)

The BUL1-1-1030.57 sample was chosen to determine whether the Belchen Member, the uppermost unit of the Keuper Group, is present or not. It does not look like; instead the sandy, calcareous marl with 42 vol.-% biogenic components (Tab. 3-1) and 28 vol.-% fine-grained quartz sand seems to be part of the Schambelen Member (Staffelegg Formation).

The five thin sections of the Beggingen Member (BUL1-1-1025.00, 1024.54, 1022.64, 1022.08, 1021.30) demonstrate the lithological diversity (*cf.* Tab. 3-1) of this unit. The two lowermost samples (BUL1-1-1025.00 and 1024.54) have a significant quartz content (14 and 26 vol.-%, resp., Tab. 3-1), of which one part consists of 0.20 mm-sized quartz grains and the other of up to 2 mm quartzite rock fragments (Fig. B-8). All five thin sections contain varying proportions of iron-ooids (9 – 42 vol.-%), in one case (BUL1-1-1022.08) with flattened limonitic iron-ooids and beautiful chamositic iron-ooids in the adjacent horizon, and in another case of goethitic/limonitic origin, together with iron-oolitic and iron-stromatolithic intraclasts (BUL1-1-1021.30; Fig. B-9). They are deposited together with echinoderm and bivalve fragments or limonitic echinoderm in a micritic matrix or limonitic micrite matrix or have been cemented during diagenesis (BUL1-1-1025.00 and BUL1-1-1024.54, Tab. 3-1, Fig. B-8).

The uppermost two thin sections, BUL1-1-1008.20 and BUL1-1-1007.70, come from condensed beds of the Grünschholz Member. Both are packstones (biomicrites), consisting of countless biogenic components (in total, 48 and 42 vol.-%, resp., Tab. 3-1), mainly bivalves, and embedded in a phosphoritic (BUL1-1-1007.70) micritic matrix. BUL1-1-1008.20 contains some phosphoritic intraclasts (3 vol.-%) and glauconite (12 vol.-%), as "normal" grains or grown within biogenic fragments.

Opalinus Clay (BUL1-1-976.02, 967.64, 919.32, 912.44, 908.54, 908.33 & 904.47)

These thin section samples have been chosen to study the sedimentary and diagenetic history of the Opalinus Clay.

Thin section BUL1-1-976.02 and BUL1-1-919.32 represent two "normal" Opalinus Clay facies: the upper sample (BUL1-1-919.32) consists of alternating argillaceous quartz silt (mean 0.05 mm) laminae and calcite-cemented, bioclast-containing, fine-sand (0.07 mm) laminae (34 vol.-% quartz in total, Tab. 3-1). The lower one (BUL1-1-976.02) is not as finely laminated and has slightly less and finer-grained quartz (28 vol.-%, Tab. 3-1).

Another composition can be found in BUL1-1-967.64, possibly a hardground in the lower Opalinus Clay: micritic nodules (42 vol.-%, counted in the "intraclasts" column, Tab. 3-1), intraclasts or possibly small septarians nodule are embedded in a silty to fine sandy (13 vol.-%) argillaceous matrix with few biogenic components.

BUL1-1-912.44, another hardground, is a biomicrite (22 vol.-% echinoderm and 5 vol.-% bivalve fragments, Tab. 3-1) with iron-stromatolithic intraclasts (12 vol.-%) (Fig. B-10).

The BUL1-1-908.54 and BUL1-1-908.33 thin sections have a very similar composition: iron-oolitic micrite-intraclasts (15 – 20 vol.-% iron-ooids, 80 – 85 vol.-% micrite matrix); whereas the iron-ooids are almost completely replaced by calcite, some of them show relicts of iron-mineral layers (Fig. B-11), and biomicritic intraclasts are the dominant components (65 and 75 vol.-%, resp., Tab. 3-1). The calcified iron-ooids have sizes up to 1 mm.

BUL1-1-904.47, made of a horizon consisting of bored micritic nodules, shows an unusual microfacies with a dominance of pyrite (37 vol.-%, Tab. 3-1), up to 4 mm long nodules with calcite veins and small framboids. It also contains bored, pyritic, micritic intraclasts (15 vol.-%), echinoderm components and five iron-ooids.

«Murchisonae-Oolith Formation» (BUL1-1-891.55, 884.38), Wedelsandstein Formation (BUL1-1-883.33, 870.35 & 860.36) and «Humphriesioolith Formation» (BUL1-1-855.52 & 854.98)

Iron-oolitic and calcareous/quartz-rich beds are the focus of the analysis for these three formations: BUL1-1-891.55, 884.38, 855.52 and 854.98 are iron-oolitic beds of the «Murchisonae-Oolith Formation» and the «Humphriesioolith Formation», BUL1-1-883.33 and BUL1-1-870.35 are calcareous/quartz-rich beds of the Wedelsandstein Formation; BUL1-1-860.36 represents the normal argillaceous facies of the Wedelsandstein Formation.

BUL1-1-891.55 and BUL1-1-884.38 are similar: both consist mainly of biogenic fragments, in total 40 vol.-% (partly limonitic) and 28 vol.-% (all limonitic), respectively, and iron-ooids (20 and 19 vol.-%, resp.) (Fig. B-12). BUL1-1-884.38 contains more (18 vol.-% *vs.* 6 vol.-%) and coarser (0.10 *vs.* 0.06 mm) quartz sand.

The two analysed calcareous/quartz-rich beds (BUL1-1-883.33 and 870.35) show quite different origins: the first one is a limonitic biomicrite, consisting of 56 vol.-% (Tab. 3-1) of mainly limonitic, biogenic components in a micritic calcite matrix. The second one is a calcareous silt- to sandstone (argillaceous, bioclastic) with 43 vol.-% quartz and 28 vol.-% biogenic fragments (Fig. B-13). Thin section BUL1-1-860.36 represents a shaly Wedelsandstein facies, i.e. a silty marl and consists of 32 vol.-% (Tab. 3-1) silt-sized quartz, 15 vol.-% biogenic components and 45 vol.-% argillaceous matrix.

The BUL1-1-855.52 sample is a hardground with iron-oolitic intraclasts (70 vol.-%, Tab. 3-1; Fig. B-14). In contrast, the BUL1-1-854.98 sample consists of irregularly formed, 0.1 – 1.5 mm iron-ooids (23 vol.-%, Tab. 3-1), mostly of chamositic origin, as well as numerous biogenic fragments (22 vol.-% echinoderms, 9 vol.-% bivalves and 3 vol.-% limonitic echinoderms) embedded in a fine-grained sandy, limonitic, argillaceous matrix.

«Herrenwis Unit» (BUL1-1-850.27, 848.42, 833.21, 825.22, 820.22 & 812.08)

Thin section BUL1-1-850.27 shows a lot of serpulids (38 vol.-%, Tab. 3-1), "living tubes of worms" (Fig. B-15) which, in orthogonal sections, resemble ooids when looked at in macroscopically. The serpulids are embedded in a silty (10 vol.-% quartz) marly matrix.

Thin section BUL1-1-848.42 has a corresponding limestone bed that, seen macroscopically, seems to have ooids, but is a "normal" biosparite, i.e. a biodetritical "arenite" consisting of echinoderm fragments (28 vol.-%, Tab. 3-1), bivalves (16 vol.-%) and other biogenic components (18 vol.-%) with a significant amount of foraminifera, all in a sparitic calcite cement.

All four thin sections from the reef facies limestones, BUL1-1-833.21, 825.22, 820.22 and 812.08, show crystalline calcite rocks – a mosaic of calcite crystals that replace primary aragonitic corals, as well as pore-filling calcite and dolomite (saddle dolomite, in BUL1-1-825.22) that formed during later diagenesis (Figs. B-16, B-17). The distinction between calcite-replacing coral and calcite-filling primary pore space is often difficult. Therefore, it cannot be said with certainty that the proportion of the corals listed in Tab. 3-1 is correct.

«Parkinsoni-Württembergica-Schichten» (BUL1-1-811.78 & 809.21) and Wutach Formation (BUL1-1-806.17)

The analysed iron-oolitic bed (BUL1-1-811.78: ?«Parkinsoni-Oolith») shows fewer, but well-formed, limonitic, 0.1 – 3 mm iron-ooids (12 vol.-%, Tab. 3-1, Fig. B-18) with a small fibrous calcite cement rim. The matrix (42 vol.-%) consists of calcite micrite with very small dolomite crystals and silt-sized quartz grains (11 vol.-%).

The BUL1-1-809.21 thin section shows a marly facies, rich in bivalves: 28 vol.-% bivalve debris (Tab. 3-1) with primary calcite shells, 12 vol.-% echinoderm debris and 12 vol.-% quartz. All components are sedimented with a marly matrix.

The one thin section (BUL1-1-806.17) of the iron-oolitic Wutach Formation consists mainly of iron-ooids and bivalves, sedimented with a micritic matrix. The iron-ooids (27 vol.-%, Tab. 3-1) are 0.2 – 2 mm long and consist of limonite, primarily goethite. Several of them have a somewhat distorted and pitted outline (Fig. B-19): pressure-solution and neomorphism of the encircling matrix and ooid rim are responsible for this. Within the matrix, which is a mixture of calcite micrite, limonitic calcite micrite and microsparite, numerous small (0.05 – 0.20 mm) bivalve and echinoderm clasts and a few larger brachiopods and pelecypodes (bivalves) are present.

Wildegg Formation (BUL1-1-805.13, 802.68 & 779.21)

The BUL1-1-805.13 sample of the «Glaukonitsandmergel Bed» *sensu* Gygi (1977, 2000, 2012) shows a strange microfacies: 22 vol.-% sand-sized (0.15 – 0.25 mm) glauconite grains, 8 vol.-% quartz (0.10 mm), 50 vol.-% iron-oolitic intraclasts and few iron-ooids; all components are embedded in a marly matrix (12 vol.-%, Tab. 3-1). The iron-ooids (mean size: 1 mm) of the intraclasts have been mostly replaced by calcite (Fig. B-20).

The micritic bed near the base of the Effingen Member (TS BUL1-1-802.68) contains only a few (10 vol.-%, Tab. 3-1) small bioclasts (echinoderms, bivalves) and few silt-sized quartz grains and glauconite. The BUL1-1-779.21 thin section, taken from a nodular limestone horizon, consists of sponge nodules (18 vol.-%) and an ammonite (22 vol.-%, listed in the column under "other biogenes"), as well as some bivalve and echinoderm clasts, all sedimented in a micritic matrix.

Villigen Formation (BUL1-1-735.84, 703.37 & 694.80)

The BUL1-1-735.84 sample is a grey to dark-grey mottled micrite, where the thin section shows small (0.05 – 0.1 mm) pellets (38 vol.-%, Tab. 3-1) and tiny biogenic components (15 vol.-%). BUL1-1-703.37 is a sponge biomicrite with a partially recognisable sponge structure.

The BUL1-1-694.80 sample is a calcareous marl with limestone nodules and intraclasts. The thin section shows a dolomitic marl with numerous echinoderm particles (16 vol.-%, Tab. 3-1), serpulids (18 vol.-%), serpulid-bearing intraclasts (8 vol.-%) and micrite parts (40 vol.-%) (Fig. B-21). Dolomite (18 vol.-%) is present as very small (0.01 – 0.03 mm) rhombohedrons. However, it could instead be dedolomite: it seems that the rhombohedrons consist of few smaller crystals. The interpretation "dolomite" is supported by the colouration: the crystals are not coloured.

Schwarzbach Formation (BUL1-1-676.10 & 653.67)

The BUL1-1-676.10 thin section is an echinoderm biomicrite: 32 vol.-% (Tab. 3-1) echinoderm particles, with sizes up to 4 mm, are embedded together with a few bivalves, pellets and glauconite grains in a calcareous, partly marly matrix (58 vol.-%, Tab. 3-1).

In contrast, BUL1-1-653.67 has a complex composition: many different small (1 cm) rounded nodules, together with biogenic components (thin bivalves, echinoderm particles, 20 vol.-%, Tab. 3-1, Fig. B-22), few glauconite grains (4 vol.-%) and pyrite (3 vol.-%) in a partially marly and partially calcareous matrix. Several of the rounded nodules seem to be pellets, some are micritic sponge components, some are biomicritic intraclasts and others show encrusting foraminifera.

«Felsenkalke» / «Massenkalk» (BUL1-1-641.26, 636.67, 626.21, 594.92, 575.05, 550.77 & 536.16)

The «Felsenkalke» / «Massenkalk» formation is composed of two principal lithologies: the well-bedded micritic «Felsenkalke» and the «Massenkalk» that consists of massive, limestone (saccharoidal), formerly sponge limestones. They have undergone intense changes during diagenesis as calcite replacement for the biogenic bodies, then dolomitisation and dedolomitisation. The result is a so-called "saccharoidal limestone" ("zuckerkörniger Kalkstein"). During core description it is not always easy to differentiate micrites, dolomites, microsparites and dedolomites and to identify the original limestone.

In the lower part, a grey dedolomitic biopelmicrite (BUL1-1-641.26) appears with up to 2 mm-sized black nodules of glauconite (6 vol.-%, Tab. 3-1). Some of the components are pellets, some intraclasts, and some sponge particles; perhaps all are micritic sponge fragments.

The BUL1-1-626.22 sample is a coarser crystalline limestone composed of microsparite with micrite spots and interpreted as dedolomite (70 vol.-%, Tab. 3-1, Fig. B-23). It also contains druses of bigger calcite cement crystals (22 vol.-%) of which some enclose echinoderm fragments (8 vol.-%). BUL1-1-575.05 looks like a micrite, but the thin section yields a microsparite, a very finely crystalline calcite mosaic with micrite spots. Rhombohedrons can occasionally be identified, but they are full of small inclusions (Fig. B-24). Nonetheless, the limestone is interpreted as dedolomite (97 vol.-%, Tab. 3-1).

Sample BUL1-1-594.92, a dedolomitic biopelmicrite, consists of sponges (30 vol.-%, Tab. 3-1), pellets (25 vol.-%) and bivalves (7 vol.-%), in a dedolomitic (15 vol.-%) micrite matrix (20 vol.-%). The thin section shows that when dolomitisation and subsequent dedolomitisation do not affect the entire rock, it is easier to identify rhombohedrons filled with calcite crystals and relicts of sponge structures.

The BUL1-1-550.77 sample derived from a foreign object in the karstified section is a brown iron-mineralised and calcareous, concentric component, probably a calc-sinter crust. It belongs to the Siderolithic Group.

Tab. 3-1: Microfacies analysis from BUL1-1 (536.16 – 1'034.81 m) and BUL1-1B (1'042.16 – 1'317.79 m); numbers in vol.-%

Microfacies analysis BUL1-1 (536.16 - 1'034.81 m) BUL1-1B (1'042.16 - 1'317.79 m)	clay matrix, micrite, microsparite	dolomitic matrix	limonitic matrix	components (and biohermal organisms)															cements, diagenesis											
				calcitic biogenes							Fe-stromat+strom.clasts	allochems					detritial quartz + silic.rock fragm.	quartz grainsize (mm)												
				echinoderms	bivalves	limonitic echinod. + bivalves	serpulids	corals	sponges, spicules	other biogenes		pellets, peloids	ooids	oncoids	Fe-ooids	intraclasts			calcite cement	"stellate cement" (s) cone-in-cone calcite (c)	(Fe)-dolomite	dedolomite	anhydrite, gypsum	quartz cement	pyrite	limonite,Fe-min.nodules	siderite	glauconite	mica	porosity
536.16m: micrite *«Felsenkalke» / «Massenkalk»*	87			4	2					2												5							
550.77m: calc-sinter crust (?) *Siderolithic Group*																									100				
575.05m: dedolomite *«Felsenkalke» / «Massenkalk»*																	3	0.03				97							
594.92m: biopelmicrite, dedolomitic *«Felsenkalke» / «Massenkalk»*	20				7				30			25										15		3					
626.22m: dedolomite *«Felsenkalke» / «Massenkalk»*				8															22			70							
636.67m: biopelmicrite *«Felsenkalke» / «Massenkalk»*	43			3	10				14			18							4			6			2				
641.26m: biopelmicrite, dedol., glauc. *«Felsenkalke» / «Massenkalk»*	32			5	6				5			17				3						26					6		
653.67m: calc. marl, biocl., intraclasts *Schwarzbach Fm.*	35			9	11				8			22				8									3		4		
676.10m: biomicrite *Schwarzbach Fm.*	58			32	3							4															3		
694.80m: calc. marl, biocl, intracl. *Villigen Fm.*	40			16			18									8				18									
703.37m: biomicrite *Villigen Fm.*	10						2		75			8							5										
735.84m: biopelmicrite *Villigen Fm.*	44			2	6				4	3		38					3	0.02											
779.21m: biomicrite, dedolomitic *Wildegg Fm. (Effingen Mb.)*	37			6	3				18	22									6			8							
802.68m: biomicrite, silty *Wildegg Fm. (Effingen Mb.)*	75			5	5							3					4	0.04				6					2		
805.13m: sandy marl, glauconitic *Wildegg Fm. («Glaukonitsandmergel Bed»)*	12			5											3	50	8	0.10									22		
806.17m: iron-oolite, calcareous *Wutach Fm.*	17		17	8	17					4					27		5	0.06	5										
809.21m: calc. marl, bioclastic *«Parkinsoni-Württembergica-Sch.»*	40			12	28					2							12	0.05							6				
811.78m: biomicrite, iron-oolitic *«Parkinsoni-Württembergica-Sch.»*	42			12	4					2					12		11	0.05	4		10				3				
812.08m: biosparite, dolom. *«Herrenwis Unit»*			8	6				43											13		30								
820.22m: biosparite (boundstone?) *«Herrenwis Unit»*								20											80										
825.22m: biosparite, dolomitic *«Herrenwis Unit»*	10			5				35											15		18								17
833.21m: biomicrosparite, dolomitic *«Herrenwis Unit»*	28			12	12		15		2								4	0.05	10		12			5					
848.42m: biosparite *«Herrenwis Unit»*				28	16					18									38										
850.27m: calcareous marl, bioclastic *«Herrenwis Unit»*	28			12	6		38			3							10	0.05						3					
854.98m: marl, Fe-ool., biocla., sandy *«Humphriesioolith Fm.»*			24	22	9	3									23		14	0.07	5										
855.52m: hardground with intraclasts *«Humphriesioolith Fm.»*	9			10	3										5	70	3	0.06											
860.36m: silty marl *Wedelsandstein Fm.*	45			9	6												32	0.05			4							4	
870.35m: calc. sandstone (arg., biocl.) *Wedelsandstein Fm.*	26			18	8					2							43	0.08	3										
883.33m: biomicrite, limonitic *Wedelsandstein Fm.*	34			8	6	42									4					6									
884.38m: biomicrite, iron-oolitic, sandy *«Murchisonae-Oolith Fm.»*			28			28									19		18	0.10	7										
891.55m: biosparite, iron-oolitic *«Murchisonae-Oolith Fm.»*			14	18	5	14				3					20		6	0.06	15	5									
904.47m: hardground, pyritic *Opalinus Clay*	22			5											1	15	8	0.04	8	4					37				
908.33m: hardground, Fe-ool. intracla. *Opalinus Clay*	8			5												75	7	0.05		5									
908.54m: hardground, Fe-ool. intracla. *Opalinus Clay*	13			10												65	5	0.05							7				
912.44m: hardground *Opalinus Clay*	47			22	5						12					4	10	0.04											
919.32m: arg. siltstone / silty claystone *Opalinus Clay*	56			2	2												34	0.07	4									2	
967.64m: hardground *Opalinus Clay*	33			2	4											42	13	0.06	4	2									
976.02m: silty claystone *Opalinus Clay*	60			2	2												28	0.05	6									2	
1'007.70m: hardground *Staffelegg Fm. (Grünschholz Mb.)*	42			5	34					3									4			12							
1'008.20m: biomicrite, glauconitic *Staffelegg Fm. (Grünschholz Mb.)*	20			4	38					6						3	6	0.05	4						7		12		
1'021.30m: hardground, Fe-oolite, calc. *Staffelegg Fm. (Beggingen Mb.)*	42			9	8										28	13													
1'022.08m: hardground, Fe-oolite, calc. *Staffelegg Fm. (Beggingen Mb.)*	37			6	7										36		8	0.04	6										
1'022.64m: hardground, Fe-oolite, calc. *Staffelegg Fm. (Beggingen Mb.)*			21		8	14									42				15										
1'024.54m: hardground, biospa., Fe-ool. *Staffelegg Fm. (Beggingen Mb.)*				9		31				3					17		14	0.20	22							4			
1'025.00m: biosparite, sandy, limonitic *Staffelegg Fm. (Beggingen Mb.)*				8		37									9		26	0.20	20										
1'030.57m: calc. marl, bioclastic, sandy *Staffelegg Fm. (Schmabelen Mb.)*	24			34	8												28	0.15							4			2	
1'034.81m: dolomicrite *Klettgau Fm. (Gruhalde Mb.)*		92															8	0.04											
1'042.16m: dolomicrite *Klettgau Fm. (Seebi Mb.)*		94															3	0.10			3								
1'043.65m: sandstone, dolomitic *Klettgau Fm. (Seebi Mb.)*		17														5	70	0.30				8							
1'051.53m: dolomicrite, stromatolithe *Klettgau Fm. (Gansingen Mb.)*		87																				13							
1'055.72m: sandstone, argillaceous *Klettgau Fm. (Ergolz Mb.)*	15																68	0.08				17							
1'065.22m: argillaceous siltstone *Klettgau Fm. (Ergolz Mb.)*	40																50					6						4	
1'082.87m: dolomicrite, silty *Bänkerjoch Fm.*		74															18	0.03				5						3	
1'091.12m: dolomite pseudomorph *Bänkerjoch Fm.*	8																				52	40							
1'112.37m: anhydrite, dolomitic *Bänkerjoch Fm.*																					18	78				4			
1'123.99m: calcite pseudomorph gypsum *Bänkerjoch Fm.*	18																		82										
1'131.60m: dolomicrite, anhydritic *Bänkerjoch Fm.*		78																				22							
1'142.62m: dolostone (pelsparite) *Schinznach Fm. (Stamberg Mb.)*		14		3						2		37				3					24								17
1'152.47m: dolostone (oolite) *Schinznach Fm. (Stamberg Mb.)*													73																27
1'156.20m: dolostone (oolite) *Schinznach Fm. (Stamberg Mb.)*					10								55											5					30
1'179.39m: biosparite *Schinznach Fm. (Leutsch. + Kienb. Mb.)*	5			16	31					3						11			26		4								4
1'203.66m: oosparite, anhydritic *Schinznach Fm. (Leutsch. + Kienb. Mb.)*													53						16		9		22						
1'240.72m: anhydrite, dolomitic *Zeglingen Fm. («Obere Sulfatzone»)*																					15	85							
1'268.42m: anhydrite *Kaiseraugst Fm. («Orbicularismergel»)*																					8	92							
1'306.01m: sandstone, dolo., ?stromato. *Kaiseraugst Fm. («Wellendolomit»)*		28															61	0.30			9							2	
1'306.32m: sandstone, dolomitic *Dinkelberg Fm.*		45															55	0.12											
1'308.34m: sandstone, quartz-cemented *Dinkelberg Fm.*																	59	0.40				12	16						13
1'317.79m: sandstone, anhydritic *Dinkelberg Fm.*																	66	1.00			8	15	5						6

3.2 Ammonite stratigraphy

The amount of determinable material was distributed very differently in the different core sections. Ammonites were frequently found in the Toarcian, in the earliest Aalenian, in the Bathonian (although very poorly determinable) and in the Oxfordian. In the late Aalenian and in the Bajocian we found only very few ammonites. This can probably be attributed to the somewhat unexpected approximately 30 m-thick reef facies («Herrenwis Unit») encountered in the Bajocian. A selection of ammonites was documented photographically on five plates (Plates I – V) in Appendix C. In general, several ammonite samples could not be prepared, or the remains extracted from the borehole were so badly preserved or so small that determining them was not possible.

In general, the more determinable ammonites present in a profile section, the more precisely we can determine the biostratigraphic classification of that section (Tabs. 3-2a and 3-2b). Furthermore, it has to be taken into account that not all ammonites have the same index value and that the preservation state of the objects also plays an important role. In this respect, a certain error margin must always be expected. This is in the range of about one ammonite Subzone (SZ) but can be as high as one ammonite Zone (Z) when the available data are insufficient.

Staffelegg Formation (BUL1-1)

1'030.41 m: One completely recrystallised ammonite and one ammonite cross-section (unprepared). The preservation of the ammonite is rather poor; it probably stems from the Early Hettangian *Psiloceras*? sp. Lithology: grey bioclastic limestone with echinoderm ossicles and probably ammonite shell fragments.

1'022.91 m: Two ammonite fragments. Neither could be determined because the fragment of the larger of the two ammonites shows only a small section of the ventral side and the smaller one is so strongly encrusted that it could not be exposed. Lithology: rusty-brown iron-oolite with green-grey, micritic intraclasts. Several bivalves are present.

1'016.77 m: A small ammonite fragment that has only three ribs. It could be a representative of the Asteroceratids. The fragment is too small for a definite determination. Probably Late Sinemurian, Obtusum Zone?. Lithology: grey siltstone with sulphidic burrows. The ammonite fragment is illustrated on Plate I, Fig. 1 (Appendix C, for all figures in this Section 3.2).

1'002.75 m: *Harpoceras* sp. The specimen is too incomplete for a reliable determination. However, the ammonite originates from the Falcifer Zone. Lithology: dark grey, bituminous shale. The ammonite is illustrated on Plate I, Fig. 2.

1'000.58 m: The incomplete ammonite can be assigned to the genus *Catacoeloceras*. It occurs from the late Bifrons Zone (Crassum Subzone) to the Variabilis Zone. Lithology: grey, limestone (argillaceous) with lighter patches and numerous burrows. The ammonite fragment is illustrated on Plate I, Figs. 3a and b.

999.78 m: A largely flattened, sculptureless ammonite that is assigned to the species *Perilytoceras jurense* (Zieten 1830). It is often found in the Late Toarcian in the Swiss Jura, especially in the Thouarsense Zone. Lithology: dark grey marl with pyrite concretions, ammonite fragments, and belemnites (*Acrocoelites* sp.). The ammonite is illustrated on Plate I, Fig. 4.

997.17 m: *Pleydellia*? sp. The specimen is too poorly preserved for a reliable determination. If it is a representative of the genus *Pleydellia*, it would belong to the Aalensis Zone. Lithology: dark grey marl with biodetritus and small ?phosphoric concretions. The ammonite is illustrated on Plate I, Fig. 5.

996.64 m: *Pleydellia dudelangense* (Maubeuge 1950) and *Pleydellia* sp. The former suggests the Aalensis Zone, Aalensis Subzone. Lithology (also for samples 996.62 – 996.58 m): dark grey claystone with belemnites and biodetritus. The ammonite is illustrated on Plate II, Fig. 1.

996.62 m: *Pleydellia* ex gr. *buckmani* (Maubeuge 1947). A flattened sculpture steinkern. Despite the apparently large umbilicus, the specimen can be assigned to the ammonite group around *Pleydellia buckmani*. Age: Aalensis Zone, Torulosum Subzone. The ammonite is illustrated on Plate II, Fig. 2.

996.60 m: (Plate II, Fig. 3) see above (Plate II, Fig. 2).

996.58 m: (without illustration) see above (Plate II, Fig. 2).

996.29 m: *Pleydellia misera* (Buckman 1902). Aalensis Zone, Torulosum Subzone. Lithology: grey bioclastic calcareous marl (echinoderm ossicles, etc.). The ammonite is illustrated on Plate II, Fig. 4.

Opalinus Clay (BUL1-1)

995.88 m: *Leioceras*? sp. ex gr. *subglabrum* (Buckman 1902). This form belongs to the early Opalinum Subzone of the Opalinum Zone. Lithology: dark grey claystone. The ammonite is illustrated on Plate II, Fig. 5.

995.78 m: *Leioceras*? sp. ex gr. *subglabrum* (Buckman 1902). This form belongs to the early Opalinum Subzone of the Opalinum Zone. Lithology: dark grey claystone.

995.53 m: *Leioceras undatum* (Buckman 1899) belongs to the Opalinum Subzone of the Opalinum Zone. Lithology: dark grey claystone. The ammonite is crushed, and its core is partly preserved in pyrite. The ammonite is illustrated on Plate III, Fig. 1.

969.10 m: *Leioceras opalinum* (Reinecke 1818), microconch, belongs to the Opalinum Subzone of the Opalinum Zone. Lithology: grey, somewhat silty claystone with mica. The ammonite is a flattened steinkern with some oyster growth. The ammonite is illustrated on Plate III, Fig. 2.

959.52 m: *Leioceras* sp. Juvenile microconch. Lithology: dark grey claystone.

959.07 m: *Leioceras opalinum* (Reinecke 1818), microconch, belongs to the Opalinum Subzone of the Opalinum Zone. Lithology: dark grey claystone, mica-bearing. The ammonite is crushed and preserved with recrystallised calcitic shell. The ammonite is illustrated on Plate III, Fig. 3.

908.22 m: *Leioceras* sp. This ammonite belongs to the Opalinum Zone, Opalinum Subzone. Lithology: bioclastic (echinoderm skeletal elements), grey to brownish limestone (partly argillaceous) with intraclasts and brown veins. The ammonite fragment is illustrated on Plate III, Fig. 4.

897.43 m: Indeterminable fragment of an ammonite. Lithology: somewhat silty claystone.

«Murchisonae-Oolith Formation» (BUL1-1)

891.63 m: *Brasilia* ex gr. *bradfordensis*. Belongs to the Bradfordensis Zone, Bradfordensis Subzone. Lithology: limestone (iron-oolitic) with intraclasts of different lithology, fossil-rich: ammonites, ammonite fragments and shells. The ammonite is illustrated on Plate III, Figs. 5a and b.

Wedelsandstein Formation (BUL1-1)

882.71 m: Graphoceratidae *Hyperlioceras*? sp. Truncated ammonite preserved as steinkern. Age: Early Bajocian, probably Discites Zone. Lithology: dark grey-brown, marl (iron-oolitic) with mica. The iron-ooids are limonitic/goethitic with a diameter of up to 0.5 mm. The ammonite is illustrated on Plate III, Figs. 6a and b.

«Herrenwis Unit» (BUL1-1)

852.11 m: Ammonite fragment, although in addition biloxite (white corundum) was used the fragment was not preparable. The recrystallised steinkern is connected inseparably with the cement of the sediment.

832.36 m: *Diplopodia*? sp., cannot be dissected.

829.82 m: *Caenocidaris cucumifera* (Agassiz 1840). Has been found in a dated layer at only one locality in the Swiss Jura. This is in the deeper coral facies in the La Malcôte quarry, Canton Jura. There the age could be determined to the Laeviuscula/Sauzei Zone boundary. In general, the species is mostly cited from the Bajocian (e.g. Hess 1975). The sea urchin spine is illustrated on Plate III, Fig. 7.

«Parkinsoni Württembergica-Schichten» (BUL1-1)

812.03 m: *Pseudogarantiana* sp. The genus occurs in the Garantiana Zone and extends into the early Parkinsoni Zone. Lithology: marl (iron-oolitic) with belemnites and bivalves. The ammonite fragment is illustrated on Plate III, Fig. 8.

810.58 m: *Procerites*? sp.: Probably Early Bathonian. Lithology: iron-ooid-bearing, brown, somewhat limestone (argillaceous). The ammonite is illustrated on Plate IV, Figs. 1a and b.

Wutach Formation (BUL1-1)

806.21 m: *Oecotraustes* sp. occurs in the Bathonian. As only an incomplete internal coil remains, the ammonite cannot be determined more precisely (without illustration). Lithology: brown to rust-red iron-oolite with bivalves and gastropods.

806.33 m: Ammonite fragment, Perisphinctoidea indet., not determinable and therefore without illustration. Lithology: limestone (iron-oolitic), somewhat argillaceous with shells.

805.80 m: *Siemiradzkia*? sp. Probably of Bathonian age. Lithology: brown to brown-grey iron-oolitic limestone with shells. The ammonite fragment is illustrated on Plate IV, Fig. 2.

805.70 m: Indeterminable ammonite fragment. Lithology: brown limestone (iron-oolitic).

805.37 m: Indeterminable ammonite fragment. Lithology: brown limestone (iron-oolitic).

Wildegg Formation (BUL1-1)

803.77 m: *Perisphinctes*? sp. Probably Transversarium Zone. Lithology: dark grey marl with crinoid stem fragments. The ammonite is illustrated on Plate IV, Fig. 3.

802.85 m: *Glochiceras subclausum* (Oppel 1863) occurs in the Transversarium Zone up to the Stenocycloides Subzone of the Bifurcatus Zone. Probably Transversarium Zone (is much rarer in the Bifurcatus Zone). Lithology: dark grey marl with ammonite fragments, crinoid stem fragments and intraclasts. The ammonite is illustrated on Plate IV, Fig. 4.

802.61 m: *Subdiscosphinctes* sp. The genus occurs in the Swiss Jura from the Transversarium Zone, Luciaeformis Subzone to the Schilli Subzone (see Gygi 2001). Lithology: dark grey, glauconite-bearing marl with intraclasts and belemnites. The ammonite fragment is illustrated on Plate IV, Fig. 5.

801.65 m *Perisphinctes* sp. Middle to early Late Oxfordian. Lithology: grey marl with individual echinoderm ossicles. The ammonite fragment is illustrated on Plate IV, Fig. 6.

Tab. 3-2a: Ammonite and other macrofossil determination from BUL1-1

Depth [m]	**Identification**	**Ammonite Zone (Subzone) or Age**
801.65	*Perisphinctes* sp.	(Middle to early Late Oxfordian)
802.61	*Subdiscosphinctes* sp.	Transversarium Z (Luciaeformis–Schilli SZ)
802.85	*Glochiceras subclausum* (Oppel 1863)	Transversarium Zone to Bifurcatus Zone, Stenocycloides SZ
803.77	*Perisphinctes*? sp.	Transversarium Zone?
805.37	Indeterminable ammonite fragment	
805.70	Indeterminable ammonite fragment	
805.80	*Siemiradzkia*? sp.	(probably Bathonian)
806.33	Perisphinctoidea indet.	
806.21	*Oecotraustes* sp.	(Bathonian)
810.58	*Procerites*? sp.	(probably Early Bathonian)
812.03	*Pseudogarantiana* sp.	Garantiana to early Parkinsoni Zone
829.82	*Caenocidaris cucumifera* (Agassiz 1840)	Early Bajocian
832.36	*Diplopodia*? sp.	
852.11	Ammonite fragment (not preparable)	
882.71	*Hyperlioceras*? sp.	Discites Zone?
891.63	*Brasilia* ex gr. *bradfordensis*	Bradfordensis Zone (Bradfordensis SZ)
897.43	Indeterminable ammonite fragment	
908.22	*Leioceras* sp.	Opalinum Zone (Opalinum SZ)
959.07	*Leioceras opalinum* (Reinecke 1818)	Opalinum Zone (Opalinum SZ)
959.52	*Leioceras* sp.	
969.10	*Leioceras opalinum* (Reinecke 1818)	Opalinum Zone (Opalinum SZ)
995.53	*Leioceras undatum* (Buckman 1899)	Opalinum Zone (Opalinum SZ)
995.78	*Leioceras*? sp. ex gr. *subglabrum* (Buckman 1902)	Opalinum Zone (Opalinum SZ)
995.88	*Leioceras*? sp. ex gr. *subglabrum* (Buckman 1902)	Opalinum Zone (Opalinum SZ)
996.29	*Pleydellia misera* (Buckman 1902)	Aalensis Zone (Torulosum SZ)
996.58	*Pleydellia* ex gr. *buckmani* (Maubeuge 1947)	Aalensis Zone (Torulosum SZ)
996.60	*Pleydellia* ex gr. *buckmani* (Maubeuge 1947)	Aalensis Zone (Torulosum SZ)
996.62	*Pleydellia* ex gr. *buckmani* (Maubeuge 1947)	Aalensis Zone (Torulosum SZ)
996.64	*Pleydellia dudelangense* (Maubeuge 1950) and *Pleydellia* sp.	Aalensis Zone (Aalensis SZ)
997.17	*Pleydellia*? sp.	Aalensis Zone?
999.78	*Perilytoceras jurense* (Zieten 1830)	Thouarsense Zone?
1'000.58	*Catacoeloceras* sp.	Bifrons Z (Crassum SZ) to Variabilis Z
1'002.75	*Harpoceras* sp.	Falcifer Zone
1'016.77	Asteroceratid?	Obtusum Zone?
1'022.91	Two indeterminable ammonite fragments	
1'030.41	*Psiloceras*? sp.	(Early Hettangian)

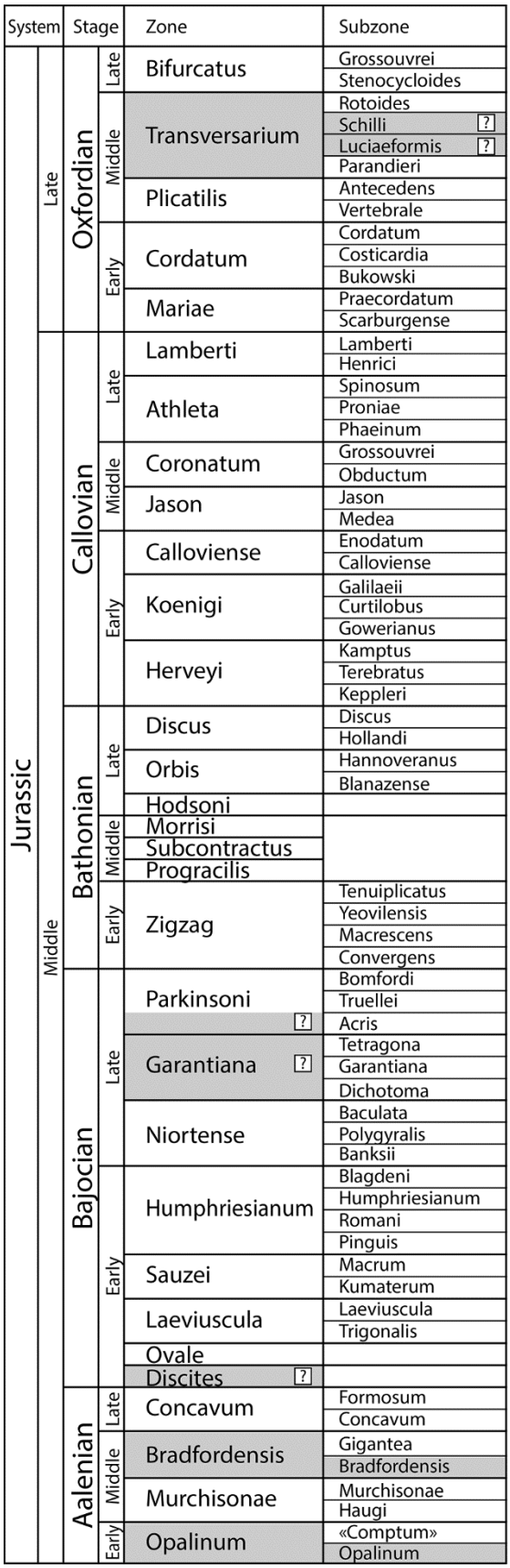

System	Stage		Zone	Subzone
Jurassic	Late	Late	Bifurcatus	Grossouvrei
				Stenocycloides
		Middle	Transversarium	Rotoides
				Schilli ?
				Luciaeformis ?
				Parandieri
			Plicatilis	Antecedens
				Vertebrale
		Early	Cordatum	Cordatum
				Costicardia
				Bukowski
			Mariae	Praecordatum
				Scarburgense
	Middle	Late	Lamberti	Lamberti
				Henrici
			Athleta	Spinosum
				Proniae
				Phaeinum
		Middle	Coronatum	Grossouvrei
				Obductum
			Jason	Jason
				Medea
		Early	Calloviense	Enodatum
				Calloviense
			Koenigi	Galilaeii
				Curtilobus
				Gowerianus
			Herveyi	Kamptus
				Terebratus
				Keppleri
		Late	Discus	Discus
				Hollandi
			Orbis	Hannoveranus
				Blanazense
			Hodsoni	
		Middle	Morrisi	
			Subcontractus	
			Progracilis	
		Early	Zigzag	Tenuiplicatus
				Yeovilensis
				Macrescens
				Convergens
		Late	Parkinsoni	Bomfordi
				Truellei
			?	Acris
			Garantiana ?	Tetragona
				Garantiana
				Dichotoma
			Niortense	Baculata
				Polygyralis
				Banksii
		Early	Humphriesianum	Blagdeni
				Humphriesianum
				Romani
				Pinguis
			Sauzei	Macrum
				Kumaterum
			Laeviuscula	Laeviuscula
				Trigonalis
			Ovale	
			Discites ?	
	Early	Late	Concavum	Formosum
				Concavum
		Middle	Bradfordensis	Gigantea
				Bradfordensis
			Murchisonae	Murchisonae
				Haugi
		Early	Opalinum	«Comptum»
				Opalinum

System	Stage		Zone	Subzone
Jurassic	Early	Late	Aalensis	Torulosum
				Aalensis ?
			Levesquei	Moorei
				Levesquei
			Insigne	Dispansum
				Insigne
			Thouarsense ?	Fallaciosum
				Thouarsense
			Variabilis ?	
		Early	?	Crassum
			Bifrons	Fibulatum
				Commune
			Falcifer	Falcifer
				Elegans
				Exaratum
				Elegantulum
			Tenuicostatum	Semicelatum
				Clevelandicum
				Paltum
		Late	Spinatum	Hawskerense
				Apyrenum
			Margaritatus	Gibbosus
				Subnodosus
				Stokesi
		Early	Davoei	Figulinum
				Capricornus
				Maculatum
			Ibex	Luridum
				Valdani
				Masseanum
			Jamesoni	Jamesoni
				Brevispina
				Polymorphus
				Taylori
		Late	Raricostatum	Aplanatum
				Macdonnelli
				Raricostatum
				Densinodulum
			Oxynotum	Oxynotum
				Simpsoni
			Obtusum ?	Denotatus
				Stellare
				Obtusum
		Early	Turneri	Turneri
			Semicostatum	Sauzeanum
				Scipionanum
				Charlesi
			Bucklandi	Bucklandi
				Rotiforme
				Conybeari
	Hettangian		Angulata	Complanata
				Extranodosa
			Liasicus	Laquaeus
				Portlocki
			Planorbis	Johnstoni
				Planorbis

BUL1-1

Grey highlighted zones and subzones are documented in the drill core with ammonites. Fields with additional interrogation points are not surely proven with ammonites.

Biostratigraphy modified after Cariou & Hanzpergue (1997)

Fig. 3-1a: Zones and subzones documented based on ammonites in BUL1-1

Staffelegg Formation (BUL1-1B)

1'005.06 m: *Dactylioceras* sp. Probably Falcifer Zone because of the finer ribbing. Lithology: laminated bituminous shale. The ammonite is illustrated on Plate V, Fig. 1.

1'004.11 m: *Dactylioceras* ex gr. *commune*? (Sowerby 1815) The ammonite belongs to the Bifrons Zone, probably Commune Subzone. Lithology: laminated bituminous shale. The ammonite is illustrated on Plate V, Fig. 2.

999.05 m: *Pseudogrammoceras fallaciosum* (Bayle 1878). This ammonite is common in the Thouarsense Zone, Fallaciosum Subzone. Lithology: light grey limestone (argillaceous). The ammonite is illustrated on Plate V, Fig. 3.

998.16 m: *Dumortieria* sp. occurs in the Levesquei Zone. Lithology: light grey, splintered limestone.

997.67 m: *Dumortieria* sp. occurs in the Levesquei Zone. Lithology: grey marl with bivalves, belemnites and echinid remains.

997.63 m: *Dumortieria* ex gr. *levesquei* (d'Orbigny 1844) occurs in the Levesquei Zone, Levesquei Subzone. Lithology: grey marl with belemnites. The ammonite fragment is illustrated on Plate V, Fig. 4.

997.36 m: *Dumortieria* ex gr. *moorei* (Lycett 1857) occurs in the Levesquei Zone, Moorei Subzone. Lithology: grey marl. The ammonite is illustrated on Plate V, Fig. 5.

997.10 m: *Dumortieria* sp. occurs in the Levesquei Zone. Lithology: grey marl. The two ammonites are illustrated on Plate V, Fig. 6.

996.84 m: *Pleydellia* sp. various fragments and one internal coil. Furthermore, a belemnite *Rhabdobelus exilis* (d'Orbigny 1842). The fossils belong to the Aalensis Zone. A more precise determination is not possible because of the incomplete ammonites. Lithology: dark grey marl with biodetritus and belemnites as well as phosphoritised intraclasts.

996.67 m: *Pleydellia* sp. and a belemnite *Rhabdobelus exilis* (d'Orbigny 1842) that both occur in the Aalensis Zone. Lithology: dark grey bioclastic marl with belemnites.

Tab. 3-2b: Ammonite determination from BUL1-1B

Depth [m]	**Identification**	**Ammonite Zone (Subzone) or Age**
996.67	*Pleydellia* sp.	Aalensis Zone
996.84	*Pleydellia* sp.	Aalensis Zone
997.10	*Dumortieria* sp.	Levesquei Zone
997.36	*Dumortieria* ex gr. *moorei* (Lycett 1857)	Levesquei Zone (Moorei SZ)
997.63	*Dumortieria* ex gr. *levesquei* (d'Orbigny 1844)	Levesquei Zone (Levesquei SZ)
997.67	*Dumortieria* sp.	Levesquei Zone
998.16	*Dumortieria* sp.	Levesquei Zone
999.05	*Pseudogrammoceras fallaciosum* (Bayle 1878)	Thouarsense Zone (Fallaciosum SZ)
1'004.11	*Dactylioceras* ex gr. *commune*? (Sowerby 1815)	Bifrons Zone (Commune SZ?)
1'005.06	*Dactylioceras* sp.	Falcifer Zone?

System		Stage		Zone	Subzone
Jurassic	Late	Oxfordian	Late	Bifurcatus	Grossouvrei
					Stenocycloides
			Middle	Transversarium	Rotoides
					Schilli
					Luciaeformis
					Parandieri
				Plicatilis	Antecedens
					Vertebrale
			Early	Cordatum	Cordatum
					Costicardia
					Bukowski
				Mariae	Praecordatum
					Scarburgense
	Middle	Callovian	Late	Lamberti	Lamberti
					Henrici
				Athleta	Spinosum
					Proniae
					Phaeinum
			Middle	Coronatum	Grossouvrei
					Obductum
				Jason	Jason
					Medea
			Early	Calloviense	Enodatum
					Calloviense
				Koenigi	Galilaeii
					Curtilobus
					Gowerianus
				Herveyi	Kamptus
					Terebratus
					Keppleri
		Bathonian	Late	Discus	Discus
					Hollandi
				Orbis	Hannoveranus
					Blanazense
				Hodsoni	
			Middle	Morrisi	
				Subcontractus	
				Progracilis	
			Early	Zigzag	Tenuiplicatus
					Yeovilensis
					Macrescens
					Convergens
		Bajocian	Late	Parkinsoni	Bomfordi
					Truellei
					Acris
				Garantiana	Tetragona
					Garantiana
					Dichotoma
				Niortense	Baculata
					Polygyralis
					Banksii
			Early	Humphriesianum	Blagdeni
					Humphriesianum
					Romani
					Pinguis
				Sauzei	Macrum
					Kumaterum
				Laeviuscula	Laeviuscula
					Trigonalis
				Ovale	
				Discites	
		Aalenian	Late	Concavum	Formosum
					Concavum
			Middle	Bradfordensis	Gigantea
					Bradfordensis
				Murchisonae	Murchisonae
					Haugi
			Early	Opalinum	«Comptum»
					Opalinum

System		Stage		Zone	Subzone
Jurassic	Early	Toarcian	Late	Aalensis	Torulosum
					Aalensis
				Levesquei	Moorei
					Levesquei
				Insigne	Dispansum
					Insigne
				Thouarsense	Fallaciosum
					Thouarsense
				Variabilis	
			Early	Bifrons	Crassum
					Fibulatum
					Commune ?
				Falcifer ?	Falcifer
					Elegans
					Exaratum
					Elegantulum
				Tenuicostatum	Semicelatum
					Clevelandicum
					Paltum
		Pliensbachian	Late	Spinatum	Hawskerense
					Apyrenum
				Margaritatus	Gibbosus
					Subnodosus
					Stokesi
			Early	Davoei	Figulinum
					Capricornus
					Maculatum
				Ibex	Luridum
					Valdani
					Masseanum
				Jamesoni	Jamesoni
					Brevispina
					Polymorphus
					Taylori
		Sinemurian	Late	Raricostatum	Aplanatum
					Macdonnelli
					Raricostatum
					Densinodulum
				Oxynotum	Oxynotum
					Simpsoni
				Obtusum	Denotatus
					Stellare
					Obtusum
			Early	Turneri	Turneri
				Semicostatum	Sauzeanum
					Scipionanum
					Charlesi
				Bucklandi	Bucklandi
					Rotiforme
					Conybeari
		Hettangian		Angulata	Complanata
					Extranodosa
				Liasicus	Laquaeus
					Portlocki
				Planorbis	Johnstoni
					Planorbis

BUL1-1B

Grey highlighted zones and subzones are documented in the drill core with ammonites. Fields with additional interrogation points are not surely proven with ammonites.

Biostratigraphy modified after Cariou & Hanzpergue (1997)

Fig. 3-1b: Zones and subzones documented based on ammonites in BUL1-1B

3.3 Palynostratigraphy

The studied samples mostly yielded good palynological residues with rich and diverse palynofloras. Preservation is good. The palynomorph assemblages are mainly composed of dinoflagellate cysts, pollen and spores. Minor components are prasinophytes, acritarchs, fungal remains, foraminiferal test linings and green algae (e.g. *Botryococcus*). A total of 201 dinoflagellate cyst taxa, 22 other aquatic palynomorphs and 56 pollen and spore taxa were recorded.

Some reworked sporomorphs (*Densosporites* spp., *Rhaetipollis germanicus, Ricciisporites tuberculatus*) indicate erosion of Triassic sediments in the source area. Other reworking is indicated by the occurrence of a few single specimens of the dinoflagellate cyst *Luehndea spinosa*, a typical Early Jurassic species with a main distribution in the Late Pliensbachian and earliest Toarcian.

The studied samples from the Bülach-1-1 core are dated to span the interval from the Aalenian/ Toarcian boundary to the Oxfordian. 22 sample intervals were differentiated and, where possible, assigned to ammonite biostratigraphy. A list of the analysed samples and the age dating of each sample are given in Tab. 3-3. The indicated ages, zones (Z) and subzones (SZ) for each sample are the result of palynostratigraphical analysis and interpretation. The results of the quantitative analysis are illustrated in a range chart (Appendix D1). A Depth/Age plot is illustrated in Appendix D2.

Sample interval 996.31 – 995.90 m (2 samples): Late Toarcian, Aalensis Zone to Early Aalenian, Opalinum Zone, Opalinum Subzone

The palynoflora of the two samples in this interval is characterised by very high abundances of one species, *Evansia*? cf. *granochagrinata*. This species dominates the palynoflora, reaching 42 % or more than 65 %, respectively, of all palynomorphs counted. Other dinoflagellate cysts present, though in low numbers, belong to the family Phallocystaceae (*Andreedinium* sp. 2, *Dodekovia* spp., *D. bullula, D. knertensis, D. pseudochytroeides, Parvocysta*? *tricornuta, Reutlingia nasuta, Susadinium scrofoides*) and to the family Valvaeodiniaceae (*Valvaeodinium* spp*., V. cavum, V. sphaerechinatum, V. spongiosum, V. vermipellitum*). There are species of *Nannoceratopsis* (*Nannoceratopsis* spp., *N. gracilis* s.s. and s.l., *N. triangulata*), species of *Scriniocassis* (*Scriniocassis limbicavatus, S. priscus, S. weberi*), as well as *Kallosphaeidium praussii, Mancodinium semitabulatum, Hystrichodinium*? sp. and *Wallodinium laganum*.

The sample interval is defined by the dominant occurrence of *Evansia*? cf. *granochagrinata*.

The composition of the dinoflagellate cyst assemblages is typical for the interval straddling the Toarcian/Aalenian boundary. *Evansia*? cf. *granochagrinata* and *Wallodinium laganum* have their FADs (First Appearance Datums) in the Late Toarcian, probably Levesquei Zone. *Kallosphaeridium praussii* and *Nannoceratopsis triangulata* first appear in the latest Toarcian or close to the Toarcian/Aalenian boundary. The very high abundance or dominance of *Evansia*? cf. *granochagrinata* is typical for an age of the samples straddling the Toarcian/Aalenian boundary (Aalensis Zone/Opalinum Zone, Opalinum Subzone). This characteristic bioevent at the Early to Middle Jurassic boundary defines the palynostratigraphic unit A of Feist-Burkhardt & Pross (2010).

Sample interval 995.55 – 910.02 m (6 samples): Early Aalenian, Opalinum Zone, Opalinum Subzone

The composition of the dinoflagellate cyst assemblages is similar to the interval below. *Evansia*? cf. *granochagrinata* is still common to abundant, but abundance decreases. The diversity of Phallocystaceae and Valvaeodiniaceae increases with the occurrence of further species such as *Andreedinium* aff. *elongatum*, *Comparodinium punctatum, Dodekovia "penicillus"*, *D. syzygia, D. tegillata, Moesiodinium raileanui* (questionable), *Ovalicysta hiata, Parvocysta bjaerkei, Phallocysta eumekes, Phallocysta*? *frommernensis* (common), *Reutlingia cardobarbata* and *R. fausta*. *Nannoceratopsis dictyambonis* and *Nannoceratopsis* sp. B have their first occurrence.

The interval is defined by the first occurrence of *Phallocysta*? *frommernensis* to the last occurrence and top acme of *Phallocysta*? *frommernensis*, and the last occurrence of unquestionable *Evansia*? cf. *granochagrinata* and *Nannoceratopsis triangulata*. The species *Wallodinium laganum* also has its last occurrence in this interval.

According to Feist-Burkhardt & Pross (2010), there are four marker species for the Early Aalenian Opalinuston Formation (German stratigraphy): *Kallosphaeridium praussii, Phallocysta*? *frommernensis, Nannoceratopsis triangulata* and *Wallodinium laganum*. All four marker species occur in this interval. The acme of *Phallocysta*? *frommernensis* defines the palynostratigraphical unit B of Feist-Burkhardt & Pross (2010) of the Opalinuston Formation.

The sample interval is therefore dated as Early Aalenian Opalinum Zone, Opalinum Subzone, and corresponds to palynostratigraphic unit B of Feist-Burkhardt & Pross (2010).

Sample interval 897.41 – 891.89 m (2 samples): Early Aalenian, Opalinum Zone, possibly «Comptum» Subzone to (?) Middle Aalenian, Murchisonae Zone

Assemblages in this interval are strongly reduced in the diversity of phallocystacean dinoflagellate cysts. The base of the interval is characterised by the first abundant occurrence of *Nannoceratopsis plegas* with its subspecies *N. plegas plegas* and *N. plegas brevicorna*, and the first occurrence of species of *Batiacasphaera* (abundant), with *Batiacasphaera* sp. A and sp. B.

The interval is defined from the first occurrence of *Batiacasphaera* spp. at the base, to the first occurrence of *Evansia*? *spongogranulata* in the interval above.

Batiacasphaera spp. has its FAD in the upper part of the Opalinum Zone. *Batiacasphaera* sp. A is known to be abundant in the «Comptum» Subzone of Opalinum Zone. *Evansia*? *spongogranulata* has its FAD in the Murchisonae Zone.

The interval is dated Opalinum Zone, possibly «Comptum» Subzone to (?)Murchisonae Zone.

The occurrence of *Luehndea spinosa* indicates reworking of Early Jurassic Late Pliensbachian to earliest Toarcian sediments in the source area.

Sample 891.70 m (1 sample): Middle Aalenian, Murchisonae to Bradfordensis Zone

The sample is characterised by the first occurrence of *Evansia*? *spongogranulata*. *Nannoceratopsis plegas* is still abundant. *Andreedinium elongatum* also has its first occurrence. Representatives of the genus *Dissiliodinium* are not yet present but have their first occurrence in the interval above.

Evansia? *spongogranulata* has its FAD in the Murchisonae Zone. *Dissiliodinium* spp. have an FAD within the Bradfordensis Zone.

The sample is dated Murchisonae to Bradfordensis Zone.

Sample interval 891.63 – 885.59 m (4 samples): Middle Aalenian, Bradfordensis Zone

The assemblages are characterised by the occurrence of the first species of *Dissiliodinium, D. lichenoides* and *Dissiliodinium* spp. Species of *Scriniocassis* (*S. limbicavatus, S. plegas, S. weberi*) have their last occurrence in this interval. *Nannoceratopsis dictyambonis* is common to superabundant. *Andreedinium elongatum* is quite common.

The interval is defined as reaching from the first occurrence of *Dissiliodinium lichenoides* to the first occurrence of *Evansia*? *eschachensis* in the interval above.

The FADs of *Dissiliodinium* spp. and *Dissiliodinium lichenoides* are within the Bradfordensis Zone. The LAD (Last Appearance Datum) of *Scriniocassis* spp. is in the Bradfordensis Zone. The FAD of *Evansia*? *eschachensis* is in the Concavum Zone.

The sample interval is dated Bradfordensis Zone.

Sample interval 884.80 – 884.42 m (2 samples): Late Aalenian, Concavum Zone

Assemblages are characterised by the first occurrence of *Evansia*? *eschachensis*. *Andreedinium elongatum* is common to abundant and the acritarch *Fromea tornalis* is common.

The interval is defined as reaching from the first occurrence of *Evansia*? *eschachensis* to the first occurrence of *Dissiliodinium* aff. *giganteum* in the interval above.

The FAD of *Evansia*? *eschachensis* is in the Concavum Zone. The FAD of *Dissiliodinium* aff. *giganteum* is in the Discites Zone. The common occurrence of *Andreedinium elongatum* and the acritarch *Fromea tornatilis* is typical for an age close to the Aalenian/Bajocian boundary.

The interval is dated Concavum Zone.

Sample interval 883.98 – 883.24 m (2 samples): Early Bajocian, Discites Zone

Samples in this interval show the first occurrence of *Dissiliodinium* aff. *giganteum*, *Gongylodinium erymnoteichon* (questionable), and the only occurrence of *Pareodinia* sp. 4.

The interval is defined as reaching from the first occurrence of *Dissiliodinium* aff. *giganteum* to the first occurrence of *Dissiliodinium giganteum* (sensu stricto) in the interval above.

Dissiliodinium aff. *giganteum* and *Gongylodinium erymnoteichon* have an FAD in the Discites Zone. *Dissiliodinium giganteum* has an FAD in the Ovale Zone. *Pareodinia* sp. 4 has so far only been observed in the Discites Zone.

The interval is dated Discites Zone.

Sample interval 880.02–869.81 m (3 samples): Early Bajocian, Ovale Zone

Assemblages in this interval are characterised by the first occurrence of *Dissiliodinium giganteum*, common *Gongylodinium erymnoteichon* and the first occurrence of the spore *Lycopodiumsporites gristhorpensis*. In the uppermost sample, *Cavatodissiliodinium hansgochtii* and *Durotrigia daveyi* have their first occurrence. Last occurrences in this interval have *Andreedinium elongatum* and *Evansia*? *eschachensis*.

The interval is defined as reaching from the first occurrence of *Dissiliodinium giganteum* to the last occurrence of *Evansia*? *eschachensis*.

The FAD of *Dissiliodinium giganteum* is in the Ovale Zone. The LADs of *Andreedinium elongatum* and *Evansia*? *eschachensis* are in the Ovale Zone.

The interval is dated Ovale Zone.

Sample interval 869.64 – 854.98 m (8 samples): Early Bajocian, Laeviuscula Zone

In addition to the species known from below, the dinoflagellate cyst assemblages are characterised by the consistent occurrence of *Cavatodissiliodinium hansgochtii, Durotrigia daveyi* and *Durotrigia* spp. The species *Durotrigia daveyi* may become very abundant in samples of the upper part of the sample interval. *Batiacasphaera laevigata* appears with the first questionable specimens at the base of the interval. *Batiacasphaera* spp. are abundant and very diverse, showing a wide variety of wall structures and surface ornamentation.

In the upper part of the interval, several specimens of two peculiar dinoflagellate cyst species, *Bradleyella* sp. 1 and *Gresslyodinium mirabile,* are recorded. *Bradleyella* sp. 1 is close to, or possibly conspecific with, *Bradleyella adela*, a rare species first described from the Bajocian of the UK. *Gresslyodinium mirabile* is a flashily ornamented species with a peculiar morphology. This is the first record of the species since its first description by Below (1990) from Dogger gamma sediments of Franconia in South Germany. Since then, the species has not been reported in the literature.

The interval is defined as reaching from the first questionable occurrence of *Batiacasphaera laevigata* to the first questionable occurrence of *Kallosphaeridium hypornatum* in the interval above.

The FAD of *Batiacasphaera laevigata* is in the Laeviuscula Zone. The FAD of *Kallosphaeridium hypornatum* is in the Sauzei Zone.

The interval is dated Laeviuscula Zone.

Sample interval 853.99 – 832.36 m (6 samples): Early Bajocian, Sauzei Zone

Assemblages of the lower part of the interval resemble those from below. Assemblages in the upper part of the interval are poorer and less diverse, and the topmost sample yielded very little palynological residue. *Kallosphaeridium hypornatum* has its first (questionable) occurrence at the base and occurs intermittently throughout the interval and above. *Evansia*? *spongogranulata* occurs intermittently and shows its last occurrence in the sample just above the top of the interval. Last occurrences in this interval include *Cavatodissiliodinium hansgochtii, Dissiliodinium giganteum* and consistent *Mancodinium semitabulatum*. There is an unusal occurrence of a few single specimens of *Phallocysta* spp. and *Phallocysta eumekes* in the upper part of the interval.

The interval is defined as reaching from the first questionable occurrence of *Kallosphaeridium hypornatum* to the first occurrence of *Acanthaulax crispa, Cavatodissiliodinium* sp. 1, sp. 2, sp. 3, *Durotrigia filapicata, Phallocysta thomasii* and *Wanaea* sp. 1 in the interval above.

The FAD of *Kallosphaeridium hypornatum* is in the Sauzei Zone. The FADs of *Acanthaulax crispa, Cavatodissiliodinium* sp. 1, sp. 2, sp. 3, *Durotrigia filapicata, Phallocysta thomasii* and *Wanaea* sp. 1 are in the Humphriesianum Zone. *Evansia*? *spongogranulata* was so far considered to have its LAD in the Sauzei Zone.

The age of the sample interval is interpreted to be Sauzei Zone.

Sample 827.38 m (1 sample): Early Bajocian, Humphriesianum Zone, Romani – Humphriesianum Subzone

The sample is characterised by numerous first occurrences: *Acanthaulax crispa, Cavatodissiliodinium* sp. 1, sp. 2 and sp. 3, *Durotrigia filapicata, Phallocysta thomasii*, *Valensiella/ Ellipsoidictyum* spp. (questionable) and *Wanaea* sp. 1. The species *Evansia*? *spongogranulata* has its last occurrence. *Phallocysta thomasii* only occurs in this sample.

The interval is defined by the first and last occurrence of *Phallocysta thomasii*.

Acanthaulax crispa, Cavatodissiliodinium sp. 1, sp. 2 and sp. 3, *Durotrigia filapicata, Phallocysta thomasii* and *Wanaea* sp. 1 all have their FADs in the Humphriesianum Zone. The range of *Phallocysta thomasii* is considered to be restricted to the Romani and Humphriesianum subzones of the Humphriesianum Zone. *Evansia*? *spongogranulata* was so far considered to have its LAD in the Sauzei Zone, but its range may reach into the early Humphriesianum Zone.

The sample is dated Humphriesianum Zone, Romani to Humphriesianum Subzone.

Sample interval 822.35 – 818.03 m (2 samples): Early Bajocian, Humphriesianum Zone

Samples of this interval are similar to before but lack *Phallocysta thomasii*. In addition, there are the first occurrences of *Atopodinium* sp. 1, *Meiourogonyaulax* sp. 2, questionable *Nannoceratopsis spiculata, Rhynchodiniopsis*? sp. 1 and *Wanaea* sp. 2.

All species mentioned have their FADs within the Humphriesianum Zone.

The sample interval is dated Humphriesianum Zone (undifferentiated).

Sample 813.27 m (1 sample): dating not possible

The sample yielded very little residue with only a few single grains. Dating is not possible.

Sample interval 812.19 – 812.05 m (2 samples): Early Bajocian, Humphriesianum Zone, Blagdeni Subzone and Late Bajocian, Niortense Zone

The assemblages are characterised by numerous first occurrences. In the basal sample, these include *Aldorfia aldorfensis* (questionable), *Batiacasphaera* sp. 1, *Ctenidodinium* spp. (questionable), *Gonyaulacysta pectinigera, Korystocysta gochtii, Meiourogonyaulax valensii, Nannoceratopsis spiculata* and *Rhynchodiniopsis? regalis*. In the second sample, the first

occurrences include *Atopodinium polygonale, Ctenidodinium continuum* (questionable), *Endoscrinium asymmetricum, Gongylodinium hocneratum* and *Valvaeodinium spinosum*. The species *Durotrigia daveyi* is common in both samples, and the top of its acme is in the upper sample of this interval. Last occurrence in this interval has also *Nannoceratopsis gracilis* s.l.

The FADs of the first occurring species are in the Blagdeni Subzone of the Humphriesianum Zone (*Aldorfia aldorfensis* and *Rhynchodiniopsis*? *regalis*), the Niortense Zone (*Atopodinium polygonale, Ctenidodinium continuum, Korystocysta gochtii, Gonyaulacysta pectinigera, Valvaeodinium spinosum*) and higher within Niortense Zone (*Endoscrinium asymmetricum, Ctenidodinium ornatum, Gongylodinium hocneratum*). The LAD of *Nannoceratopsis gracilis* s.l. is in the Niortense Zone. The top of consistently occurring *Durotrigia daveyi* is considered to be in the Humphriesianum Zone, but the species may reach up to the Garantiana Zone.

The dinoflagellate cyst taxa indicate an age corresponding to the Niortense Zone. The concurrent common occurrence of *Durotrigia daveyi*, however, indicates a mixture with a slightly older palynoflora that corresponds to the latest Humphriesianum Zone (Blagdeni Subzone) in age.

Sample 812.01 m (1 sample): Late Bajocian, Garantiana to Parkinsoni Zone

The assemblage again shows numerous first occurrences, among many others those of *Ctenidodinium sellwoodii* group, *Gonyaulacysta eisenackii* (questionable), *Sirmiodiniopsis* sp. and *Valvaeodinium vermicylindratum*. Last occurrences are i.a. *Acanthaulax crispa, Durotrigia daveyi* and *Meiourogonyaulax valensii*.

The FAD of the *Ctenidodinium sellwoodii* group is in the Garantiana Zone, that of *Gonyaulacysta eisenackii* and *Sirmiodinium* sp. is in the Parkinsoni Zone. The LAD of *Durotrigia daveyi* is in the Garantiana Zone, that of *Acanthaulax crispa* in the Parkinsoni Zone.

The sample is dated Garantiana to Parkinsoni Zone.

Sample 810.58 m (1 sample): Early Bathonian, Zigzag Zone

The assemblage is characterised by the abundant and diverse occurrence of species of the genus *Ctenidodinium* that includes *Ctenidodinium* spp., *Ct. combazii, Ct. continuum, Ct. cornigerum, Ct. ornatum* and the *Ct. sellwoodii* group. Important first occurrences are *Ctenidodinium combazii* (abundant), *Lithodinia* spp. and *Tubotuberella dangeardii*. Last occurrences are *Endoscrinium asymmetricum* and *Gongylodinium hocneratum*, both with questionable specimens.

The FAD of *Ctenidodinium combazii* is within the upper part of the Parkinsoni Zone, those of *Lithodinia* spp. and *Tubotuberella dangeardii* are in the Zigzag Zone. The LADs of *Endoscrinium asymmetricum* and consistent *Gongylodinium hocneratum* are in the Zigzag Zone.

The high diversity and abundance of *Ctenidodinium* species and the presence of *Ctenidodinium combazii* are typical for the Bathonian and earliest Callovian.

The sample is dated Zigzag Zone.

Sample 809.21 m (1 sample): Early Bathonian, Zigzag Zone, (?) Tenuiplicatus Subzone

The assemblage of the sample is similar to that from below. In addition, it includes *Lithodinia jurassica* s.l. and the first occurrence of a chorate dinoflagellate cyst, namely *Cleistosphaeridium* spp. The species *Sirmiodinium* sp. last occurs in this sample.

The FAD of *Lithodinia jurassica* s.l. is in the Zigzag Zone, that of *Cleistosphaeridium* spp. is in the Tenuiplicatus Subzone of the Zigzag Zone. The LAD of *Sirmiodinium* sp. is in the Zigzag Zone.

The sample is interpreted Zigzag Zone, probably Tenuiplicatus Subzone.

Sample 807.09 m (1 sample): Middle Bathonian, Progracilis to Morrisi Zone

The assemblage of this sample is similar to below with abundant and diverse species of *Ctenidodinium*. In addition, there are the first occurrences of *Gonyaulacysta jurassica* and *Nannoceratopsis pellucida*. The species *Carpathodinium predae* and *Rhynchodiniopsis*? *regalis* last occur in this sample.

The FADs of *Gonyaulacysta jurassica* and *Nannoceratopsis pellucida* are in the Progracilis Zone. The LAD of *Carpathodinium predae* is in the Morrisi Zone, that of *Rhynchodiniopsis*? *Regalis* is in the Hodsoni Zone.

The sample is dated Progracilis to Morrisi Zone.

Sample interval 806.17 – 805.80 m (2 samples): Late Bathonian, Hodsoni to Discus Zone

The assemblages are similar to below with abundant and diverse species of *Ctenidodinium*. In addition, there are the first occurrences of i.a. *Atopodinium prostatum, Pareodinia prolongata* and *Rigaudella filamentosa* (questionable). The species *Gongylodinium erymnoteichon* and *Valvaeodinium spinosum* last occur at the top of this interval.

The FADs of *Atopodinium prostatum, Pareodinia prolongata* and *Rigaudella filamentosa* are in the Hodsoni Zone. The LAD of *Valvaeodinium spinosum* is in the Discus Zone. The LAD of *Gongylodinium erymnoteichon* was previously considered to be in the Hodsoni Zone, but the species has recently been observed to occur up to the Discus Zone (Feist-Burkhardt, pers. obs. 2020).

The sample interval is dated Hodsoni to Discus Zone.

Sample 805.37 m (1 sample): Early Callovian, Herveyi Zone

The composition of the dinoflagellate cyst assemblage in this sample is different to below. Species of *Ctenidodinium* are less abundant. There are several first occurrences, i.a. *Lithodinia caytonensis, Sentusidinium rioultii* s.l., *Sentusidinium*? *varispinosum*, *Sirmiodinium grossii* and *Stephanelytron scarburghense* (mainly specimens with two small coronae). Last occurrences in this sample are *Atopodinium polygonale, Ctenidodinium combazii* and *Gonyaulacysta pectinigera*.

The FADs of *Lithodinia caytonensis, Sentusidinium*? *varispinosum*, *Sirmiodinium grossii* and *Stephanelytron scarburghense* are in the Herveyi Zone. The LADs of *Atopodinium polygonale, Ctenidodinium combazii* and *Gonyaulacysta pectinigera* are also in the Herveyi Zone.

The sample is dated Herveyi Zone.

Sample 805.13 m (1 sample): Middle Callovian, Jason Zone, to Late Callovian, Lamberti Zone

The composition of the dinoflagellate cyst assemblage in this sample is different to below. Chorate dinoflagellate cysts are abundant. There are numerous first and last occurrences. First occurrences in this sample include *Acanthaulax* spp., *Belodinium asaphum*, *Compositosphaeridium*

polonicum, Endoscrinium galeritum, Gonyaulacysta centriconnata (questionable), *Korystocysta pachyderma, Liesbergia scarburghensis, Rhynchodiniopsis cladophora, Rigaudella aemula, Scriniodinium crystallinum* and *Stephanelytron redcliffense*. Last occurrences in this sample are i.a. *Ctenidodinium continuum, Lithodinia caytonensis, Nannoceratopsis spiculata, Orobodinium automobile, Pareodinia prolongata, Rigaudella filamentosa, Sentusidinium*? *varispinosum* and *Valvaeodinium vermicylindratum*.

The FADs of some species are in the Jason Zone (*Compositosphaeridium polonicum* and *Stephanelytron redcliffense*), in the Coronatum Zone (*Rigaudella aemula*), in the Athleta Zone (*Scriniodinium crystallinum* and *Gonyaulacysta centriconnata*) and in the Lamberti Zone (*Belodinium asaphum, Endoscrinium galeritum* and *Liesbergia scarburghensis*). The LADs of some species are at the base of the Jason Zone (*Valvaeodinium vermicylindratum* and *Sentusidinium*? *varispinosum*), in the Jason Zone (*Nannoceratopsis spiculata*), in the Coronatum Zone (*Orobodinium automobile, Rigaudella filamentosa* and *Lithodinia caytonensis*) and in the Lamberti Zone (*Pareodinia prolongata*).

The occurrence of all these species in the one sample indicates a mixture of palynofloras of different age. The sample is dated Jason Zone to Lamberti Zone.

Sample 804.49 m (1 sample): Middle Oxfordian, Plicatilis-Tranversarium Zone to Late Oxfordian, Bifurcatus Zone

The composition of the dinoflagellate cyst assemblage in this sample is different to below. Chorate dinoflagellate cysts are abundant, as are *Rhynchodiniopsis cladophora* and *Sentusidinium rioultii.* There are numerous first occurrences, i.a. *Amphorula dodekovae, Dingodinium tuberosum, Glossodinium dimorphum, Leptodinium arcuatum, L. mirabile, Systematophora areolata* and *Tehamadinium* spp. Other important taxa present in this sample include *Compositosphaeridium polonicum, Ctenidodinium ornatum, Endoscrinium galeritum, Gonyaulacysta eisenackii,* a single specimen of *Korystocysta pachyderma, Liesbergia scarburghensis, Nannoceratopsis pellucida, Scriniodinium crystallinum* and *Sirmiodiniopsis orbis*.

There are species with FADs in the Plicatilis Zone (*Glossodinium dimorphum, Leptodinium arcuatum, L. mirabile, Systematophora areolata*) and in the Bifurcatus Zone (*Amphorula dodekovae, Dingodinium tuberosum*). The LADs of some species are considered to be in the Plicatilis Zone (*Korystocysta pachyderma, Scriniodinium crystallinum*) and in the Transversarium Zone (*Compositosphaeridium polonicum, Ctenidodinium ornatum, Endoscrinium galeritum, Gonyaulacysta eisenackii, Liesbergia scarburghensis, Nannoceratopsis pellucida* and *Sirmiodiniopsis orbis*).

The oldest age possible is the Plicatilis Zone. There are a few single specimens of *Korystocysta pachyderma* and *Scriniodinium crystallinum,* species that are considered to have their LADs in the Plicatilis Zone, but these are single specimens that may have been reworked. Most dinoflagellate cysts present have an LAD in the Tranversarium Zone (*Compositosphaeridium polonicum, Ctenidodinium ornatum, Endoscrinium galeritum, Gonyaulacysta eisenackii, Liesbergia scarburghensis, Nannoceratopsis pellucida* and *Sirmiodiniopsis orbis*). It is unusual that these species co-occur with several good specimens of unambiguous *Amphorula dodekovae* and *Dingodinium tuberosum,* as both species are considered to have an FAD in the Bifurcatus Zone.

The co-occurrence of these taxa is interpreted to correspond most likely to an age at the transition between the Transversarium Zone and Bifurcatus Zone.

Tab. 3-3: List of analysed palynology samples from BUL1-1

Depth [m]	**Age**	**Zone & Subzone**
804.49	Late – Middle Oxfordian	Bifurcatus Zone to Transversarium – Plicatilis Zone
805.13	Late – Middle Callovian	Lamberti – Jason Zone
805.37	Early Callovian	Herveyi Zone
805.80	Late Bathonian	Discus – Hodsoni Zone
806.17	Late Bathonian	Discus – Hodsoni Zone
807.09	Middle Bathonian	Morrisi – Progracilis Zone
809.21	Early Bathonian	Zigzag Zone (? Tenuiplicatus SZ)
810.58	Early Bathonian	Zigzag Zone
812.01	Late Bajocian	Parkinsoni – Garantiana Zone
812.05	Late + Early Bajocian	Niortense Z + Humphriesianum Z (Blagdeni SZ)
812.19	Late + Early Bajocian	Niortense Z + Humphriesianum Z (Blagdeni SZ)
813.27	dating impossible	dating impossible
818.03	Early Bajocian	Humphriesianum Zone
822.35	Early Bajocian	Humphriesianum Zone
827.38	Early Bajocian	Humphriesianum Z (Humphriesianum – Romani SZ)
832.36	Early Bajocian	Sauzei Zone
837.64	Early Bajocian	Sauzei Zone
842.62	Early Bajocian	Sauzei Zone
847.28	Early Bajocian	Sauzei Zone
850.27	Early Bajocian	Sauzei Zone
853.99	Early Bajocian	Sauzei Zone
854.98	Early Bajocian	Laeviuscula Zone
855.14	Early Bajocian	Laeviuscula Zone
855.47	Early Bajocian	Laeviuscula Zone
855.56	Early Bajocian	Laeviuscula Zone
856.09	Early Bajocian	Laeviuscula Zone
860.40	Early Bajocian	Laeviuscula Zone
865.49	Early Bajocian	Laeviuscula Zone
869.64	Early Bajocian	Laeviuscula Zone
869.81	Early Bajocian	Ovale Zone
874.97	Early Bajocian	Ovale Zone
880.02	Early Bajocian	Ovale Zone
883.24	Early Bajocian	Discites Zone
883.98	Early Bajocian	Discites Zone
884.42	Late Aalenian	Concavum Zone
884.80	Late Aalenian	Concavum Zone
885.59	Middle Aalenian	Bradfordensis Zone
886.96	Middle Aalenian	Bradfordensis Zone
891.15	Middle Aalenian	Bradfordensis Zone
891.63	Middle Aalenian	Bradfordensis Zone
891.70	Middle Aalenian	Bradfordensis – Murchisonae Zone
891.89	?Middle – Early Aalenian	?Murchisonae – Opalinum Z (? «Comptum» SZ)
897.41	?Middle – Early Aalenian	?Murchisonae – Opalinum Z (? «Comptum» SZ)
910.02	Early Aalenian	Opalinum Zone (Opalinum SZ)
930.34	Early Aalenian	Opalinum Zone (Opalinum SZ)
949.78	Early Aalenian	Opalinum Zone (Opalinum SZ)
969.94	Early Aalenian	Opalinum Zone (Opalinum SZ)
990.00	Early Aalenian	Opalinum Zone (Opalinum SZ)
995.55	Early Aalenian	Opalinum Zone (Opalinum SZ)
995.90	E. Aalenian – L. Toarcian	Opalinum Z (Opalinum SZ) – Aalensis Zone
996.31	E. Aalenian – L. Toarcian	Opalinum Z (Opalinum SZ) – Aalensis Zone

3.4 Chemostratigraphy

The sampling of the BUL1-1 and BUL1-1B cores focused primarily on the Lias Group (Figs. 3-2 and 3-3) and Dogger Group (Figs. 3-4 to 3-7) and, therefore inter alia on clay mineral-rich layers of the Opalinus Clay. Figures 3-8 and 3-9 illustrate the fully analysed interval from the topmost Klettgau Formation up to the Wildegg Formation (1'031.20 – 797.07 m). The data presented here (applies for all subsequent figures in this section) is shown in comparison to other data collected during the drilling campaign: simplified stratigraphic profile modified after Dossier III, Dry Clay values in wt.-% with vertical axis in m MD log depth (*cf.* Dossier X), XRD measurements (calcite: blue, dolomite/ankerite: green, siderite: red; *cf.* Dossier VIII) and C(org) measurements in blue (*cf.* Dossier VIII). In addition, formation boundaries were highlighted with black lines and other formal or informal subintervals with grey lines. For some of the data 5-point moving averages were plotted in grey in the background of the plottet data (represented by black points). Following stratigraphic abbreviations were used in Figs. 3-2 to 3-9: GBR = Grünschholz Member, Breitenmatt Member & Rickenbach Member; OPA = Opalinus Clay; «M.O.» and «Murch.-O.» = «Murchisonae-Oolith Formation»; «Hum.» = «Humphriesioolith Formation»; «P.W.» = «Parkinsoni-Württembergica-Schichten»; V. = Variansmergel Formation; W. = Wutach Formation.

The data will be discussed in three intervals: Lias Group, the lower part of the Dogger Group – mainly Opalinus Clay and the upper part of the Dogger Group. Not all data are discussed to the same extent as for example the $\delta^{18}O_{carb}$ & $\delta^{15}N_{org}$ data. The oxygen isotopes are strongly influenced by diagenesis. The nitrogen isotopes may not be as meaningful in some cases, because the combined $\delta^{13}C_{org}$ and $\delta^{15}N_{org}$ measurements showed a too low concentration of N in most of the measurements.

In addition to the continuous samples (roughly in metre resolution), some specific samples were taken (Appendix E1) to complete the information about the calcareous beds. Some of the hardground samples were drilled directly from the remaining thin section blocks to correlate the bulk geochemical data with the microfacies analysis. All these data are distinguished in different colours on the following Fig. 3-4 (calcareous samples in blue, septarian nodules in violet and macrofossils in green), but may not shown on the individual plots because of the data ranges (see Appendix E1 for data).

In contrast to the carbonate measurements, the organic measurements were not always measured in metre resolution, depending on the variability of the expected isotope data. If no major isotope changes occur over a longer succession, as is to be expected in the middle section of Opalinus Clay, only every second sample was analysed. However, this procedure also depends on the carbonate content. At a high carbonate content – as for example in the «Herrenwis Unit» – there was simply too little organic material in the drilled sample for a continuous measurement.

Lias Group

Starting from the bottom up (Fig. 3-2), the oldest sediments measured belong to the Late Triassic (Norian and/or Rhätian?), in analogy to the Weiach borehole (Looser et al. 2018). The measurements between 1'031.20 m and 1'030.60 m (three samples) represent the uppermost part of the Gruhalde Member from the Klettgau Formation. The three samples show semi-quantitative carbonate content (TCarb) values between 40 and 60 wt.-%. The $\delta^{13}C_{carb}$ (-4.1 ‰) and the $\delta^{13}C_{org}$ values (ca. -26.7 ‰) are very stable. The C/N ratio is quite low with values around 7.

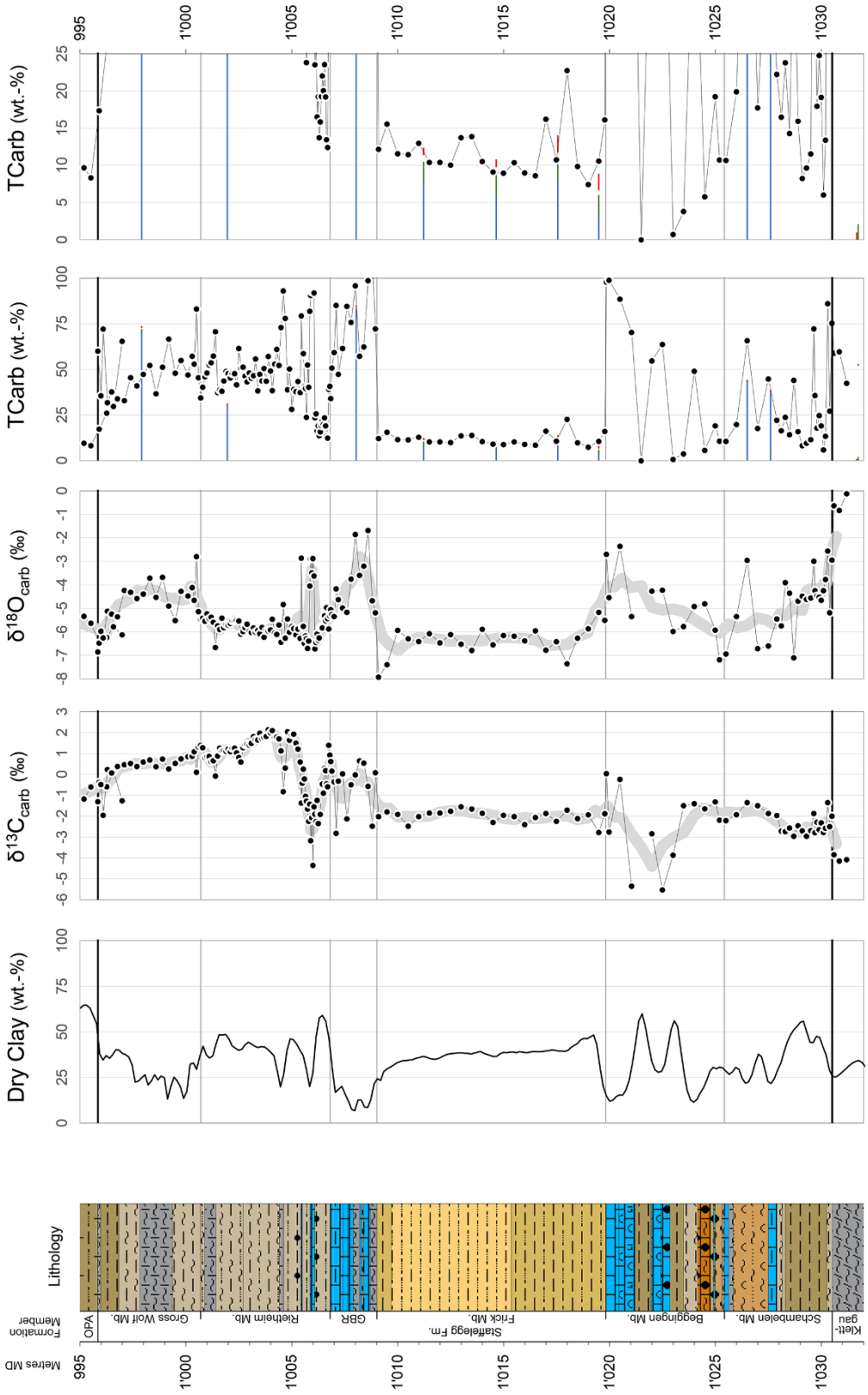

Fig. 3-2: Bulk rock (carbonate) isotopic data from the Lias Group (995.00 – 1'032.00 m)

Additional explanations and references see text at the beginning of Section 3.4.

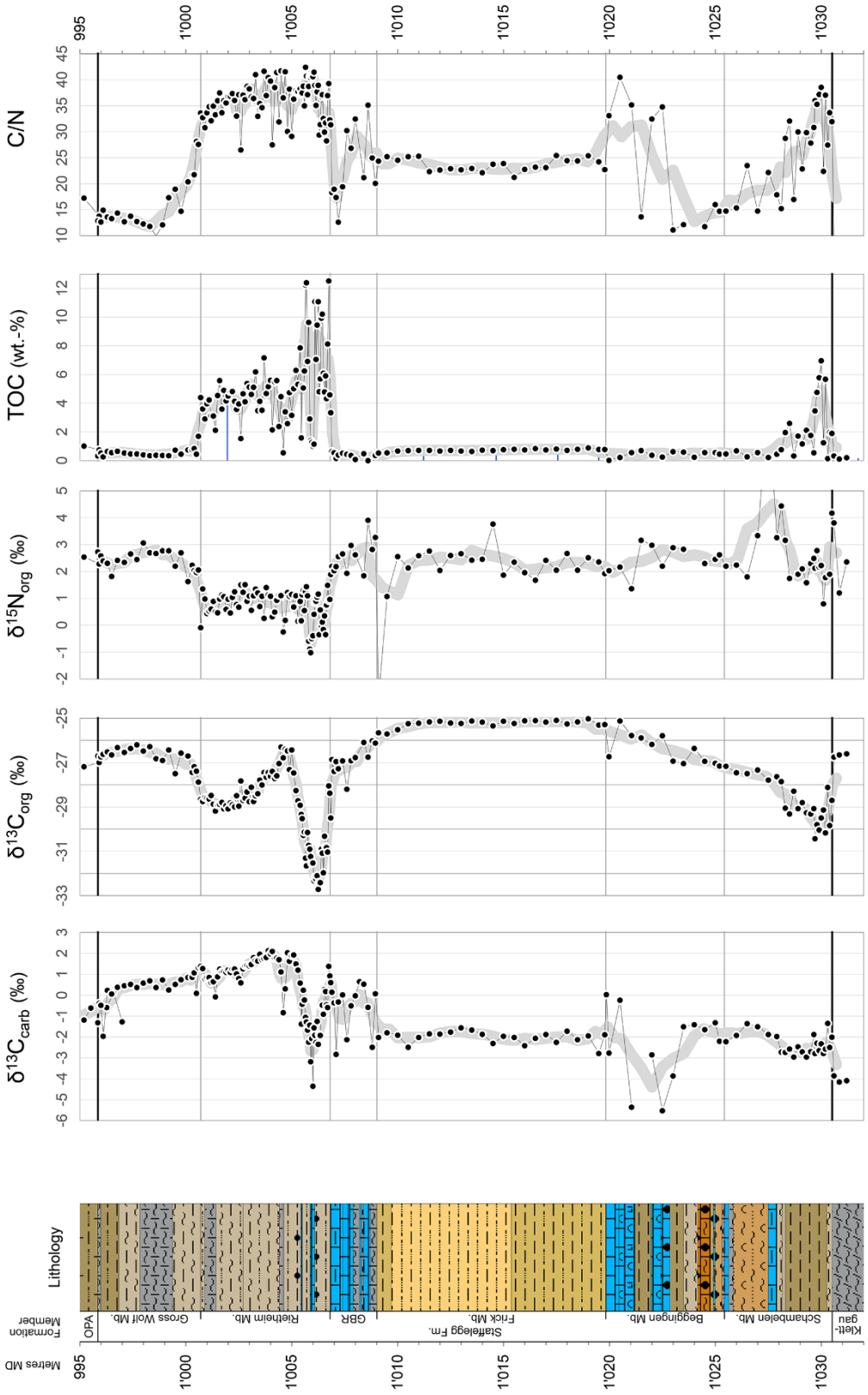

Fig. 3-3: Organic isotopic data from the Lias Group (995.00 – 1'032.00 m)

Additional explanations and references see text at the beginning of Section 3.4.

For the lowermost sediments of the Staffelegg Formation, quite different geochemical data were analysed. The semi-quantitative carbonate content decreases to lower values between 10 and 20 wt.-%. The variations in the results from the overlying members reflect the variations between claystones and argillaceous to calcareous marls as well as to limestone beds. The individual members are well represented by carbonate data with lower contents (~ 10 – 20 wt.-%) in the Schambelen and Frick Members and higher contents (≥ 40 wt.-%) in the Beggingen, Breitenmatt, Grünschholz, Rickenbach, Rietheim and Gross Wolf Members. The latter two Members also show a larger variation in their individual measurements, which can be explained by the higher sampling resolution (some intervals in the Rietheim Member with 5 cm spacing during the negative carbon isotope event, see discussion in next paragraphs) as well as by the nodular calcareous lithology (Gross Wolf Member). Although the calculated carbonate content is only a semi-quantitative method, the values presented here correspond well to the XRD values measured at the University of Bern (*cf.* Dossier VIII). The XRD data are illustrated in the following Fig. 3-2 to provide a visual comparison between the new data presented here and those from the Dossier VIII. As discussed in Wohlwend et al. (2019b) based on measurements from the BDB-1 borehole at the Mont Terri Rock Laboratory, the values calculated here follow the calcite wt.-% with an additional mixed signal from the other carbonates since, during the reaction time of 60 min at 72 °C, a complete reaction does not take place for all carbonates.

The $\delta^{13}C_{carb}$ values in the Schambelen Member fall into two individual sections. The lower one at the base to around 1'028.00 m shows values between -3.0 ‰ and -2.5 ‰. The values in the upper section stay quite stable (-2.2 ‰ to -1.3 ‰) up to the lower part of the Beggingen Member. The upper Beggingen Member (~ 1'023.00 – 1'019.82 m) with a limestone (partly iron-oolitic) and claystone alternation, shows mainly lower values in comparison to the lower part. The Frick Member is represented by very stable $\delta^{13}C_{carb}$ values around -2.0 ‰. Major $\delta^{13}C_{carb}$ isotope variations (positive and negative shifts) were measured in the overlying condensed interval (Grünschholz, Breitenmatt and Rickenbach Members) and the hanging Rietheim Member. The latter comprises one of the major Mesozoic negative carbon-isotope excursions (CIE) to -4.4 ‰ (the Toarcian-Oceanic Anoxic Event: T-OAE) followed by a rapid increase to positive values around 2.0 ‰. The values normalise thereafter to the top of the Gross Wolf Member and decrease to around -0.5 ‰.

The $\delta^{13}C_{org}$ values (Fig. 3-3) show similar variations to the inorganic ones; however, the amplitudes are much larger. The $\delta^{13}C_{org}$ values show two negative excursions. The lower one at the lowermost metre of the Schambelen Member (-30.4 ‰) can be correlated to the top-Planorbis CIE; see also Looser et al. (2018) for more detailed information about the Triassic-Jurassic boundary records in Northern Switzerland. After the negative excursion in the lowermost Schambelen Member, the organic carbon isotopes clearly show an increasing trend up to the top of the Beggingen Member and stabilise throughout the Frick Member by around -25.5 ‰. In contrast to the inorganic carbon isotope values, the organic values already start with a decreasing trend in the uppermost Frick Member at 1'010.00 m up to the top of the Rickenbach Member, followed by a major negative CIE in the sediments from the lower Rietheim Member, which – as already mentioned above – can be correlated with the T-OAE. The most negative values with -32.7 ‰ (at 1'006.25 m) can be found in the 0.73 m-thick, very bituminous interval below the «Unterer Stein» (1'006.08 – 1'005.86 m). The other hanging, informal marker horizons *sensu* Kuhn & Etter (1994) («Homogene Kalkbänke»: 1'005.50 – 1'005.43 m and «Oberer Stein»: 1'004.62 – 1'004.42 m) lie on the upper increasing trend and are followed by a smaller negative trend in the upper Rietheim Member up to the uppermost calcareous marl bed (?«Monotisbank» around 1'001.40 m; *sensu* Kuhn & Etter 1994). The overlying sediment interval (1'001.20 – 1'000.70 m) comprises slightly higher $\delta^{13}C_{org}$ values before a clear jump in the isotope values can be seen at the lithological

boundary to the overlying Gross Wolf Member. The values increase to around -26.5 ‰ in the middle part of the Gross Wolf Member before they shift to slightly lower values at the top Staffelegg Formation.

Together with the negative CIE of the T-OAE, very high semi-quantitative organic carbon content (TOC) values also occur with values close to 12 wt.-%. The very bituminous interval from the base of the Rietheim Member up to the «Homogene Kalkbänke» (1'005.50 – 1'005.43 m) has an average TOC content of around 6 – 8 wt.-%, which is slightly higher than the content in the upper part (1'005.43 – 1'000.70 m) with values around 4 – 5 wt.-%. Although the calculated TOC is only a semi-quantitative method, the values presented here correspond well with the C(org) values measured at the University of Bern (*cf.* Dossier VIII). As mentioned before, the new data demonstrate the trend, which, in lower resolution, can also be seen in the C(org) measurements, even though there is small offset to slightly higher values calculated there. The underestimation of the carbonate content (see above and/or Wohlwend et al. 2019b) partly explains the overestimation during the calculation of the TOC from the carbonate free organic content (TOC_{decarb}) (see Chapter 2 methods for the calculations).

The C/N ratios from the uppermost Klettgau Formation, with values around 7 (not shown on Fig. 3-3), can be separated from the overlying Schambelen Member with the highest values around 35 – 40 in the lowermost metres (parallel to the negative $\delta^{13}C_{org}$ values). The upper Schambelen to lower Beggingen Members show a clear trend to lower C/N ratios with the lowest values (~ 11 at 1'023.00 m) in the lower Beggingen Member. The upper Beggingen Member shows higher values with a clear shift at the lithological boundary to the hanging Frick Member with ratios around 22. The highest ratios were measured in the Rietheim Member (35 – 40 with few values up to 43). The overlying Gross Wolf Member shows a decreasing trend to ratios around 10 – 12 in the lower part (at 998.60 m) followed by a slight increase up to the top of the Staffelegg Formation.

Lower part of the Dogger Group – mainly Opalinus Clay

The interval described in the following section – the lower part of the Dogger Group (the Opalinus Clay, «Murchisonae-Oolith Formation» and the lower part of the Wedelsandstein Formation) – is also the interval at the main focus of these investigations (Figs. 3-4 and 3-5).

The semi-quantitative carbonate content (TCarb) values from the more homogeneous clay mineral-dominated lithologies compared to those from the underlying Staffelegg Formation (Fig. 3-4) are rather low and very stable with values around 5 – 15 wt.-% in the lower succession of the Opalinus Clay («Clay-rich sub-unit», «Mixed clay-silt-carbonate sub-unit» and «Upper silty sub-unit»; *cf.* Dossier III). Only the uppermost informal sub-unit («Sub-unit with silty calcareous beds») shows a clear trend to very low values between two calcareous beds from 912.55 m to 904.48 m; *cf.* Dossier III) followed by an increasing trend to values reaching almost 24 wt.-% at 899.63 m. The carbonate content decreases upwards to contents around 5 – 10 wt.-% at the top of the Opalinus Clay. The decreasing trend continues in the overlying «Murchisonae-Oolith Formation» and reaches the lowest carbonate contents of around 2 wt.-% at 886.40 m. The upper part of the «Murchisonae-Oolith Formation» shows an increase in the carbonate content up to the top of the informal formation with iron-oolitic limestone beds. The hanging Wedelsandstein Formation can be divided into two parts showing an increase twice in the carbonate contents with the highest values, reaching almost 70 wt.-% below a hardground (869.70 – 869.76 m). The overlying silty claystone again comprises very low contents below 10 wt.-% at the beginning which then increase up to values close to 24 wt.-%.

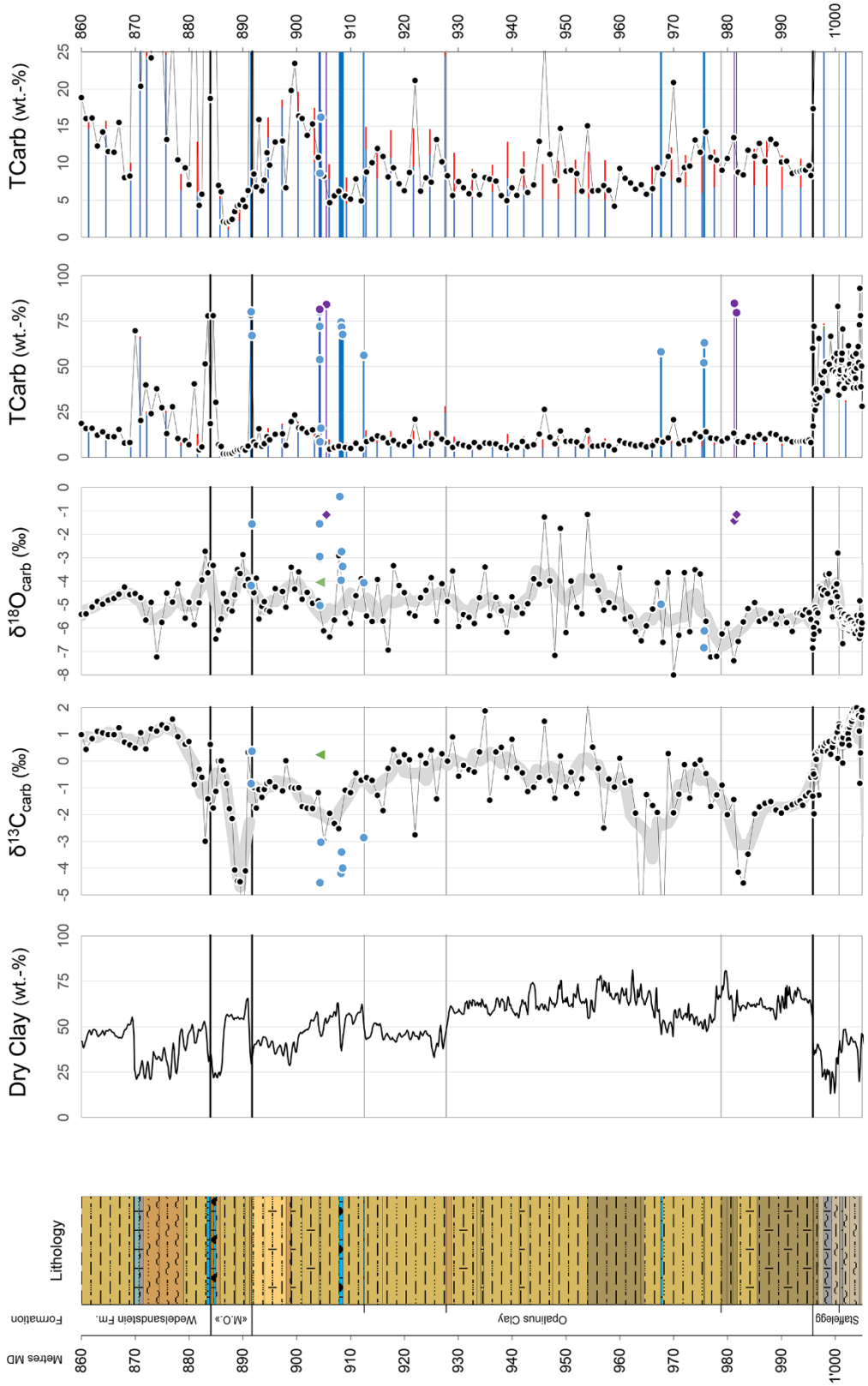

Fig. 3-4: Bulk rock (carbonate) isotopic data from the lower Dogger Group – mainly Opalinus Clay (860.00 – 1'005.00 m)

Additional explanations and references see text at the beginning of Section 3.4.

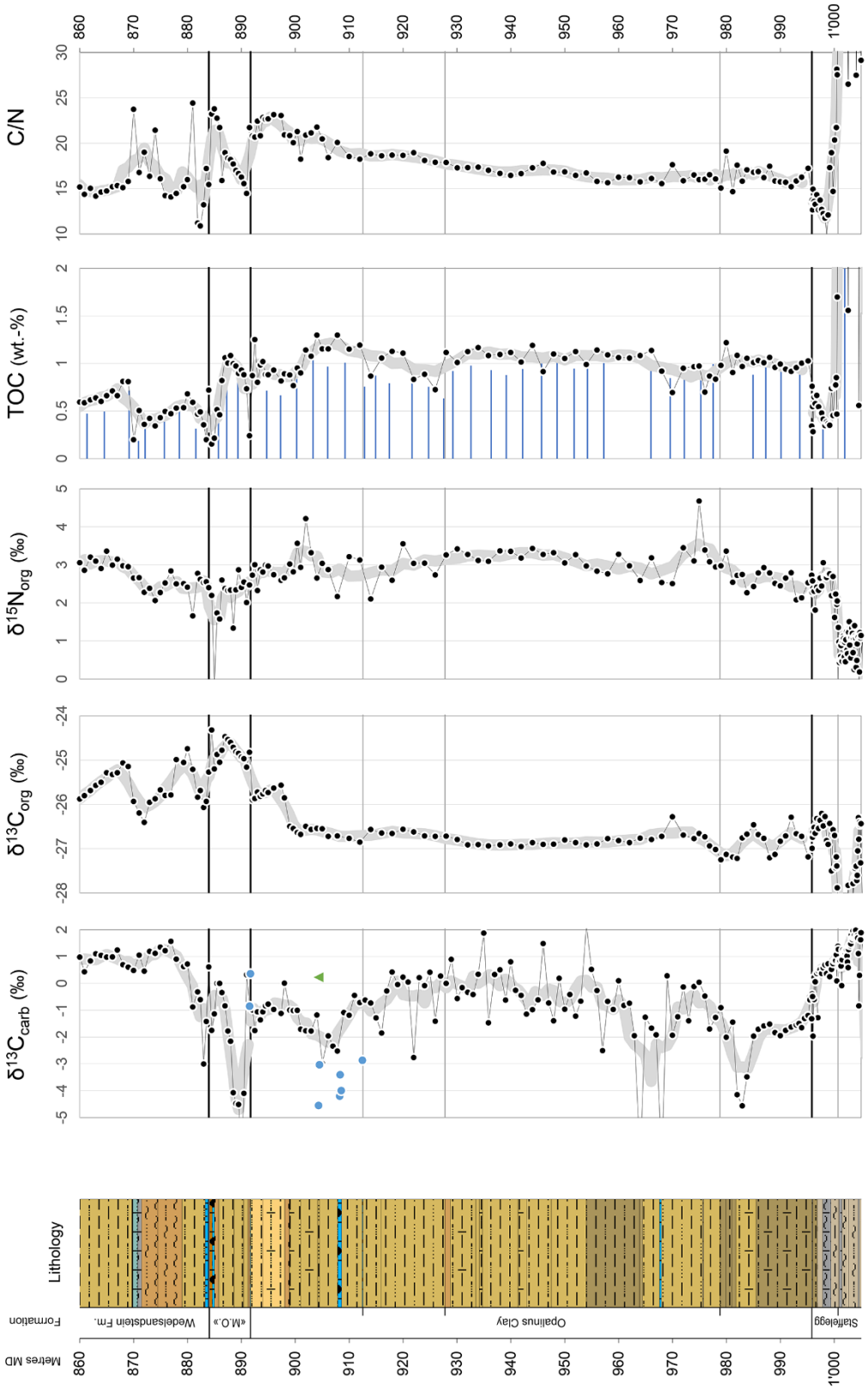

Fig. 3-5: Organic isotopic data from the lower Dogger Group – mainly Opalinus Clay (860.00 – 1'005.00 m)

Additional explanations and references see text at the beginning of Section 3.4.

The above-mentioned Opalinus Clay interval comprises several calcareous beds (see Appendix E1 for data). They are illustrated in Fig. 3-4 by thicker blue lines ending with blue dots marking the TCarb values. Two of these calcareous beds can be found in the lower part of the «Mixed clay-silt-carbonate sub-unit» (975.70 – 975.60 m, 967.93 – 967.58 m). The other three calcareous beds are located in the uppermost «Sub-unit with silty calcareous beds» (912.55 – 912.45 m, 908.60 – 907.90 m, 904.48 – 904.18 m). Most of them comprise semi-quantitative carbonate contents that are typical for calcareous marls. The values from the uppermost interval (904.48 – 904.18 m) include also measurments from calcareous intraclasts, which could be designated as limestones. Two intervals of the Opalinus Clay with septarian nodules were analysed, the lower one at 981.67 – 981.26 m and the upper one at 905.50 m. The data are illustrated with violet diamonds and lines in Fig. 3-4. Both horizons seem to be correlatable to the Weiach-1 borehole. In addition, one belemnite was measured at 904.28 m; the data are illustrated in the figure with a green triangle (data Appendix E1).

The $\delta^{13}C_{carb}$ data show two, possibly three, negative excursions: a lower one in the lowermost «Clay-rich sub-unit» and an upper one in the uppermost «Sub-unit with silty calcareous beds». The succession in between shows a trend towards more positive values, with a smaller third negative interval between 970 and 962 m. Noticeable are the two "major" negative excursions, both of which were represented by clearly decreasing and increasing trends. The lower negative excursion reaches the most negative values (-4.5 ‰ at 982.95 m) just below the lower calcareous septarian nodules mentioned above at 981.67 m. The upper negative excursion starts within the three upper calcareous beds and reaches the lowest values (-3 ‰ at 904.47 m) between the central and upper hardground, where the septarian nodule with calcite-filled shrinkage cracks could be found at 905.50 m. The calcareous nodules and the calcareous intraclasts are possibly an early diagenetic product (see also Wetzel & Allia 2000). The nodules are probably the only macroscopic features with very negative $\delta^{13}C_{carb}$ values (-30 ‰, Appendix E1). Very fine authigenic calcite was probably also precipitated in the very fine porosity of the Opalinus Clay, which led to the more negative $\delta^{13}C_{carb}$ values (see also Wohlwend et al. 2016.). Also remarkable is the scatter of the individual measurements (metre resolution). There are intervals in the «Clay-rich sub-unit» and «Sub-unit with silty calcareous beds» with a very small scatter (~ 0.5 ‰) and other intervals with a scatter up to 2 – 3 ‰ («Mixed clay-silt-carbonate sub-unit» and «Upper silty sub-unit»). The interval with the higher scatter comprises several silt lenses, some of them up to one decimetre thick, some of them very thin. It was therefore not always possible to sample only the clay mineral-rich sediments. The scatter can be explained by varying amounts of silt, which probably comprises very thin calcite fillings in the primary porosity of these lenses.

The $\delta^{13}C_{carb}$ data from the «Murchisonae-Oolith Formation» show an analogy to the above-mentioned carbonate content. The lower, very clay mineral-rich interval is also visible in the carbon isotope values with strongly diagenetic overprinted values (up to -6.4 ‰ at 890.02 m). The upper, more calcareous part and the overlying lower part of the Wedelsandstein Formation comprise $\delta^{13}C_{carb}$ values showing a trend towards more positive values around 0.5 – 1.0 ‰.

The $\delta^{13}C_{org}$ data (Fig. 3-5) show a different picture compared to the $\delta^{13}C_{carb}$ values. The curve is relatively stable in the central part («Mixed clay-silt-carbonate sub-unit» and «Upper silty sub-unit»). The organic carbon isotopes indicate variations only at the base of the Opalinus Clay («Clay-rich sub-unit») and at the top (uppermost part of the «Sub-unit with silty calcareous beds»). At the base, three individual negative trends or peaks can be recognised (995.19 m: -27.2 ‰; 988.02 m: -27.2 ‰; 978.98 m: -27.3 ‰). In the «Mixed clay-silt-carbonate sub-unit», there is an overall trend towards +0.5 ‰ heavier values in the lowermost 15 metres, followed by the same amount to lower values in the upper part. The «Upper silty sub-unit» again shows slightly heavier values (+0.5 ‰). In the uppermost part of the Opalinus Clay and at the lithological boundary to the overlying «Murchisonae-Oolith Formation», two significant shifts

can be recognised in the $\delta^{13}C_{org}$ data: the lower one, with a positive shift of almost +1 ‰ to average values of ca. -25.8 ‰, occurred between the two samples 899.00 m and 898.00 m; the upper one, with another +1 ‰ positive shift to average values of > -25.0 ‰, occurred between the two samples 892.05 m and 891.53 m.

The C/N ratio show an increase from a stable interval in the lower part (~ 17) to a ratio of around 23 at the top of the Opalinus Clay. The «Murchisonae-Oolith Formation» once more shows the same increasing trend with almost the same numbers.

Upper part of the Dogger Group

The interval described in the following section – the upper part of the Dogger Group («Murchisonae-Oolith Formation», Wedelsandstein Formation, «Humphriesioolith Formation», «Herrenwis Unit», «Parkinsoni-Württembergica-Schichten», Variansmergel Formation, Wutach Formation and Wildegg Formation) – covers in terms of time the entire Middle Aalenian, Bajocian, Bathonian, Callovian and Middle Oxfordian stages (Figs. 3-6 and 3-7). The «Murchisonae-Oolith Formation» and the lower part of the Wedelsandstein Formation were already described in the previous part as part of the upper confining unit of the Opalinus Clay.

The semi-quantitative carbonate content (Fig. 3-6) represents the alternation of silty claystones, calcareous marls and limestones. However, the TCarb contents are underestimated because of the sampling strategy of not sampling every limestone bed (focus on the clay mineral-rich sediments, exception for carbonate-rich sequences like the «Herrenwis Unit»). Nevertheless, the carbonate content curve reflects the inverse wet clay content curve (*cf.* Dossier X). As mentioned above, the Wedelsandstein Formation can be divided into two parts showing two increasing trends separated by the hardground at 869.76 – 869.70 m. The overlying 41.91 m thick «Herrenwis Unit» is very prominent, and the data presented here confirm the lithostratigraphic description of the three more marly intervals of Dossier III.

Although the $\delta^{18}O_{carb}$ data were not discussed until now (too vulnerable to diagenetic overprint), the oxygen isotopes show an interesting feature in the lower «Herrenwis Unit». The lower part (853.94 – 844.00 m) comprises a prominent decreasing trend from the base of the unit to the argillaceous marl interlayer (844.50 – 843.40 m). The overlying coralligenous limestone seems to be much less affected by diagenesis and shows much more positive $\delta^{18}O_{carb}$ values.

The $\delta^{13}C_{carb}$ data indicate an increasing trend in the Wedelsandstein Formation (as already mentioned above), which can be followed upwards to the top of the «Herrenwis Unit», with the most positive values just at the top (+3.2 ‰ at 813.00 m). The same trend was documented in the time-equivalent succession from the Passwang Formation and Hauptrogenstein at Mont Terri (Wohlwend et al. 2019b), even though the shift to lower values in the overlying «Parkinsoni-Württembergica-Schichten» is not documented there (no core). The $\delta^{13}C_{carb}$ values are almost 2 ‰ lower and stay very stable until the upper part of the Wutach Formation. The sample taken 0.10 m below the top of the Wutach Formation (+1.6 ‰ at 805.35 m) shows a slightly more positive value, which later becomes much more obvious in the hanging Birmenstorf Member of the Wildegg Formation. The several per mille positive shift to values around +3.7 ‰ at 803.00 m is typical for the Callovian/Oxfordian boundary and was already documented by Rais et al. (2007) in other locations and in the Weiach borehole. The most positive $\delta^{13}C_{carb}$ values were documented in the Middle Oxfordian (Transversarium Zone; see Rais et al. 2007).

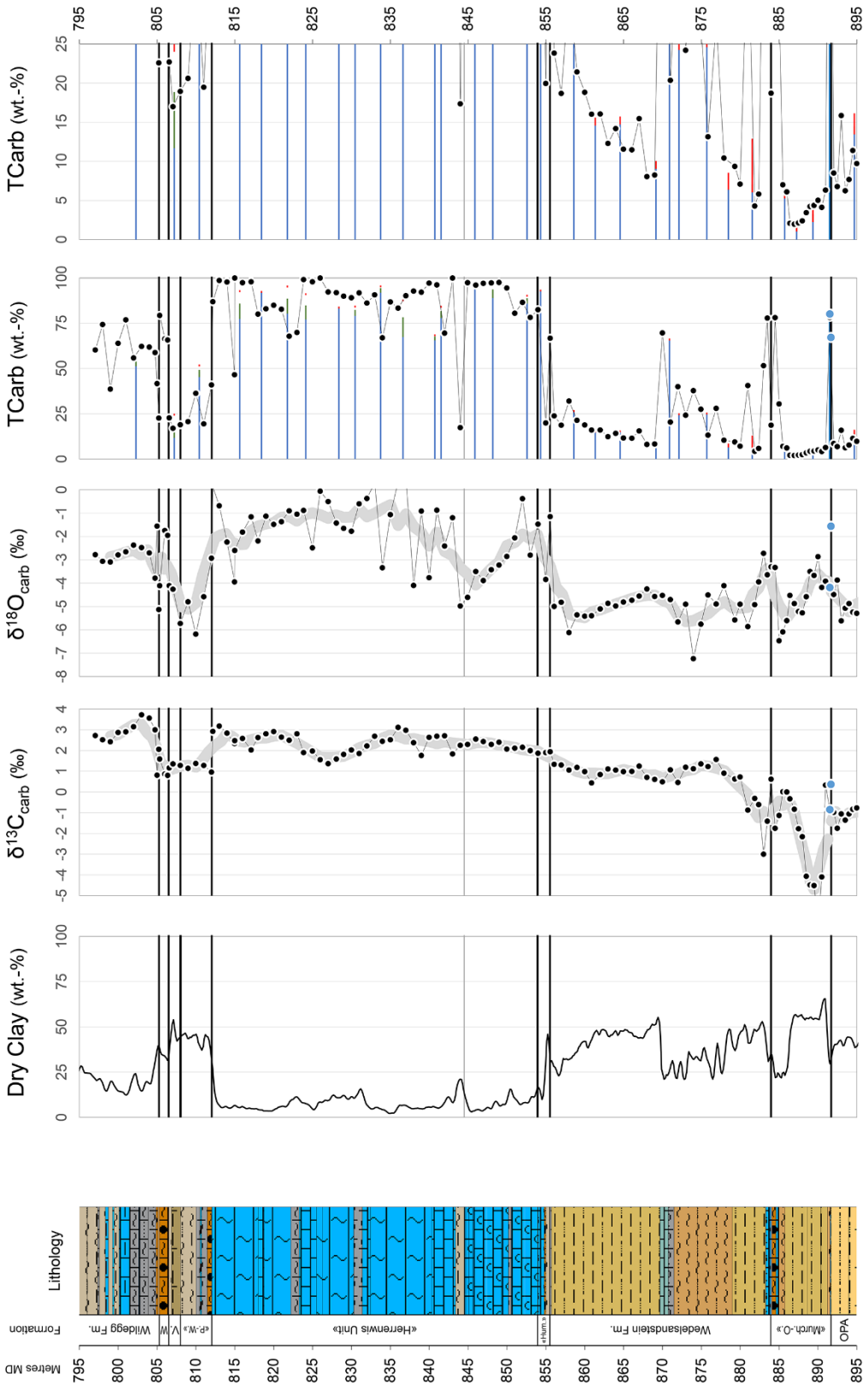

Fig. 3-6: Bulk rock (carbonate) isotopic data from the upper part of the Dogger Group (795.00 – 895.00 m)

Additional explanations and references see text at the beginning of Section 3.4.

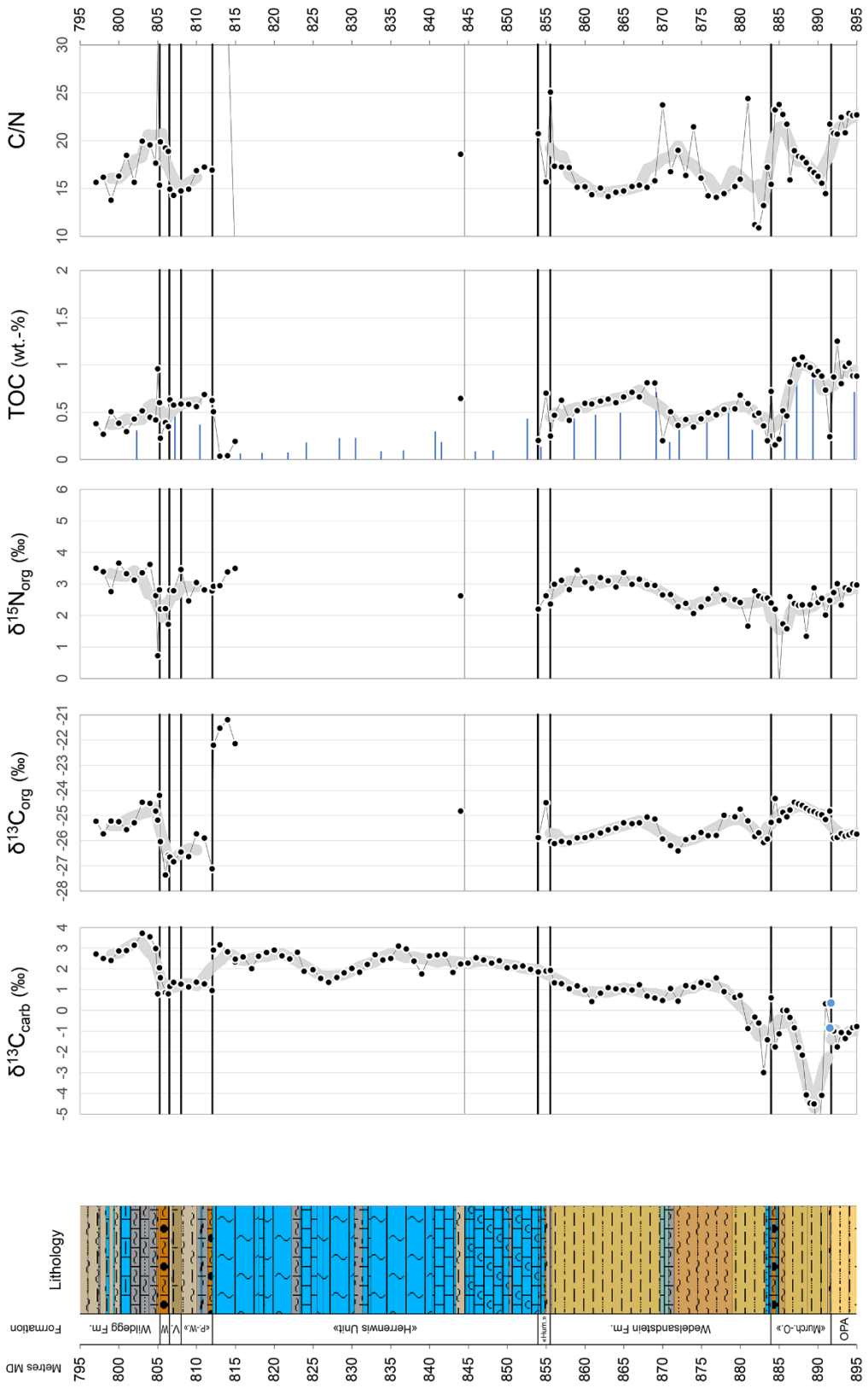

Fig. 3-7: Organic isotopic data from the upper part of the Dogger Group (795.00 – 895.00 m)
Additional explanations and references see text at the beginning of Section 3.4.

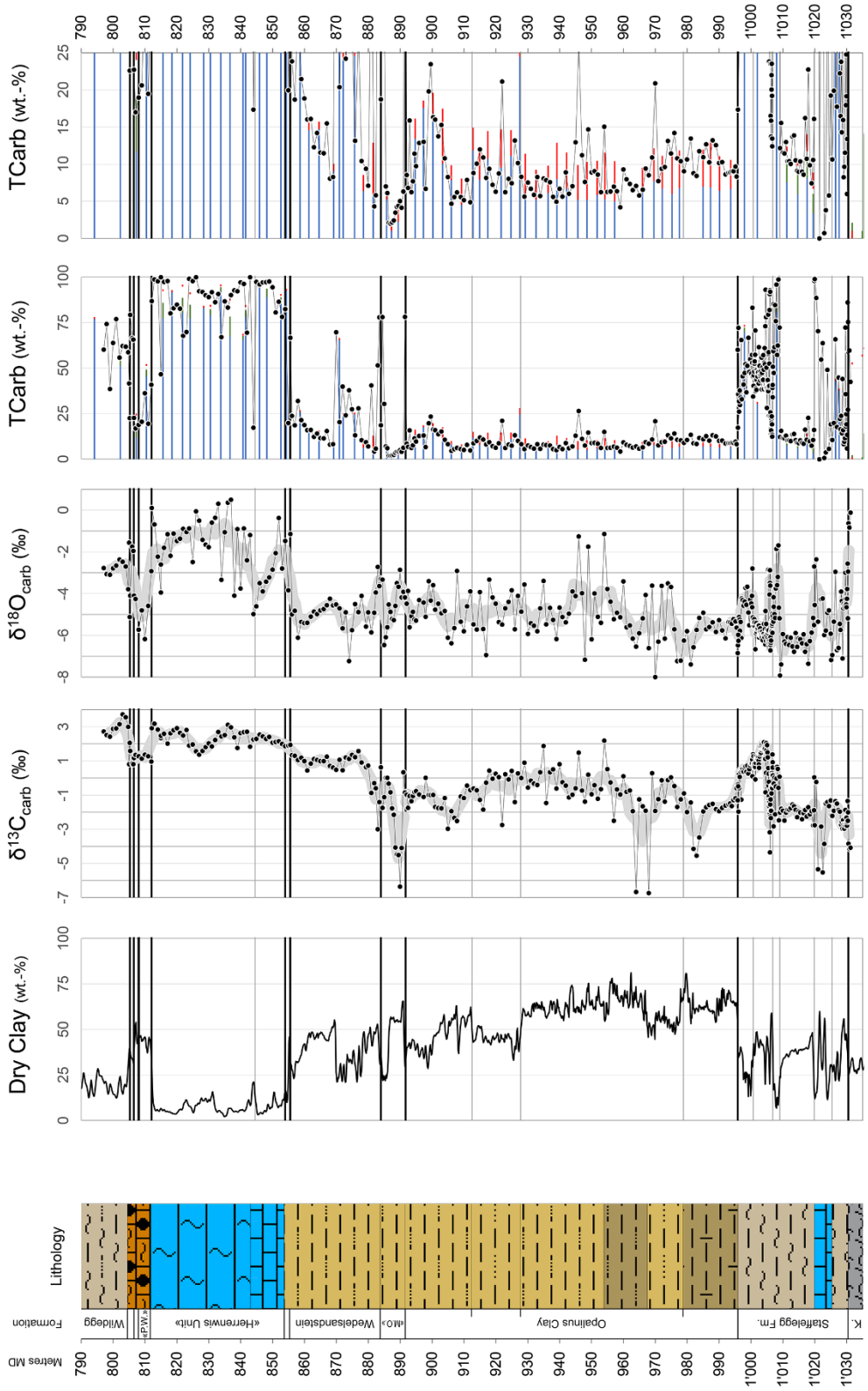

Fig. 3-8: Whole bulk rock (carbonate) isotopic data from BUL1-1 (797.07 – 997.00 m) and BUL1-1B (995.85 – 1'031.20 m)

Additional explanations and references see text at the beginning of Section 3.4.

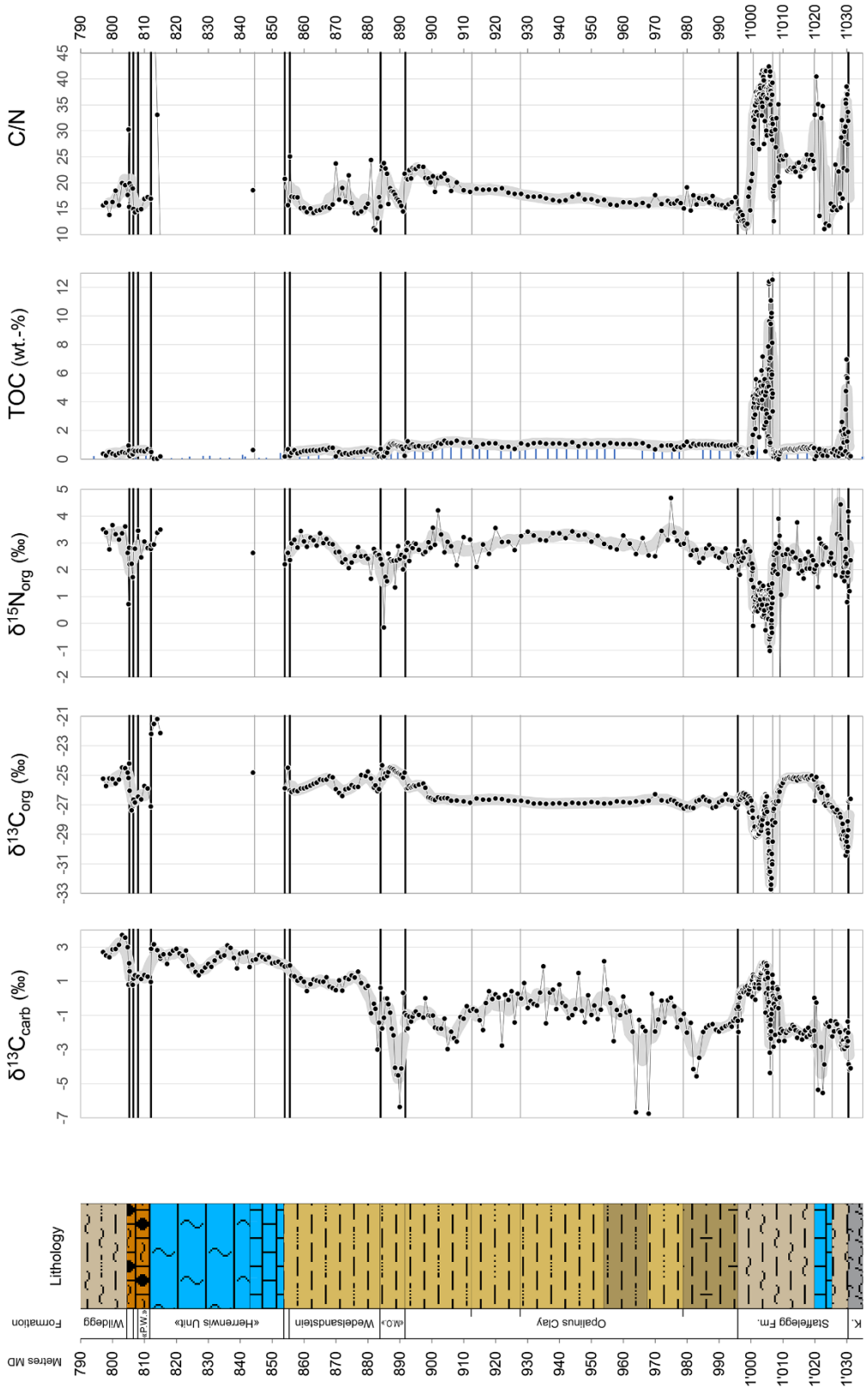

Fig. 3-9: Whole organic isotopic data from BUL1-1 (797.07 – 997.00 m) and BUL1-1B (995.85 – 1'031.20 m)

Additional explanations and references see text at the beginning of Section 3.4.

The $\delta^{13}C_{org}$ data (Fig. 3-7) from the «Murchisonae-Oolith Formation» show an increasing trend from around -25.0 ‰ at the base of the formation to -24.5 ‰ at 886.98 m, followed by a decreasing trend into the lowermost part of the Wedelsandstein Formation to values around -26.0 ‰. The trend is interrupted by a single more positive measurement at 884.50 m with a $\delta^{13}C_{org}$ value of -24.3 ‰. The $\delta^{13}C_{org}$ data from the Wedelsandstein Formation comprises a subdivision into two intervals. The lower decreasing trend includes the section from around 880.00 m up to 870.00 m and an upper decreasing trend reaches from 869.00 m up to the top of the formation at 855.53 m. The hardground at 869.76 – 869.70 m, as already mentioned in connection with the carbonate content, divides the formation. The $\delta^{13}C_{org}$ data from the overlying formations document the two shifts along with the inorganic ones, from the «Herrenwis Unit» (incomplete because there was not enough material for organic measurements from the limestones) to the overlying «Parkinsoni-Württembergica-Schichten» and from the Wutach Formation to the Wildegg Formation. However, the amplitude of the negative shift at the top «Herrenwis Unit» is much larger (-6 ‰). The four measurements from the uppermost limestones (814.98 – 812.17 m) show very positive values that have not been documented until now. However, the 1 g drilled sampling material from the limestone interval does not provide enough decarbonised material to reproduce the analyses. The higher $\delta^{13}C_{org}$ values could also be explained by a different mixing signal from terrestrial to marine organic material. The incomplete chemostratigraphic analyses from the «Herrenwis Unit» do not allow further interpretation.

The C/N ratio varies throughout the upper part of the Dogger Group with one increasing trend in the «Murchisonae-Oolith Formation», slightly varying ratios in the Wedelsandstein Formation (around 15 – 19) and a similar increase from the Dogger Group into the Malm Group.

4 Correlation of BUL1-1 and BUL1-1B

This short chapter was included to visualise (Fig. 4-1) the sampling locations (ammonites, palynological samples and thin sections) from the BUL1-1 borehole compared to the overlapping sidetrack BUL1-1B. The Lias Group was cored twice, but most of the samples were taken from the first borehole (BUL1-1), including those taken directly at the drill site (such as rock and porewater, geomechanics, mineralogy etc.; Tab. 1-2). The stratigraphic depths (core depths) are not identical, however the lateral distances are not large (within a few metres).

The core depths for the BUL1-1 core are indicated in Fig. 4-1. The variations in depth are larger in the upper part of the Staffelegg Formation (Gross Wolf Member and the upper parts of the Rietheim Member). The upper section of BUL1-1 from 995.00 m to 1'003.89 m shows an up-hole depth shift of 35 ± 5 cm when using the lithological boundaries from the BUL1-1B sidetrack as reference. Between 1'003.89 m and 1'006.00 m, the BUL1-1 core was lost due to technical problems. The top of the subsequent core retrieval was artificially set at 1'006.00 m. The lower section of BUL1-1 from 1'006.00 m to 1'040.26 m shows an up-hole depth shift of 10 ± 5 cm using the BUL1-1B sidetrack as a reference (*cf.* Dossier III). This correlation allows the ammonites, palynological samples and thin sections from BUL1-1 to be transferred to the lithologies from the BUL1-1B sidetrack (the same applies for all other samples taken from BUL1-1).

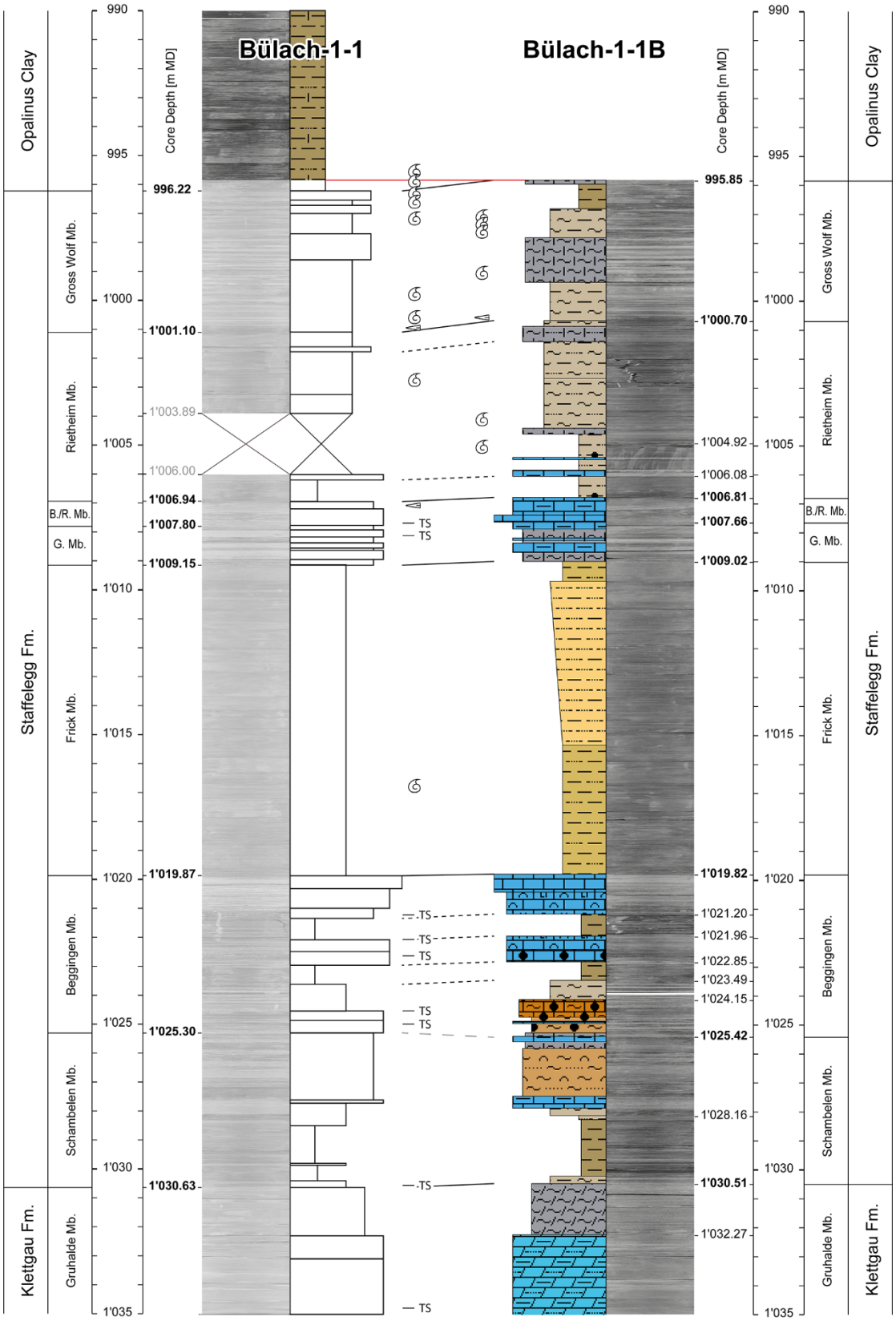

Fig. 4-1: Correlation of the double-cored interval of the Staffelegg Formation (BUL1-1 / BUL1-1B)

5 Definition of specific lithostratigraphic boundaries

The boundaries between stratigraphic units, as also shown in the stratigraphic logs of the lithostratigraphy report (Dossier III), were mostly defined based on lithological criteria. According to the guidelines on the stratigraphic nomenclature by Remane et al. (2005), the definetion of lithostratigraphic units should be based, both vertically and horizontally, on lithological variations regardless of their age. In fact, the formation boundaries, as used by Nagra for the ongoing borehole campaign of Stage 3 of the Sectoral Plan for Deep Geological Repositories (Jordan & Deplazes 2019), were not always obvious in the borehole and definitions were difficult to apply, either because of the small core diameter or because of differences in facies. The exact location of some of the formation boundaries caused discussions during core description and the process of quality control. Most of the important data for questionable boundaries were already present before the data-freeze (31.01.2020) and were used for the log descriptions and drawings. In the following paragraphs, the underlying considerations are explained to provide a better understanding of how boundaries were demarcated. We are aware of the fact that several boundaries are no longer based on lithological criteria alone and that chronostratigraphic criteria (ammonite, palyno- and chemostratigaphy) are included in the definitions.

Opalinus Clay (995.85 – 891.70 m)

In the BUL1-1B core, the lower boundary of the Opalinus Clay is set at 995.85 m at the top of a thin calcareous marl layer. This depth (995.85 m) also reflects the depth where the description of the cores shifts from BUL1-1 to the sidetrack BUL1-1B (*cf.* Dossier III). In the BUL1-1 core section, the lower boundary of the Opalinus Clay facies was defined somewhat lower, at 996.22 m. The offset was already discussed in the previous chapter and is illustrated in Fig. 4-1. Therefore, the lowermost ammonite (995.88 m) and the palynological sample (995.90 m) from BUL1-1 still belong to the Opalinus Clay, even though the core depths would indicate an attribution to the Gross Wolf Member of the Staffelegg Formation. The ammonite taken 34 cm above the lithological boundary belongs to the early Opalinum Subzone of the Opalinum Zone.

The upper boundary of the Opalinus Clay is set at 891.70 m at the erosional and bored base of a fossiliferous, limonitic, iron-oolitic hardground from 891.70 m to 891.60 m. Placing the boundary at this level was not based on lithological reasons alone. Above this hardground there are other very clay mineral-rich levels (891.25 – 885.80 m) and limestone (iron-oolitic) beds (885.02 – 884.10 m). The upper lithological boundary could have been placed at the iron-oolitic bed at 855.53 – 855.49 m or at the lower iron-oolitic bed at 885.02 – 884.63 m. However, the presence of iron-ooids is not the only evidence for the upper boundary. There are several beds within the Opalinus Clay from Bülach that also include iron-ooids (TS BUL1-1 904.47) and calcified iron-ooids (TS BUL1-1 908.54 and 908.33). Such beds are also known from other locations (e.g. Wasserflue: Wohlwend et al. 2019a). Additional evidence from ammonites, palynostratigraphy and chemostratigraphy allowed a meaningful correlation with the other boreholes (e.g. Weiach, Riniken and Benken). The ammonite (891.63 m) from the hardground at 891.70 m to 891.60 m (identified as *Brasilia* ex gr. *bradfordensis*) already belongs to the Bradfordensis Subzone of the Bradfordensis Zone (see Fig. 5-1 for the detailed location of the samples: green = palynological sampling). This indicates a hiatus and/or a very condensed interval that was also documented by the palynological samples taken at 891.89 m, 891.70 m and 891.63 m with ages from the ?Murchisonae – Opalinum Zone (?«Comptum» Subzone) below the hardground to the Bradfordensis Zone above. In addition, the positive chemostratigraphic shift of +1 ‰ in the $\delta^{13}C_{org}$ values to average values of > 25.0 ‰ occurs in that interval (Fig. 3-5). Therefore, the upper boundary of the Opalinus Clay was set at the base of the fossiliferous, limonitic, iron-oolitic hardground at 891.70 m.

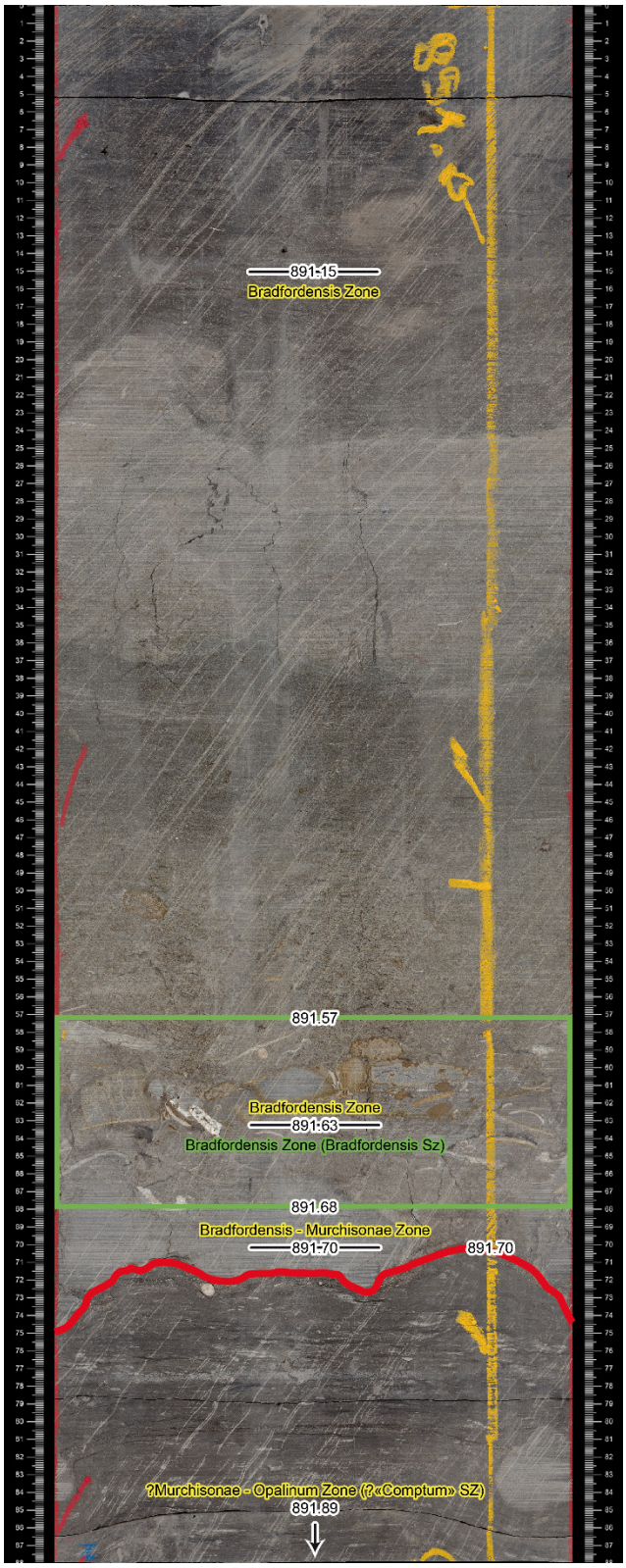

Fig. 5-1: 360° core photo (891.88 – 891.00 m) with the litho-boundary in red at 891.70 m and specific biostratigraphic datings (green: ammonite, yellow: palynomorphs)

Green rectangle: ammonite sample (with top and base), mean depth at 891.63 m.

«Murchisonae-Oolith Formation» (891.70 – 883.96 m)

In the BUL1-1 core, the lower boundary of the «Murchisonae-Oolith Formation» is set at 891.70 m at the erosional and bored base of a fossiliferous, limonitic, iron-oolitic hardground (891.70 – 891.60 m). Placing the boundary at this level was not based on lithological reasons alone; instead, the findings of ammonite stratigraphy and palyno- and chemostratigraphy flowed into the demarcation; see above for the detailed discussion about this boundary (upper boundary Opalinus Clay).

Per definition, the upper boundary of the «Murchisonae-Oolith Formation» is located at the subface of the «Sowerbyi-Oolith» (deposited during the Discites Zone), which is itself defined as the base of the Wedelsandstein Formation (German Stratigraphic Scheme; Bloos et al. 2005) and was deposited during the Discites Zone. In the BUL1-1 core, the limestone (iron-oolitic) bed (883.96 – 883.85 m) may correspond to the «Sowerbyi-Oolith». Its base at 883.96 m would therefore define the upper boundary of the «Murchisonae-Oolith Formation». However, the correlation of the «Sowerbyi-Oolith» is ambiguous. The stratigraphic position was narrowed down using biostratigraphic data that support the Early Bajocian age (Discites Zone) for the lithological boundary. The palynological sample (884.42 m) from the underlying iron-oolitic bed is dated as Late Aalenian (Concavum Zone). The following palynological interval (883.98 m – 883.24 m), including the aforementioned «Sowerbyi-Oolith», is dated as Discites Zone; the sample above at 880.02 m is dated as Ovale Zone. In addition, the ammonite at 882.71 m (identified as a Graphoceratidae *Hyperlioceras* sp.?) supports the Early Bajocian age (probably Discites Zone). The biostratigraphic data therefore frame the interval and age for the location of the «Sowerbyi-Oolith». Following this consideration above, the base of the limestone (iron-oolitic) bed (883.96 – 883.85 m) was defined as the upper boundary of the «Murchisonae-Oolith Formation» (883.96 m).

However, additional data from the ammonite preparation (ammonite sample at 882.71 m) document iron-ooids in the hanging of the above mentioned «Sowerbyi-Oolith». The polished slabs finished later on show a thicker iron-oolitic or at least limonitic interval. The upper boundary with reddish components (iron-ooids and/or limonitic components) could be drawn at around 880.77 m. A horizon (881.06 – 881.00 m) comprising limonitic components and probably a *Gryphaea* could just as well be correlated with the «Sowerbyi-Oolith». This interval is also still dated as Discites Zone.

Wedelsandstein Formation (883.96 – 855.53 m)

In the BUL1-1 core, the lower boundary of the Wedelsandstein Formation is set at 883.96 m at the subface of an limestone (iron-oolitic) bed (883.96 – 853.85 m), which is believed to correspond to the «Sowerbyi-Oolith» and therefore defines the base of the Wedelsandstein Formation (German Stratigraphic Scheme; Bloos et al. 2005). See detailed discussion for the boundary above (upper boundary of the «Murchisonae-Oolith Formation»).

In the BUL1-1 core, the upper boundary of the Wedelsandstein Formation is defined at the base of the first occurrence of iron-oolitic or limonitic sediments. These are used as lithological criteria to define the base of the overlying «Humphriesioolith Formation» (Bläsi et al. 2013, Jordan & Deplazes 2019). Based on this, the Wedelsandstein Formation ends at 855.53 m with a sharp contact overlain by limonitic and iron-oolitic intraclasts, embedded in a calcareous marl (iron-oolitic).

As already mentioned above (Section 3.4), the Wedelsandstein Formation can be subdivided into a lower increasingly calcareous unit (883.96 – 869.70 m) that includes a hardground at the top (869.76 – 869.70 m) and into an upper more marly part from 869.70 m to the top at 855.53 m. Both successions show an increasing trend in the carbonate content from the base to the top. The lower part can be dated by palynomorphs as the Discites and Ovale Zones, the upper part as the Laeviuscula Zone.

«Humphriesioolith Formation» (855.53 – 853.94 m)

In the BUL1-1 core, the lower boundary of the «Humphriesioolith Formation» discussed above is defined by the occurrence of iron-oolitic and limonitic components at 855.53 m. It overlays the calcareous marl of the topmost Wedelsandstein Formation with a sharp contact. In the lowermost 4 cm (855.53 – 855.49 m), iron-oolitic intraclasts with limonitic crusts and borings were observed.

In the BUL1-1 core, the upper boundary of the «Humphriesioolith Formation» was drawn based on the disappearance of the iron-ooids and limonitic components, which are the main lithological criteria for the «Humphriesioolith Formation». The iron-ooids and here mainly the limonitic components can be traced up to and including the calcareous marl interlayer (854.00 – 853.94 m). Therefore, the upper boundary was drawn at the top of this interlayer at 853.94 m and at the base of the hanging bioclastic, arenitic limestone.

«Herrenwis Unit» (853.94 – 812.03 m)

In the BUL1-1 core, the sedimentary succession (between 853.94 and 812.03 m) consists mainly of coral bioherm, reef detritus and crinoidal limestone. This succession corresponds to a new unit which was not previously defined formally or informally (Jordan & Deplazes 2019). Therefore, an informal working name, the «Herrenwis Unit» was chosen.

In the BUL1-1 core, the lower boundary of the «Herrenwis Unit» was defined at 853.94 m based on the disappearance of the iron-ooids and limonitic components from the underlying «Humphriesioolith Formation». The upper boundary was defined at the uppermost occurrence of the mainly coralligenous bioherm at 812.03 m with a sharp contact to the overlying iron-oolitic sediments of the «Parkinsoni-Württembergica-Schichten». Both boundaries are solely based on lithological criteria.

6 Conclusions

The present study documents data on microfacies analysis, ammonite stratigraphy and palyno-stratigraphy as well as detailed geochemical analyses (C, O and N isotopes). With this data collection, it was possible to predict the delimitation of the Mesozoic strata more accurately. Most of the important data for the boundaries in question were already present at the data-freeze (31.01.2020). Therefore, the present report complements the lithostratigraphic report of Dossier III for the deep borehole Bülach-1-1 and its sidetrack Bülach-1-1B. The lithological boundaries, and therefore the stratigraphic profile, were mostly defined by lithological criteria. Nevertheless, the customary formal and informal formation boundaries were not always obvious in the drill cores, either because of the small core diameter or changing facies conditions. The exact location of specific formation boundaries led to discussions requiring additional data to determine the exact profile description and illustration. We are aware that certain boundaries are thus no longer based solely on lithological criteria and that the definitions therefore also include chronostratigraphic criteria (ammonite stratigraphy, palyno- and chemostratigraphy).

7 References

Agassiz, L. (1840): Description des échinodermes fossiles de la Suisse. Seconde Partie, Cidarides. Denkschr. allg. schweiz. Ges. gesamt. Naturwiss. 4, 1-107.

Bayle, E. (1878): Fossiles principaux des terrains de la France. Explication de la carte géologique de la France 4/1, Paris.

Below, R. (1990): Evolution und Systematik von Dinoflagellaten-Zysten aus der Ordnung Peridiniales. III. Familie Pareodiniaceae. Palaeontographica, Abteilung B, 220/1-4, 1-96.

Bläsi, H.R., Deplazes, G., Schnellmann, M. & Traber, D. (2013): Sedimentologie und Stratigraphie des 'Braunen Doggers' und seiner westlichen Äquivalente. Nagra Arbeitsbericht NAB 12-51.

Bloos, G., Dietl, G. & Schweigert, G. (2005): Der Jura Süddeutschlands in der Stratigraphischen Tabelle von Deutschland 2002. Newsletters on stratigraphy 41, 263-277.

Buckman, S.S. (1887 – 1907): A Monograph of the Ammonites of the Inferior Oolite Series. Palaeontographical Society Monographs, London, The Palaeontographical Society, 456 pp.

Cariou, E. & Hantzpergue, P. (eds.) (1997): Biostratigraphie du Jurassique ouest-européen et méditerranéen: zonations parallèles et distribution des invertébrés et microfossiles. Bull. Centre Rech. Elf Explor. Prod.

Dickson, J. A (1965): Modified Staining Technique for Carbonates in Thin Section. Nature 205, 587.

Feist-Burkhardt, S. & Pross, J. (2010): Dinoflagellate cyst biostratigraphy of the Opalinuston Formation (Middle Jurassic) in the Aalenian type area in southwest Germany and north Switzerland. Lethaia 43, 10-31.

Fernandez, A., van Dijk, J., Müller, I.A. & Bernasconi, S.M. (2016): Siderite acid fractionation factors for sealed and open vessel digestions at 70°C and 100°C. Chemical Geology 444, 180-186.

Gygi, R.A. (1977): Revision der Ammonitengattung *Gregoryceras* (Aspidoceratidae) aus dem. Oxfordian (Oberer Jura) der Nordschweiz und von Süddeutschland. Taxonomie, Phylogenie, Stratigraphie. Eclogae geol. Helv. 70/2, 435-542.

Gygi, R.A. (2000): Annotated index of lithostratigraphic units currently used in the Upper Jurassic of northern Switzerland. Eclogae geol. Helv. 93/1, 125-146.

Gygi, R.A. (2001): Perisphinctacean ammonites of the type Transversarium Zone (Middle Oxfordian, Late Jurassic) in northern Switzerland. Schweizerische Paläontologische Abhandlungen 122, 1-171.

Gygi, R.A. (2012): Quantitative geology of Late Jurassic epicontinental sediments in the Jura Mountains of Switzerland. Springer Science & Business Media.

Hess, H. (1975): Die fossilen Echinodermen des Schweizer Juras. Veröffentlichungen aus dem Naturhistorischen Museum Basel 8, 1-130.

Isler, A., Pasquier, F. & Huber, M. (1984): Geologische Karte der zentralen Nordschweiz 1:100'000. Herausgegeben von der Nagra und der Schweiz. Geol. Komm.

Jordan, P. & Deplazes, G. (2019): Lithostratigraphy of consolidated rocks expected in the Jura Ost, Nördlich Lägern and Zürich Nordost Regions. Nagra Arbeitsbericht NAB 19-14.

Kuhn, O. & Etter, W. (1994): Der Posidonienschiefer der Nordschweiz: Lithostratigraphie, Biostratigraphie und Fazies. Eclogae geol. Helv. 87/1, 113-138.

Kukal, Z. (1971): Geology of Recent Sediments. Academie Press, New York, 490 pp.

Looser, N., Schneebeli-Hermann, E., Furrer, H., Blattmann, T.M. & Bernasconi, S.M. (2018): Environmental changes and carbon cycle perturbations at the Triassic–Jurassic boundary in northern Switzerland. Swiss Journal of Geosciences 111/3, 445-460.

Lycett, J. (1857): The Cotteswold Hills. Piper, Stephenson and Spence, London, 168 pp.

Maubeuge, P.L. (1947): Sur quelques ammonites de l'Aalénien ferrugineux du Luxembourg et sur l'échelle stratigraphique de la Formation Ferrifère Franco–Belgo–Luxembourgeoise. Archives de l'Institut Grand–Ducal de Luxembourg, Section des Sciences naturelles, physique et mathématique, Nouvelle Série 17, 73-87.

Maubeuge, P.L. (1950): Nouvelles Recherches Stratigraphiques et Paléontologiques sur l'Aalénien Luxembourgeois (Parties Moyenne et Supérieure). Archives de l'Institut Grand–Ducal de Luxembourg, Section des Sciences naturelles, physique et mathématique, Nouvelle Série 19, 365-397.

Nagra (2014): SGT Etappe 2: Vorschlag weiter zu untersuchender geologischer Standortgebiete mit zugehörigen Standortarealen für die Oberflächenanlage. Geologische Grundlagen. Dossier II: Sedimentologische und tektonische Verhältnisse. Nagra Technischer Bericht NTB 14-02.

Ogg, J.G., Ogg, G. & Gradstein, F.M. (2016): The Concise Geologic Time Scale. Cambridge University Press. 184 pp.

Oppel, A. (1862 – 1863): Über jurassische Cephalopoden. Paläont. Mitt. Mus. königl. bayer. Staat 1/3, 127-266.

d'Orbigny, A. de (1842 – 1851): Paléontologie française. Terrains jurassiques. I. Cephalopodes. Masson, Paris, 642 pp.

Parsons, T.R. (1975): Particulate organic carbon in the sea. *In:* Riey, J.P & Skirrow, G. (eds.): Chemical oceanography, Academie Press, London, 338-425.

Pietsch, J. & Jordan, P. (2014): Digitales Höhenmodell Basis Quartär der Nordschweiz – Version 2014 (SGT E2) und ausgewählte Auswertungen. Nagra Arbeitsbericht NAB 14-02.

Rais, P., Louis-Schmid, B., Bernasconi, S.M. & Weissert, H. (2007): Palaeoceanographic and palaeoclimatic reorganization around the Middle – Late Jurassic transition. Palaeogeography, Palaeoclimatology, Palaeoecology 251/3-4, 527-546.

Reinecke, J.C.M. (1818): Maris protogaei Nautilos et Argonautae vulga Cornua Ammonis in Agro Coburgico et vicinio reperiundos; descripsit et delineavit, simul Observationes de Fossilum Protypis. L.C.A. Ahlii imp., Coburg, 90 pp.

Remane, J., Adatte, T., Berger, J.P., Burkhalter, R., Dall'Agnolo, S., Decrouez, D., Fischer, H., Funk, H., Furrer, H., Graf, H.R., Gouffon, Y., Heckendorn, W. & Winkler, W. (2005): Richtlinien zur stratigraphischen Nomenklatur. Eclogae geol. Helv. 98/3, 385-405.

Scheffer, F. & Schachtschnabel, P. (1984): Lehrbuch der Bodenkunde. Enke Verlag, Stuttgart.

Sowerby, J. (1812–1846): The mineral conchology of Great Britain; or, coloured figures and descriptions of those remains of testaceous animals or shells, which have been preserved at various times and depths in the earth (vol. 1–7). Meredith, London.

Stratabugs, version 2.1 (June 2016). StrataData Ltd., UK. http://www.stratadata.co.uk.

Timescale Creator, version 7.0 (30. July 2016). Geologic TimeScale Foundation. https://engineering.purdue.edu/Stratigraphy/tscreator/.

Wetzel, A. & Allia, V. (2000): The significance of hiatus beds in shallow-water mudstones: an example from the Middle Jurassic of Switzerland. Journal of sedimentary research 70(1), 170-180.

Wohlwend, S., Hart, M. & Weissert, H. (2016): Chemostratigraphy of the Upper Albian to mid-Turonian Natih Formation (Oman) – how authigenic carbonate changes a global pattern. The Depositional Record 2/1, 97-117.

Wohlwend, S., Bläsi, H.R., Feist-Burkhardt, S., Hostettler, B., Menkveld-Gfeller, U., Dietze, V. & Deplazes, G. (2019a): Die Passwang-Formation im östlichen Falten- und Tafeljura: Fasiswald (SO) – Unt. Hauenstein (SO) – Wasserflue (AG) – Thalheim (AG) – Frickberg (AG) – Cheisacher (AG) – Böttstein (AG) – Tegerfelden (AG) – Acheberg (AG). Nagra Arbeitsbericht NAB 18-11.

Wohlwend, S., Bernasconi, S.M., Deplazes, G. & Jaeggi, D. (2019b): SO Experiment: Chemo-stratigraphic study of Late Aalenian to Early Bajocian. Mont Terri Technical Report TR 19-05. Federal Office of Topography (swisstopo), Wabern.

Wood, G.D., Gabriel, A.M. & Lawson, J.C. (1996): Palynological techniques – processing and microscopy. *In:* Jansonius, J. & McGregor, D.C.: Palynology, principles and applications. American Association of Stratigraphic Palynologists Foundation 1, 29-50.

Zieten, C.H. von (1830): Versteinerungen Württembergs, oder naturgetreue Abbildungen der in den vollständigsten Sammlungen, namentlich der in dem Kabinet des Oberamts-Arzt Dr. Hartmann befindlichen Petrefacten, mit Angabe der Gebirgs-Formationen, in welchen dieselben vorkommen und der Fundorte. Verlag & Lithographie der Expedition des Werkes unserer Zeit, Stuttgart, 102 pp.

Appendix A: List of all samples

Appendix A1a: List of all thin sections from BUL1-1 ..... A-2

Appendix A1b: List of all thin sections from BUL1-1B A-3

Appendix A2a: List of all sampled macrofossils from BUL1-1 ..... A-4

Appendix A2b: List of all sampled macrofossils from BUL1-1B A-5

Appendix A3a: List of other provisionally determined conspicuous macrofossils from BUL1-1 ..... A-6

Appendix A3b: List of other provisionally determined conspicuous macrofossils from BUL1-1B A-7

Appendix A4: List of all palynological samples from BUL1-1 ..... A-8

Appendix A1a: List of all thin sections from BUL1-1 (536.16 – 1'034.81 m)

For the description and indivual counting of the thin sections see Section 2.1; selected photos can be found in Appendix B.

Top [m]	**Bottom** [m]	**Avg. depth** [m]	**Formation**	**Retrieval date** [dd.mm.yyyy]	**Sample ID**
536.14	536.18	**536.16**	«Felsenkalke» / «Massenkalk»	17.10.2019	BUL1-1-536.16-TS
550.745	550.79	**550.77**	«Felsenkalke» / «Massenkalk»	17.10.2019	BUL1-1-550.77-TS
575.02	575.07	**575.05**	«Felsenkalke» / «Massenkalk»	17.10.2019	BUL1-1-575.05-TS
594.89	594.94	**594.92**	«Felsenkalke» / «Massenkalk»	17.10.2019	BUL1-1-594.92-TS
626.19	626.24	**626.22**	«Felsenkalke» / «Massenkalk»	17.10.2019	BUL1-1-626.22-TS
636.64	636.69	**636.67**	«Felsenkalke» / «Massenkalk»	17.10.2019	BUL1-1-636.67-TS
641.23	641.28	**641.26**	«Felsenkalke» / «Massenkalk»	17.10.2019	BUL1-1-641.26-TS
653.64	653.69	**653.67**	Schwarzbach	17.10.2019	BUL1-1-653.67-TS
676.07	676.12	**676.10**	Schwarzbach	17.10.2019	BUL1-1-676.10-TS
694.77	694.82	**694.80**	Villigen	17.10.2019	BUL1-1-694.80-TS
703.34	703.39	**703.37**	Villigen	17.10.2019	BUL1-1-703.37-TS
735.81	735.86	**735.84**	Villigen	17.10.2019	BUL1-1-735.84-TS
779.18	779.23	**779.21**	Wildegg	17.10.2019	BUL1-1-779.21-TS
802.65	802.70	**802.68**	Wildegg	21.11.2019	BUL1-1-802.68-TS
805.11	805.15	**805.13**	«Glaukonitsandmergel Bed»	21.11.2019	BUL1-1-805.13-TS
806.15	806.19	**806.17**	Wutach	21.11.2019	BUL1-1-806.17-TS
809.19	809.23	**809.21**	«Parkinsoni-Württemb.-Sch.»	21.11.2019	BUL1-1-809.21-TS
811.76	811.80	**811.78**	«Parkinsoni-Württemb.-Sch.»	21.11.2019	BUL1-1-811.78-TS
812.06	812.10	**812.08**	«Herrenwis Unit»	21.11.2019	BUL1-1-812.08-TS
820.20	820.24	**820.22**	«Herrenwis Unit»	21.11.2019	BUL1-1-820.22-TS
825.20	825.24	**825.22**	«Herrenwis Unit»	21.11.2019	BUL1-1-825.22-TS
833.19	833.23	**833.21**	«Herrenwis Unit»	21.11.2019	BUL1-1-833.21-TS
848.40	848.44	**848.42**	«Herrenwis Unit»	21.11.2019	BUL1-1-848.42-TS
850.25	850.29	**850.27**	«Herrenwis Unit»	21.11.2019	BUL1-1-850.27-TS
854.96	855.00	**854.98**	«Humphriesioolith»	21.11.2019	BUL1-1-854.98-TS
855.50	855.54	**855.52**	«Humphriesioolith»	21.11.2019	BUL1-1-855.52-TS
860.34	860.38	**860.36**	Wedelsandstein	13.12.2019	BUL1-1-860.36-TS
870.33	870.37	**870.35**	Wedelsandstein	13.12.2019	BUL1-1-870.35-TS
883.31	883.35	**883.33**	Wedelsandstein	13.12.2019	BUL1-1-883.33-TS
884.36	884.40	**884.38**	«Murchisonae-Oolith»	13.12.2019	BUL1-1-884.38-TS
891.53	891.57	**891.55**	«Murchisonae-Oolith»	13.12.2019	BUL1-1-891.55-TS
904.45	904.49	**904.47**	Opalinus Clay	13.12.2019	BUL1-1-904.47-TS
908.31	908.35	**908.33**	Opalinus Clay	13.12.2019	BUL1-1-908.33-TS
908.52	908.56	**908.54**	Opalinus Clay	13.12.2019	BUL1-1-908.54-TS
912.42	912.46	**912.44**	Opalinus Clay	13.12.2019	BUL1-1-912.44-TS
919.30	919.34	**919.32**	Opalinus Clay	13.12.2019	BUL1-1-919.32-TS
967.62	967.66	**967.64**	Opalinus Clay	13.12.2019	BUL1-1-967.64-TS
976.00	976.04	**976.02**	Opalinus Clay	13.12.2019	BUL1-1-976.02-TS
1'007.68	1'007.72	**1'007.70**	Staffelegg	12.12.2019	BUL1-1-1007.70-TS
1'008.18	1'008.22	**1'008.20**	Staffelegg	12.12.2019	BUL1-1-1008.20-TS
1'021.28	1'021.32	**1'021.30**	Staffelegg	12.12.2019	BUL1-1-1021.30-TS
1'022.06	1'022.10	**1'022.08**	Staffelegg	12.12.2019	BUL1-1-1022.08-TS
1'022.62	1'022.66	**1'022.64**	Staffelegg	12.12.2019	BUL1-1-1022.64-TS
1'024.52	1'024.56	**1'024.54**	Staffelegg	12.12.2019	BUL1-1-1024.54-TS
1'024.98	1'025.02	**1'025.00**	Staffelegg	12.12.2019	BUL1-1-1025.00-TS
1'030.55	1'030.59	**1'030.57**	Staffelegg	12.12.2019	BUL1-1-1030.57-TS
1'034.79	1'034.83	**1'034.81**	Klettgau	12.12.2019	BUL1-1-1034.81-TS

Appendix A1b: List of all thin sections from BUL1-1B (1'042.16 – 1'317.79 m)

For the description and indivual counting of the thin sections see Section 2.1; selected photos can be found in Appendix B.

Top [m]	**Bottom** [m]	**Avg. depth** [m]	**Formation**	**Retrieval date** [dd.mm.yyyy]	**Sample ID**
1'042.14	1'042.18	**1'042.16**	Klettgau	16.01.2020	BUL1-1B-1041.16-TS
1'043.63	1'043.67	**1'043.65**	Klettgau	16.01.2020	BUL1-1B-1043.65-TS
1'051.51	1'051.55	**1'051.53**	Klettgau	16.01.2020	BUL1-1B-1051.53-TS
1'055.70	1'055.74	**1'055.72**	Klettgau	16.01.2020	BUL1-1B-1055.72-TS
1'065.20	1'065.24	**1'065.22**	Klettgau	16.01.2020	BUL1-1B-1065.22-TS
1'082.85	1'082.89	**1'082.87**	Bänkerjoch	12.12.2019	BUL1-1B-1082.87-TS
1'091.10	1'091.14	**1'091.12**	Bänkerjoch	12.12.2019	BUL1-1B-1091.12-TS
1'112.35	1'112.39	**1'112.37**	Bänkerjoch	12.12.2019	BUL1-1B-1112.37-TS
1'123.97	1'124.01	**1'123.99**	Bänkerjoch	12.12.2019	BUL1-1B-1123.99-TS
1'131.58	1'131.62	**1'131.60**	Bänkerjoch	12.12.2019	BUL1-1B-1131.60-TS
1'142.60	1'142.64	**1'142.62**	Schinznach	16.01.2020	BUL1-1B-1142.62-TS
1'152.45	1'152.49	**1'152.47**	Schinznach	16.01.2020	BUL1-1B-1152.47-TS
1'156.18	1'156.22	**1'156.20**	Schinznach	16.01.2020	BUL1-1B-1156.20-TS
1'179.37	1'179.41	**1'179.39**	Schinznach	16.01.2020	BUL1-1B-1179.39-TS
1'203.64	1'203.68	**1'203.66**	Schinznach	16.01.2020	BUL1-1B-1203.66-TS
1'240.70	1'240.74	**1'240.72**	Zeglingen	03.02.2020	BUL1-1B-1240.72-TS
1'268.40	1'268.44	**1'268.42**	Kaiseraugst	16.01.2020	BUL1-1B-1268.42-TS
1'305.99	1'306.03	**1'306.01**	Kaiseraugst	16.01.2020	BUL1-1B-1306.01-TS
1'306.30	1'306.34	**1'306.32**	Dinkelberg	16.01.2020	BUL1-1B-1306.32-TS
1'308.32	1'308.36	**1'308.34**	Dinkelberg	16.01.2020	BUL1-1B-1308.34-TS
1'317.77	1'317.81	**1'317.79**	Dinkelberg	16.01.2020	BUL1-1B-1317.79-TS

Appendix A2a: List of all sampled macrofossils from BUL1-1 (801.65 – 1'030.44 m)

For the definitive determination of the individual macrofossils see Section 2.2 (Tab. 3-2a).

Top [m]	**Bottom** [m]	**Avg. depth** [m]	**Formation**	**Retrieval date** [dd.mm.yyyy]	**Sample ID**
801.65	801.665	801.66	Wildegg	24.09.2019	BUL1-1-801.65-BS(MF)
802.61	802.64	802.63	Wildegg	24.09.2019	BUL1-1-802.63-BS(MF)
802.83	802.855	802.84	Wildegg	24.09.2019	BUL1-1-802.85-BS(MF)
803.75	803.775	803.76	Wildegg	24.09.2019	BUL1-1-803.77-BS(MF)
805.355	805.39	805.37	Wutach	24.09.2019	BUL1-1-805.37-BS(MF)
805.68	805.71	805.70	Wutach	24.09.2019	BUL1-1-805.70-BS(MF)
805.76	805.83	805.80	Wutach	24.09.2019	BUL1-1-805.80-BS(MF)
806.16	806.27	806.21	Wutach	24.09.2019	BUL1-1-806.21-BS(MF)
806.31	806.34	806.33	Wutach	24.09.2019	BUL1-1-806.33-BS(MF)
810.55	810.615	810.58	«Parkinsoni-Württ.-Sch.»	24.09.2019	BUL1-1-810.58-BS(MF)
811.99	812.03	812.01	«Parkinsoni-Württ.-Sch.»	24.09.2019	BUL1-1-812.03-BS(MF)
829.81	829.83	829.82	«Herrenwis Unit»	24.09.2019	BUL1-1-829.82-BS(MF)
832.34	832.37	832.36	«Herrenwis Unit»	24.09.2019	BUL1-1-832.36-BS(MF)
852.08	852.135	852.11	«Herrenwis Unit»	24.09.2019	BUL1-1-852.11-BS(MF)
853.81	853.86	853.84	«Herrenwis Unit»	24.09.2019	BUL1-1-853.84-BS(MF)
891.57	891.68	891.63	«Murchisonae-Oolith»	24.09.2019	BUL1-1-891.63-BS(MF)
897.42	897.44	897.43	Opalinus Clay	24.09.2019	BUL1-1-897.43-BS(MF)
908.20	908.24	908.22	Opalinus Clay	24.09.2019	BUL1-1-908.22-BS(MF)
959.05	959.09	959.07	Opalinus Clay	13.11.2019	BUL1-1-959.07-BS(MF)
959.50	959.53	959.52	Opalinus Clay	13.11.2019	BUL1-1-959.52-BS(MF)
968.03	968.06	968.05	Opalinus Clay	13.11.2019	BUL1-1-969.10-BS(MF)
973.25	973.28	973.27	Opalinus Clay	13.11.2019	BUL1-1-973.27-BS(MF)
980.06	980.09	980.08	Opalinus Clay	13.11.2019	BUL1-1-980.09-BS(MF)
995.52	995.54	995.53	Opalinus Clay	12.12.2019	BUL1-1-995.53-BS(MF)
995.77	995.79	995.78	Opalinus Clay	13.11.2019	BUL1-1-995.78-BS(MF)
995.86	995.89	995.88	Opalinus Clay	13.11.2019	BUL1-1-995.88-BS(MF)
996.27	996.30	996.29	Staffelegg	13.11.2019	BUL1-1-996.29-BS(MF)
996.58	996.64	996.61	Staffelegg	13.11.2019	BUL1-1-996.61-BS(MF)
997.15	997.18	997.17	Staffelegg	13.11.2019	BUL1-1-997.17-BS(MF)
998.30	998.34	998.32	Staffelegg	13.11.2019	BUL1-1-998.32-BS(MF)
998.66	998.76	998.71	Staffelegg	13.11.2019	BUL1-1-998.71-BS(MF)
999.76	999.80	999.78	Staffelegg	13.11.2019	BUL1-1-999.78-BS(MF)
1'000.56	1'000.60	1'000.58	Staffelegg	13.11.2019	BUL1-1-1000.58-BS(MF)
1'002.73	1'002.76	1'002.75	Staffelegg	13.11.2019	BUL1-1-1002.75-BS(MF)
1'016.75	1'016.79	1'016.77	Staffelegg	13.11.2019	BUL1-1-1016.77-BS(MF)
1'022.91	1'022.96	1'022.94	Staffelegg	13.11.2019	BUL1-1-1022.94-BS(MF)
1'030.41	1'030.46	1'030.44	Staffelegg	13.11.2019	BUL1-1-1030.44-BS(MF)

Appendix A2b: List of all sampled macrofossils from BUL1-1B (996.65 – 1'005.06 m)

For the definitive determination of the individual macrofossils see Section 2.2 (Tab. 3-2b).

Top [m]	**Bottom** [m]	**Avg. depth** [m]	**Formation**	**Retrieval date** [dd.mm.yyyy]	**Sample ID**
996.65	996.68	996.67	Staffelegg	13.11.2019	BUL1-1B-996.67-BS(MF)
996.79	996.84	996.82	Staffelegg	13.11.2019	BUL1-1B-996.82-BS(MF)
997.07	997.10	997.09	Staffelegg	13.11.2019	BUL1-1B-997.09-BS(MF)
997.35	997.37	997.36	Staffelegg	13.11.2019	BUL1-1B-997.36-BS(MF)
997.61	997.64	997.63	Staffelegg	13.11.2019	BUL1-1B-997.63-BS(MF)
997.66	997.68	997.67	Staffelegg	13.11.2019	BUL1-1B-997.67-BS(MF)
998.14	998.18	998.16	Staffelegg	13.11.2019	BUL1-1B-998.16-BS(MF)
999.03	999.07	999.05	Staffelegg	13.11.2019	BUL1-1B-999.05-BS(MF)
1'004.09	1'004.13	1'004.11	Staffelegg	13.11.2019	BUL1-1B-1004.11-BS(MF)
1'005.04	1'005.08	1'005.06	Staffelegg	13.11.2019	BUL1-1B-1005.06-BS(MF)

Appendix A3a: List of other provisionally determined conspicuous macrofossils from BUL1-1 (785.50 – 1'028.74 m)

Top [m]	Bottom [m]	Fossil	Determination (provisional)
750.50	750.64	Sponges	indet.
765.59		Belemnite	indet.
770.90	770.96	Crinoids	Balanocrinus
770.90		Belemnite	indet.
780.81		Ammonites	Dichotomoceras
799.15		Belemnite	Hibolites sp.
799.50		Belemnite	Hibolites sp.
801.615		Ammonite	Subdiscosphinctes?
803.55		Bivalve	Eopecten sp
805.70	806.00	Bivalves. belemnites, gastropods	
806.22	806.54	Bivalves, gastropods, Brachiopods	
806.335	806.42	Bivalve	?Ctenostreon
806.50		Ammonite	Oppellidae indet.
807.00	808.00	Oysters	?Catinula, ?Nanogyra
807.70		Belemnite	
808.235		Ammonite fragment	Procerites?
808.575		Ammonite fragment	indet.
811.00	812.03	Belemnites, bivalves	indet
811.65		Bivalve	Pholadomya?
811.88		Belemnite	indet
812.03	844.70	Corals, echinoids, bivalves, brachiopods	
825.83		Echinoid spike	
902.92		Bivalve	Bositra buchi
904.30		Belemnite	?Acrocoelites
935.185		Oyster	indet.
958.22		Aptychi	indet.
958.39		Fossil indet.	
958.595		Ammonite fragment	Leioceras?
958.97		Ammonite	Leioceras
961.45		Ammonite	Leiopceras juvenil
961.70		Ammonite	Leioceras ex. gr.opalinum
961.85		Ammonite fragment	Leioceras sp.
962.23	962.25	Ammonites	Leioceras
963.55		Ammonite	?Leioceras
963.68		Ammonite	?Leioceras
965.16		Aptychus	?Leioceras
966.52		Bivalve	Bositra buchi
966.56		Aptychus	?Leioceras
967.33		Ammonite	Leioceras ex gr.opalinum
967.67		Ammonite	Leioceras
971.90		Aptychus	?lLeioceras
973.12		Trace fossil	indet
977.40		Aptychus	Leioceras
978.80		Aptychi	Leioceras
978.85		Ammonite	indet.
980.28		Aptychi	?lLeioceras
980.70		Shell fragment	indet.
980.73		Ammonite	indet.
981.28		Ammonite	Leioceras
981.93		Ammonite fragment	Leioceras?
983.07		Ammonite fragment	indet.
983.73		Ammonite fragment	Leioceras
995.70		Ammonite fragment	Leioceras
995.75		Ammonite fragment	Leioceras
996.59	996.61	Ammonite	Pleydellia

(continued)

Top [m]	**Bottom** [m]	**Fossil**	**Determination (provisional)**
996.61	996.64	Ammonite + bivalve	Pleydellia
997.35		Gastropods	indet.
997.40		Ammonite	Pleydellia
997.62	997.68	Ammonites	Pleydellia
998.40		Ammonite + oysters	Dumortieria
1'001.035		Bivalve	Pseudomytiloides?
1'001.065		Plant remains	indet.
1'001.60		Ammonite	Dactylioceras commune?
1'006.34		Bivalves	Pseudomytiloides dubius
1'007.08		Belemnites	Passaloteuthis sp.
1'007.46	1'007.63	Belemnites	Passaloteuthis sp.
1'008.06		Gryphaea	?Gryphaea obliqua
1'008.26		Gryphaea	?Gryphaea obliqua
1'019.91		Crinoid	Chladocrinus
1'020.87	1'021.36	Bivalves	Grtyphaea arcuata
1'022.39		?Ammonite	?
1'028.08		Bivalve	Plagiostoma
1'028.74		Brachiopods?	Modiolus

Appendix A3b: List of other provisionally determined conspicuous macrofossils from BUL1-1B (996.66 – 1'029.60 m)

Top [m]	**Bottom** [m]	**Fossil**	**Determination (provisional)**
996.66		Belemnite	Salpingoteuthis od anderer
996.73		Ammonite	Pleydellia leura?
997.48		Crinoid remains	Balanocrinus
997.78		Ammonite	Dumortieria
998.61		Ammonite	?
999.21		Ammonite	Hammatoceras?
999.53		Ammonite	indet.
1'000.93		Belemnites	Acrocoelites?
1'001.02		Ammonite	indet.
1'002.31		Belemnites	indet.
1'002.735		Bivalves	Pseudomytiloides dubius
1'002.92		Bivalves	Pseudomytiloides dubius
1'003.37		Fish scale	Schmelzschupper
1'003.88		Fish remains?	indet.
1'003.94		Aptychus	indet.
1'004.36		Belemnite	?Youngibelus?
1'005.50		?Vertebrae remains	indet.
1'006.26		Jet (type of lignite)	indet.
1'006.365		Bivalves	Pseudomytiloides dubius
1'006.605		Ammonite	Lytoceras siemensi
1'006.81	1'007.06	Belemnites	u.a. Passaloteuthis bisulcata
1'006.81		Crinoid remains	Seirocrinus subangularis
1'007.33		Ammonite	Lytoceras
1'008.09		Bivalves	Gryphaea obliqua?
1'019.83		Stromatolitic crust	indet.
1'022.83		Ammonite	Schlotheimia??
1'024.00		Bivalve	Entolium sp.
1'028.54		Bivalve	Modiolus (in BUL1-1 als Lingula bezeichnet)
1'029.60		Crab remains?	indet.

Appendix A4: List of all palynological samples from BUL1-1 (804.49 – 996.31 m)

Palynological samples in grey are taken from ammonite samples retrieved at specific depths. Sampling was always as close as possible to the ammonite.

Core	Top [m]	Bottom [m]	Avg. Depth [m]	Formation	Retrieval date [dd.mm.yyyy]	Sample ID
BUL1-1	804.47	804.50	804.49	Wildegg	21.01.2020	BUL1-1-804.49-BS(Pa)
BUL1-1	805.11	805.15	805.13	Wildegg	21.01.2020	BUL1-1-805.13-BS(Pa)
BUL1-1	805.36	805.39	805.37	Wutach	21.11.2019	BUL1-1-805.37-BS(Pa)
BUL1-1	805.76	805.83	805.80	Wutach	21.11.2019	BUL1-1-805.80-BS(Pa)
BUL1-1	806.15	806.19	806.17	Wutach	21.11.2019	BUL1-1-806.17-BS(Pa)
BUL1-1	807.07	807.11	807.09	«Variansmergel»	21.11.2019	BUL1-1-807.09-BS(Pa)
BUL1-1	809.19	809.23	809.21	«Parkinsoni-Württ.-Sch.»	21.11.2019	BUL1-1-809.21-BS(Pa)
BUL1-1	810.55	810.62	810.58	«Parkinsoni-Württ.-Sch.»	21.11.2019	BUL1-1-810.58-BS(Pa)
BUL1-1	811.99	812.03	812.01	«Parkinsoni-Württ.-Sch.»	21.11.2019	BUL1-1-812.01-BS(Pa)
BUL1-1	812.03	812.06	812.05	«Herrenwis Unit»	21.11.2019	BUL1-1-812.05-BS(Pa)
BUL1-1	812.18	812.20	812.19	«Herrenwis Unit»	21.11.2019	BUL1-1-812.19-BS(Pa)
BUL1-1	813.25	813.29	813.27	«Herrenwis Unit»	06.02.2020	BUL1-1-813.27-BS(Pa)
BUL1-1	818.00	818.05	818.03	«Herrenwis Unit»	21.11.2019	BUL1-1-818.03-BS(Pa)
BUL1-1	822.34	822.36	822.35	«Herrenwis Unit»	21.11.2019	BUL1-1-822.35-BS(Pa)
BUL1-1	827.37	827.39	827.38	«Herrenwis Unit»	21.11.2019	BUL1-1-827.38-BS(Pa)
BUL1-1	832.34	832.37	832.36	«Herrenwis Unit»	21.11.2019	BUL1-1-832.36-BS(Pa)
BUL1-1	837.62	837.65	837.64	«Herrenwis Unit»	21.11.2019	BUL1-1-837.64-BS(Pa)
BUL1-1	842.60	842.63	842.62	«Herrenwis Unit»	21.11.2019	BUL1-1-842.62-BS(Pa)
BUL1-1	847.26	847.29	847.28	«Herrenwis Unit»	21.11.2019	BUL1-1-847.28-BS(Pa)
BUL1-1	850.25	850.29	850.27	«Herrenwis Unit»	21.11.2019	BUL1-1-850.27-BS(Pa)
BUL1-1	853.98	854.00	853.99	«Humphriesioolith»	21.11.2019	BUL1-1-853.99-BS(Pa)
BUL1-1	854.96	855.00	854.98	«Humphriesioolith»	21.11.2019	BUL1-1-854.98-BS(Pa)
BUL1-1	855.13	855.15	855.14	«Humphriesioolith»	21.11.2019	BUL1-1-855.14-BS(Pa)
BUL1-1	855.45	855.48	855.47	«Humphriesioolith»	21.11.2019	BUL1-1-855.47-BS(Pa)
BUL1-1	855.54	855.58	855.56	Wedelsandstein	21.11.2019	BUL1-1-855.56-BS(Pa)
BUL1-1	856.07	856.10	856.09	Wedelsandstein	21.11.2019	BUL1-1-856.09-BS(Pa)
BUL1-1	860.38	860.41	860.40	Wedelsandstein	13.12.2019	BUL1-1-860.40-BS(Pa)
BUL1-1	865.47	865.50	865.49	Wedelsandstein	13.12.2019	BUL1-1-865.49-BS(Pa)
BUL1-1	869.62	869.66	869.64	Wedelsandstein	13.12.2019	BUL1-1-869.64-BS(Pa)
BUL1-1	869.79	869.82	869.81	Wedelsandstein	13.12.2019	BUL1-1-869.81-BS(Pa)
BUL1-1	874.95	874.98	874.97	Wedelsandstein	13.12.2019	BUL1-1-874.97-BS(Pa)
BUL1-1	880.00	880.04	880.02	Wedelsandstein	13.12.2019	BUL1-1-880.02-BS(Pa)
BUL1-1	883.22	883.25	883.24	Wedelsandstein	13.12.2019	BUL1-1-883.24-BS(Pa)
BUL1-1	883.97	883.99	883.98	«Murchisonae-Oolith»	13.12.2019	BUL1-1-883.98-BS(Pa)
BUL1-1	884.40	884.43	884.42	«Murchisonae-Oolith»	06.02.2020	BUL1-1-884.42-BS(Pa)
BUL1-1	884.78	884.82	884.80	«Murchisonae-Oolith»	13.12.2019	BUL1-1-884.80-BS(Pa)
BUL1-1	885.57	885.60	885.59	«Murchisonae-Oolith»	13.12.2019	BUL1-1-885.59-BS(Pa)
BUL1-1	886.95	886.97	886.96	«Murchisonae-Oolith»	13.12.2019	BUL1-1-886.96-BS(Pa)
BUL1-1	891.13	891.16	891.15	«Murchisonae-Oolith»	13.12.2019	BUL1-1-891.15-BS(Pa)
BUL1-1	891.57	891.68	891.63	«Murchisonae-Oolith»	13.12.2019	BUL1-1-891.63-BS(Pa)
BUL1-1	891.68	891.71	891.70	«Murchisonae-Oolith»	13.12.2019	BUL1-1-891.89-BS(Pa)
BUL1-1	891.88	891.90	891.89	Opalinus Clay	06.02.2020	BUL1-1-891.89-BS(Pa)
BUL1-1	897.39	897.42	897.41	Opalinus Clay	13.12.2019	BUL1-1-897.41-BS(Pa)
BUL1-1	910.00	910.04	910.02	Opalinus Clay	13.12.2019	BUL1-1-910.02-BS(Pa)
BUL1-1	930.33	930.35	930.34	Opalinus Clay	13.12.2019	BUL1-1-930.34-BS(Pa)
BUL1-1	949.77	949.79	949.78	Opalinus Clay	13.12.2019	BUL1-1-949.78-BS(Pa)
BUL1-1	969.93	969.95	969.94	Opalinus Clay	13.12.2019	BUL1-1-969.94-BS(Pa)
BUL1-1	989.99	990.01	990.00	Opalinus Clay	21.01.2020	BUL1-1-990.00-BS(Pa)
BUL1-1	995.54	995.56	995.55	Opalinus Clay	21.01.2020	BUL1-1-995.55-BS(Pa)
BUL1-1	995.88	995.91	995.90	Opalinus Clay?	21.01.2020	BUL1-1-995.90-BS(Pa)
BUL1-1	996.30	996.32	996.31	Staffelegg	21.01.2020	BUL1-1-996.31-BS(Pa)

Appendix B: Photos microfacies

Fig. B-1: Thin section BUL1-1B-1308.34, Dinkelberg Fm. B-2
Fig. B-2: Thin section BUL1-1B-1203.66, Schinznach Fm. B-2
Fig. B-3: Thin section BUL1-1B-1152.47, Schinznach Fm. B-2
Fig. B-4: Thin section BUL1-1B-1123.99, Bänkerjoch Fm. B-3
Fig. B-5: Thin section BUL1-1B-1091.12, Bänkerjoch Fm. B-3
Fig. B-6: Thin section BUL1-1B-1055.72, Klettgau Fm. (Ergolz Mb.) B-3
Fig. B-7: Thin section BUL1-1B-1043.65, Klettgau Fm. (Seebi Mb.) B-4
Fig. B-8: Thin section BUL1-1-1025.00, Staffelegg Fm. (Beggingen Mb.) B-4
Fig. B-9: Thin section BUL1-1-1021.30, Staffelegg Fm. (Beggingen Mb.) B-4
Fig. B-10: Thin section BUL1-1-912.44, Opalinus Clay B-5
Fig. B-11: Thin section BUL1-1-908.33, Opalinus Clay B-5
Fig. B-12: Thin section BUL1-1-884.38, «Murchisonae-Oolith Fm.» B-5
Fig. B-13: Thin section BUL1-1-870.35, Wedelsandstein Fm. B-6
Fig. B-14: Thin section BUL1-1-855.52, «Humphriesioolith Fm.» B-6
Fig. B-15: Thin section BUL1-1-850.27, «Herrenwis Unit» B-6
Fig. B-16: Thin section BUL1-1-825.22, «Herrenwis Unit» B-7
Fig. B-17: Thin section BUL1-1-820.22, «Herrenwis Unit» B-7
Fig. B-18: Thin section BUL1-1-811.71, «Parkinsoni-Württembergica-Sch.» (?«Parkinsoni-Oolith») B-7
Fig. B-19: Thin section BUL1-1-806.17, Wutach Fm. B-8
Fig. B-20: Thin section BUL1-1-805.13, «Glaukonitsandmergel Bed» B-8
Fig. B-21: Thin section BUL1-1-694.80, Villigen Fm. B-8
Fig. B-22: Thin section BUL1-1-653.67, Schwarzbach Fm. B-9
Fig. B-23: Thin section BUL1-1-626.22, «Felsenkalke» / «Massenkalk» B-9
Fig. B-24: Thin section BUL1-1-575.05, «Felsenkalke» / «Massenkalk» B-9

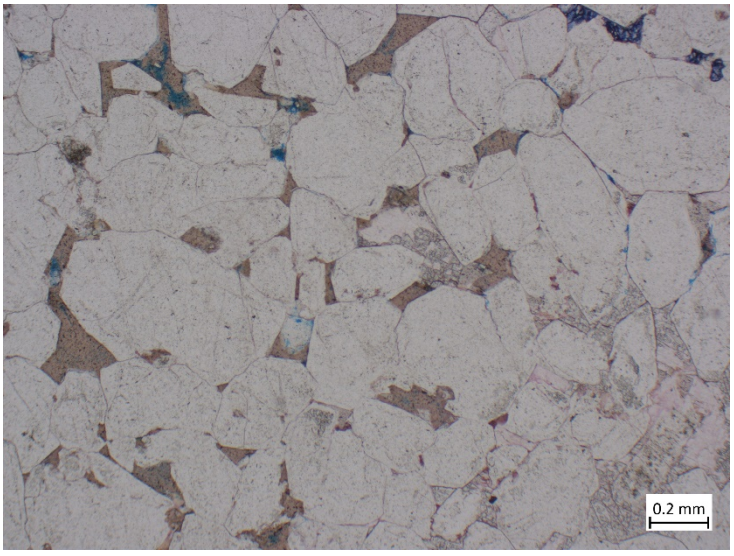

Fig. B-1:

Quartz sandstone:
detrital quartz grains with idiomorphic quartz cement overgrowths; open pore space (reddish), calcite (blue) as well as anhydrite cement (lower right corner, bright colours)

Thin section (TS) photo,
TS stained for calcite

BUL1-1B-1308.34
Dinkelberg Fm.

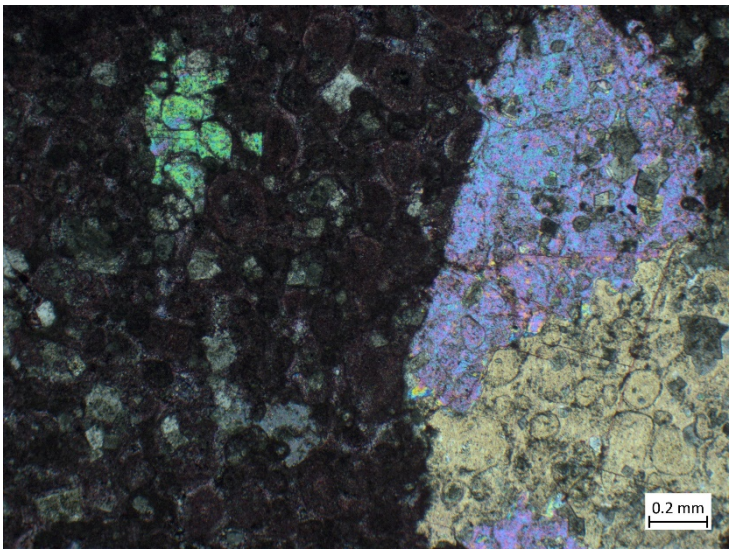

Fig. B-2:

Oosparite:
calcite ooids and cement (darker part), partly replaced by large anhydrite crystals (pastel-coloured)

Thin section photo, crossed nicols

BUL1-1B-1203.66
Schinznach Fm.

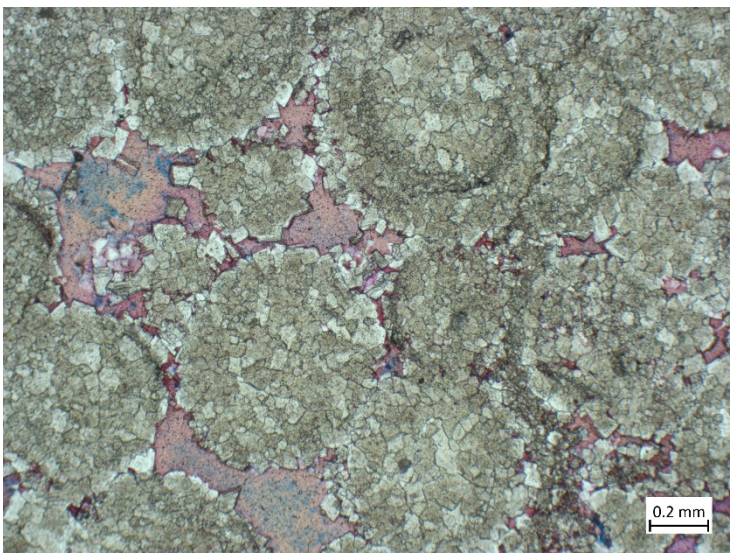

Fig. B-3:

Dolomitic oosparite:
ooids entirely replaced by dolomite rhombohedrons, open pore space (reddish)

Thin section photo,
TS stained for calcite

BUL1-1B-1152.47
Schinznach Fm.

Selected photos of microfacies of the Dinkelberg Formation and Schinznach Formation

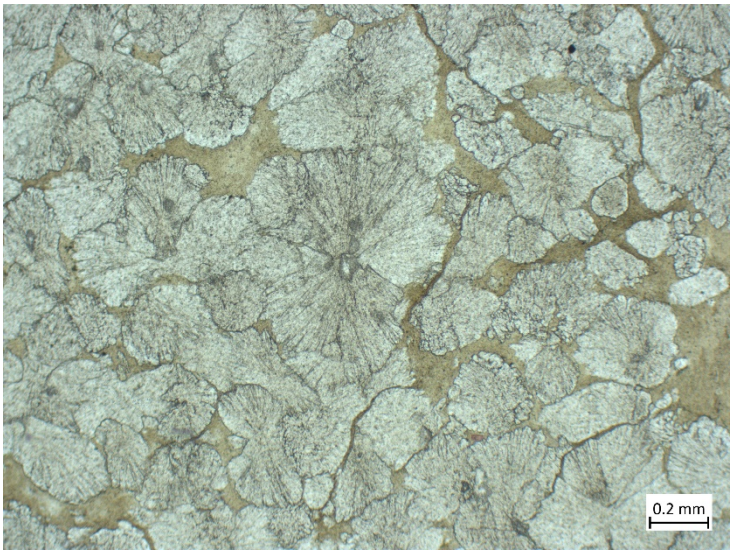

Fig. B-4:

Calcite rosettes forming a limestone layer:
calcite pseudomorph replacing twinned gypsum crystals

Thin section photo

BUL1-1B-1123.99
Bänkerjoch Fm.

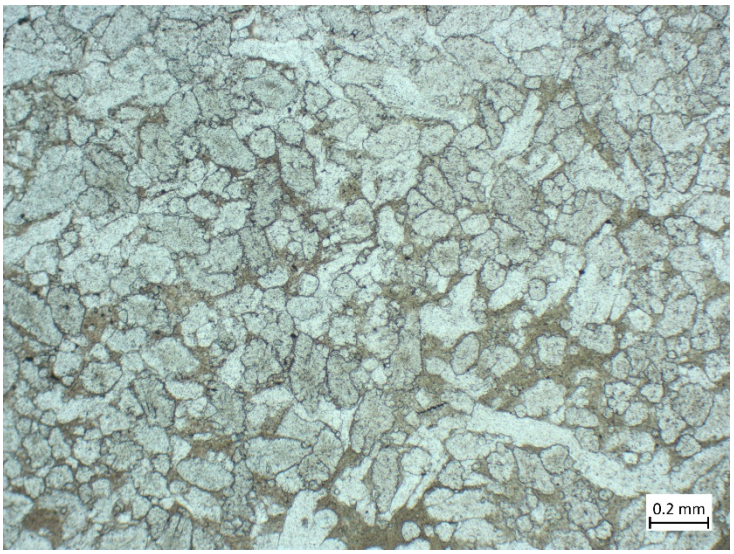

Fig. B-5:

Dolomite rhombohedrons, forming an dolostone (argillaceous) bed:
dolomite crystals pseudomorph replacing gypsum crystals

Thin section photo

BUL1-1B-1091.12
Bänkerjoch Fm.

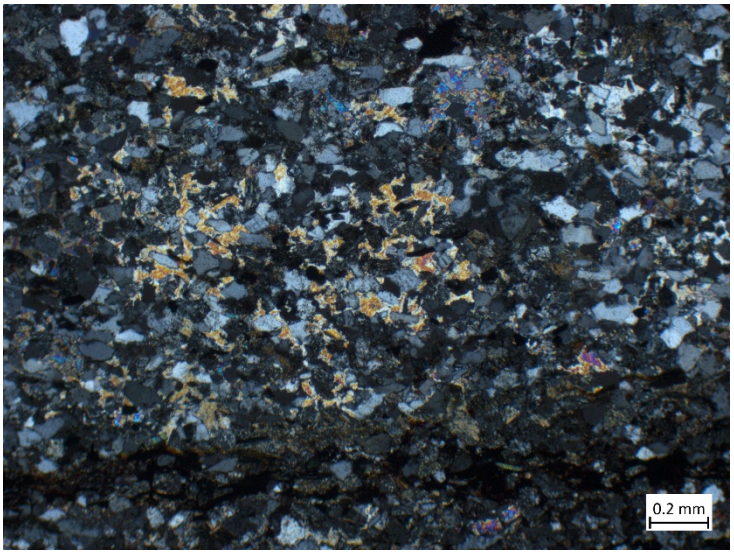

Fig. B-6:

Sandstone, fine-grained, anhydritic and argillaceous:
detritic quartz grains (grey) and siliciclastic rock fragments (mainly darker grey) with anhydrite cement (orange) and clay matrix (lower part; darker part)

Thin section photo, crossed nicols

BUL1-1B-1055.72
Klettgau Fm. (Ergolz Mb.)

Selected photos of microfacies from the Bänkerjoch Formation and Klettgau Formation

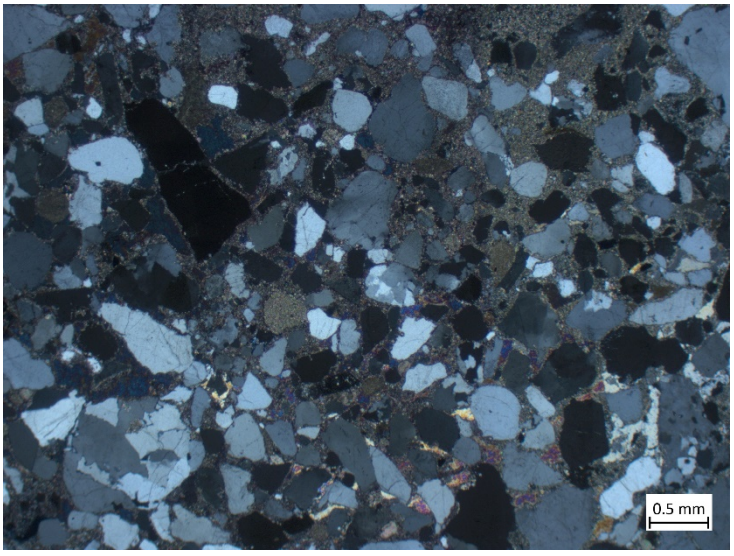

Fig. B-7:

Sandstone, coarse-grained: detritic quartz grains (grey) and siliciclastic rock fragments (grey) with anhydrite cement and dolomicritic matrix (orange)

Thin section photo, crossed nicols

BUL1-1B-1043.65
Klettgau Fm. (Seebi Mb.)

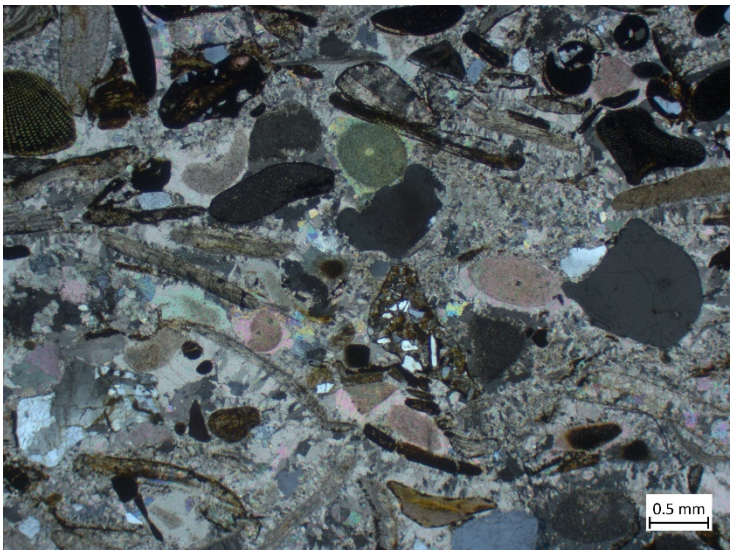

Fig. B-8:

Biosparite, sandy: echinoderm (reddish and greenish) and bivalve detritus (brown) as well as quartz and quartzite grains (grey); echinoderms with syntaxial calcite cement (pastel-coloured)
Thin section photo, crossed nicols

BUL1-1-1025.00
Staffelegg Fm. (Beggingen Mb.)

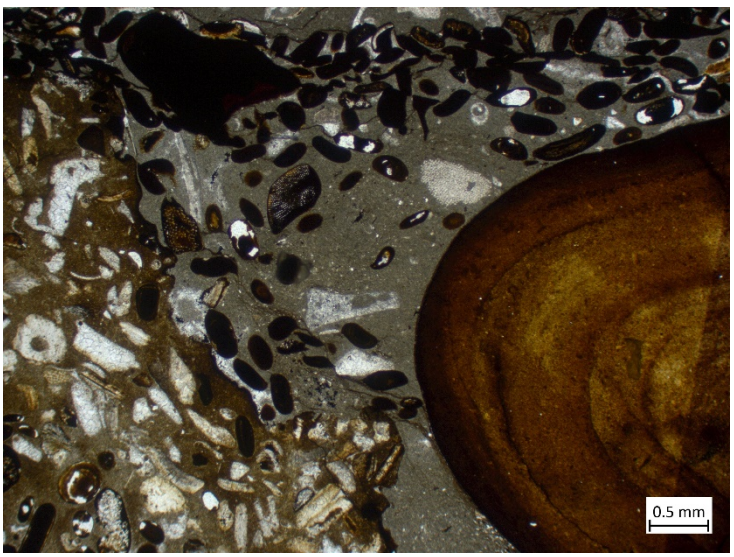

Fig. B-9:

Hardground: iron-oolite with limonitic biomicrite intraclast and iron-stromatolite intraclast

Thin section photo

BUL1-1-1021.30
Staffelegg Fm. (Beggingen Mb.)

Selected photos of microfacies from the Klettgau Formation and Staffelegg Formation

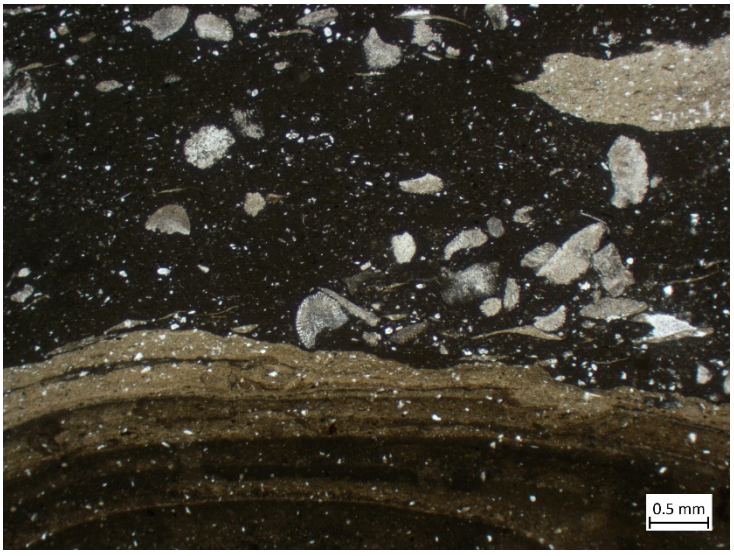

Fig. B-10:

Hardground with iron-stromatolite intraclast in the lower part and biodetritus above in a clay mineral-rich matrix

Thin section photo

BUL1-1-912.44
Opalinus Clay

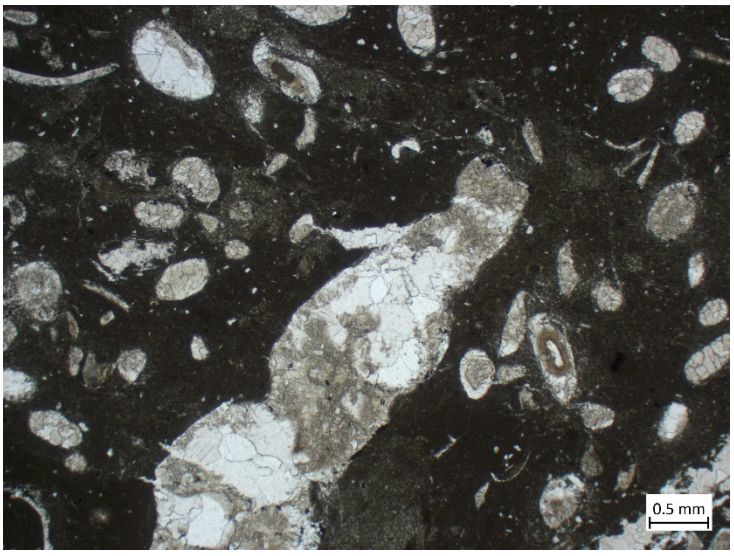

Fig. B-11:

Hardground with micritic iron-oolite intraclast: all iron-ooids are replaced by calcite; only a few show relicts of iron mineral layers (one in the lower right part)

Thin section photo

BUL1-1-908.33
Opalinus Clay

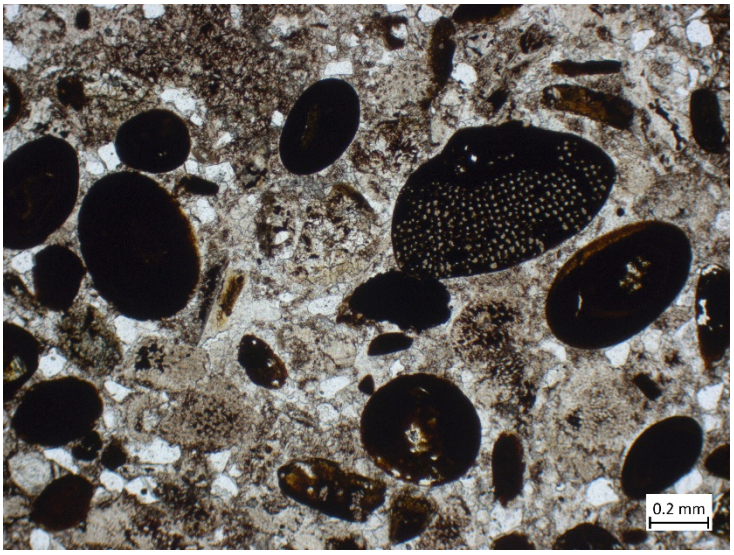

Fig. B-12:

Limonitic, iron-oolitic biomicrite: iron-ooids, more or less structureless, and limonitic bioclasts, such as echinoderms, sedimented in a limonitic micrite matrix

Thin section photo

BUL1-1-884.38
«Murchisonae-Oolith Fm.»

Selected photos of microfacies from the Opalinus Clay and «Murchisonae-Oolith Formation»

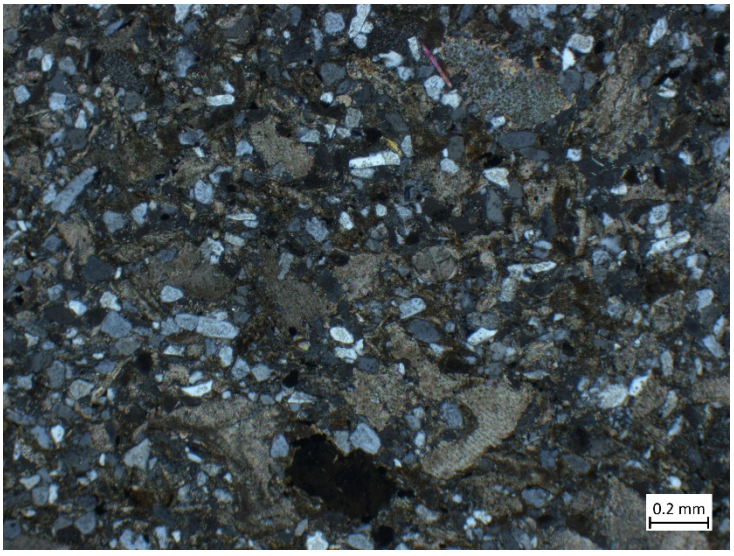	**Fig. B-13:** calcareous, quartz-rich bed: Calcareous silt- to sandstone (argillaceous, bioclastic): fine-grained detritic quartz and echinoderm fragments in a argillaceous, calcareous matrix Thin section photo, crossed nicols BUL1-1-870.35 Wedelsandstein Fm.
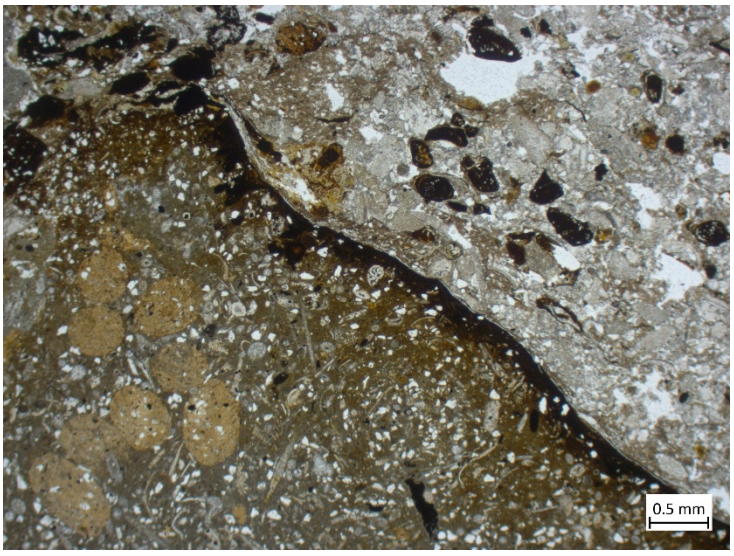	**Fig. B-14:** Hardground: iron-oolitic intraclast with limonitic crust Thin section photo BUL1-1-855.52 «Humphriesioolith Fm.»
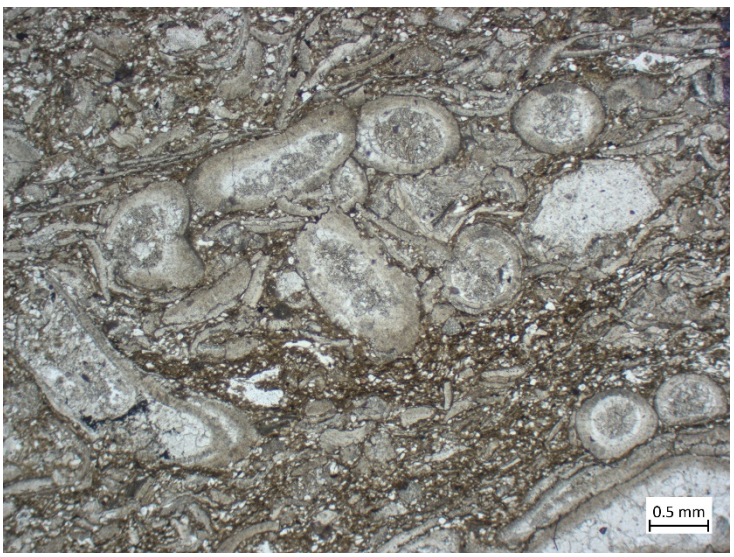	**Fig. B-15:** Bioclastic calcareous marl: with numerous serpulids - calcareous tubes made by worms Thin section photo BUL1-1-850.27 «Herrenwis Unit»

Selected photos of microfacies from Wedelsandst. Fm., «Humphriesiool. Fm.», «Herrenwis Unit»

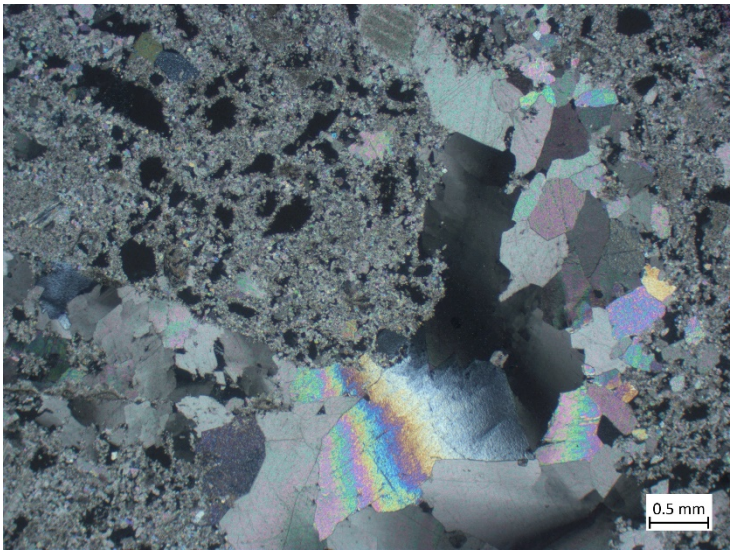

Fig. B-16:

Dolomitic biosparite with saddle dolomite (curved crystal faces) filling primary or secondary pore space

Thin section photo, crossed nicols

BUL1-1-825.22
«Herrenwis Unit»

Fig. B-17:

Calcite mosaic (interpreted as biosparite, ?boundstone): Calcite replacing aragonite of the corals and/or filling primary pore space

Thin section photo

BUL1-1-820.22
«Herrenwis Unit»

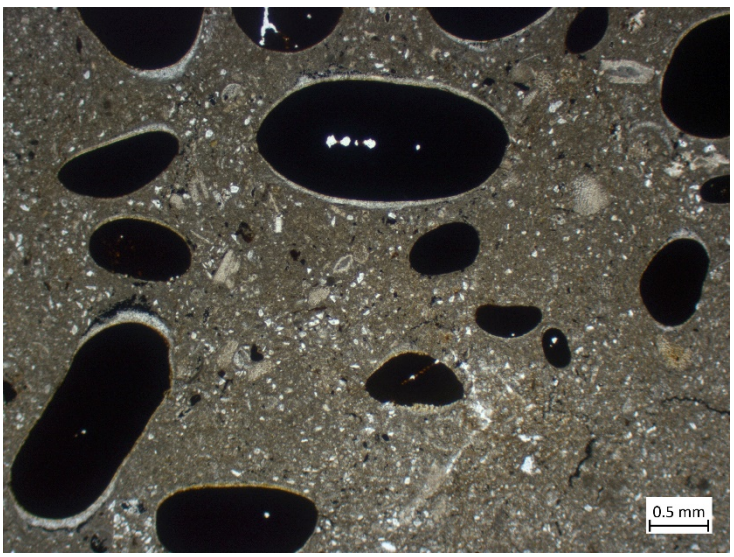

Fig. B-18:

Iron-oolitic biomicrite: Well formed limonitic iron-ooids with small calcite cement rims in a micritic matrix with some bioclasts and quartz silt

Thin section photo

BUL1-1-811.71
«Parkinsoni-Württembergica-Sch.»
(?«Parkinsoni-Oolith»)

Selected photos of microfacies from «Herrenwis Unit» and «Parkinsoni-Oolith»

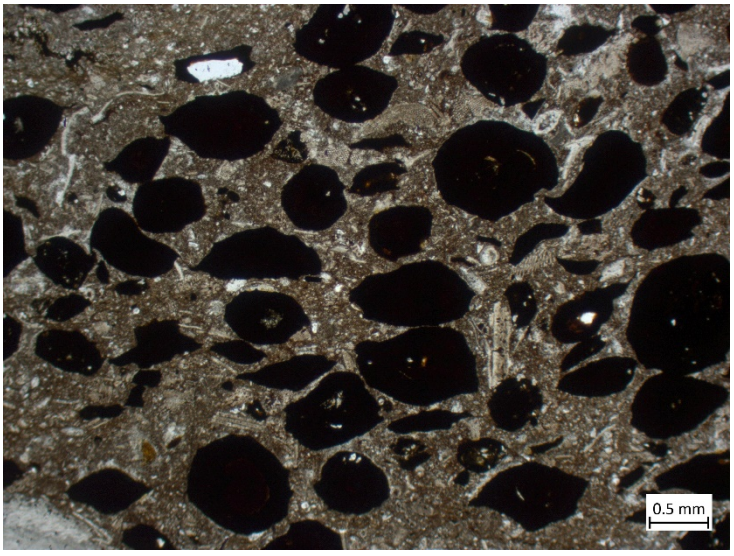

Fig. B-19:

Iron-oolite, calcareous: some of the iron-ooids show pitted outlines

Thin section photo

BUL1-1-806.17
Wutach Fm.

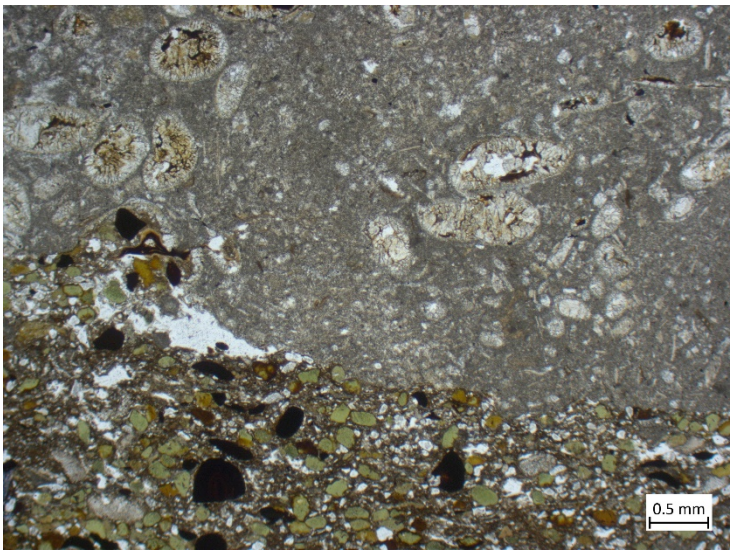

Fig. B-20:

Limestone (iron-oolitic) (intraclast, iron-ooids replaced by calcite) and glauconitic, sandy marl underneath

Thin section photo

BUL1-1-805.13
«Glaukonitsandmergel Bed»)

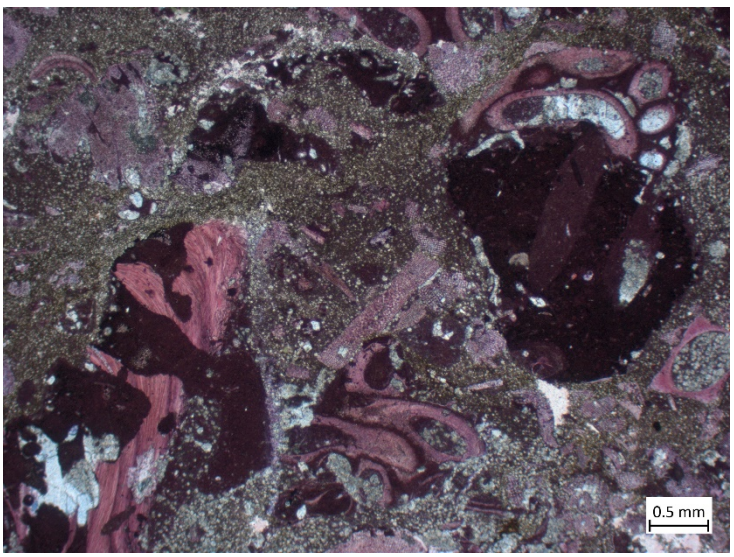

Fig. B-21:

Calcareous marl with limestone nodules: some of them are serpulids bearing intraclasts

Thin section photo, TS stained for calcite (= red)

BUL1-1-694.80
Villigen Fm.

Selected photos of microfacies from Wutach Fm., «Glaukonitsandmergel Bed» and Villigen Fm.

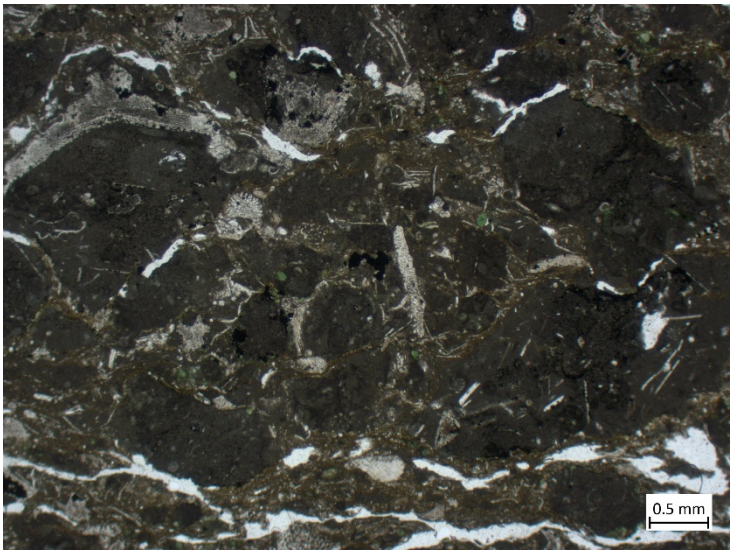

Fig. B-22:

Calcareous marl with micritic and biomicritic limestone nodules/intraclasts

Thin section photo

BUL1-1-653.67
Schwarzbach Fm.

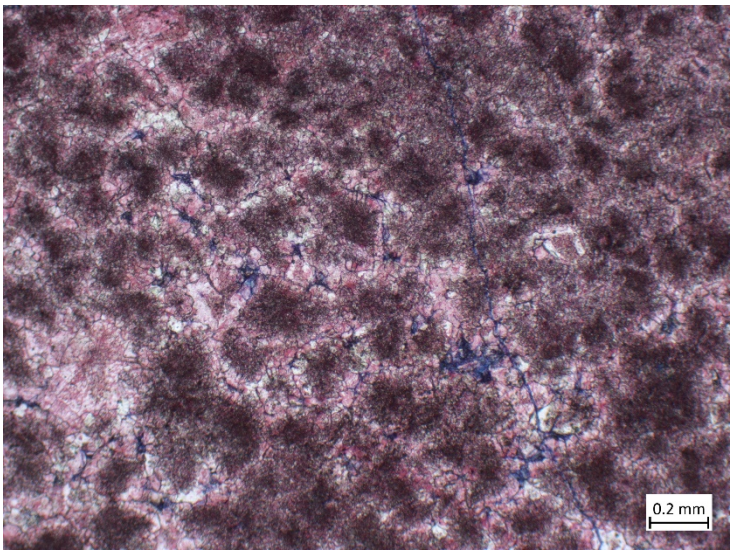

Fig. B-23:

Dedolomite:
mosaic of small calcite crystals and micrite patches. Rhombohedron outlines show that calcite is replacing dolomite and therefore "dedolomite"

Thin section photo, TS stained for calcite

BUL1-1-626.22
«Felsenkalke» / «Massenkalk»

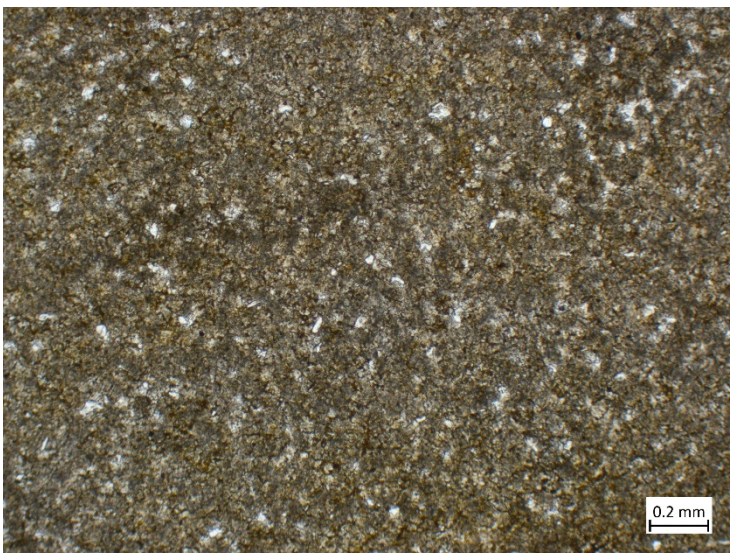

Fig. B-24:

Dedolomite:
as above, but finer crystalline

Thin section photo

BUL1-1-575.05
«Felsenkalke» / «Massenkalk»

Selected photos of microfacies from Schwarzbach Fm. and «Felsenkalke» / «Massenkalk»

Appendix C: Plates of ammonites

Plate I: BUL1-1 (1'016.77 – 997.17 m) C-3

Plate II: BUL1-1 (996.64 – 995.88 m) C-5

Plate III: BUL1-1 (995.53 – 812.03 m) C-7

Plate IV: BUL1-1 (810.58 – 801.65 m) C-9

Plate V: BUL1-1B (997.10 – 1'005.06 m) C-11

Plate I BUL1-1 (1'016.77 – 997.17 m)

Fig. 1: *Asteroceras*? sp., depth: 1'016.77 m, Staffelegg Fm. (Frick Mb.), Obtusum Zone?
Fig. 2: *Harpoceras* sp., depth: 1'002.75 m, Staffelegg Fm. (Rietheim Mb.), Falcifer Zone.
Figs. 3a, b: *Catacoeloceras* sp., depth: 1'000.58 m, Staffelegg Fm. (Gross Wolf Mb.), Bifrons Zone, Crassum Subzone to Variabilis Zone.
Fig. 4: *Perilytoceras jurense* (Zieten, 1830), depth: 999.78 m, Staffelegg Fm. (Gross Wolf Mb.), Thouarsense Zone?.
Fig. 5: *Pleydellia*? sp., depth: 997.17 m, Staffelegg Fm. (Gross Wolf Mb.), Aalensis Zone?.

Most of the figures are illustrated on the original scale; otherwise black bars indicate 1 cm.

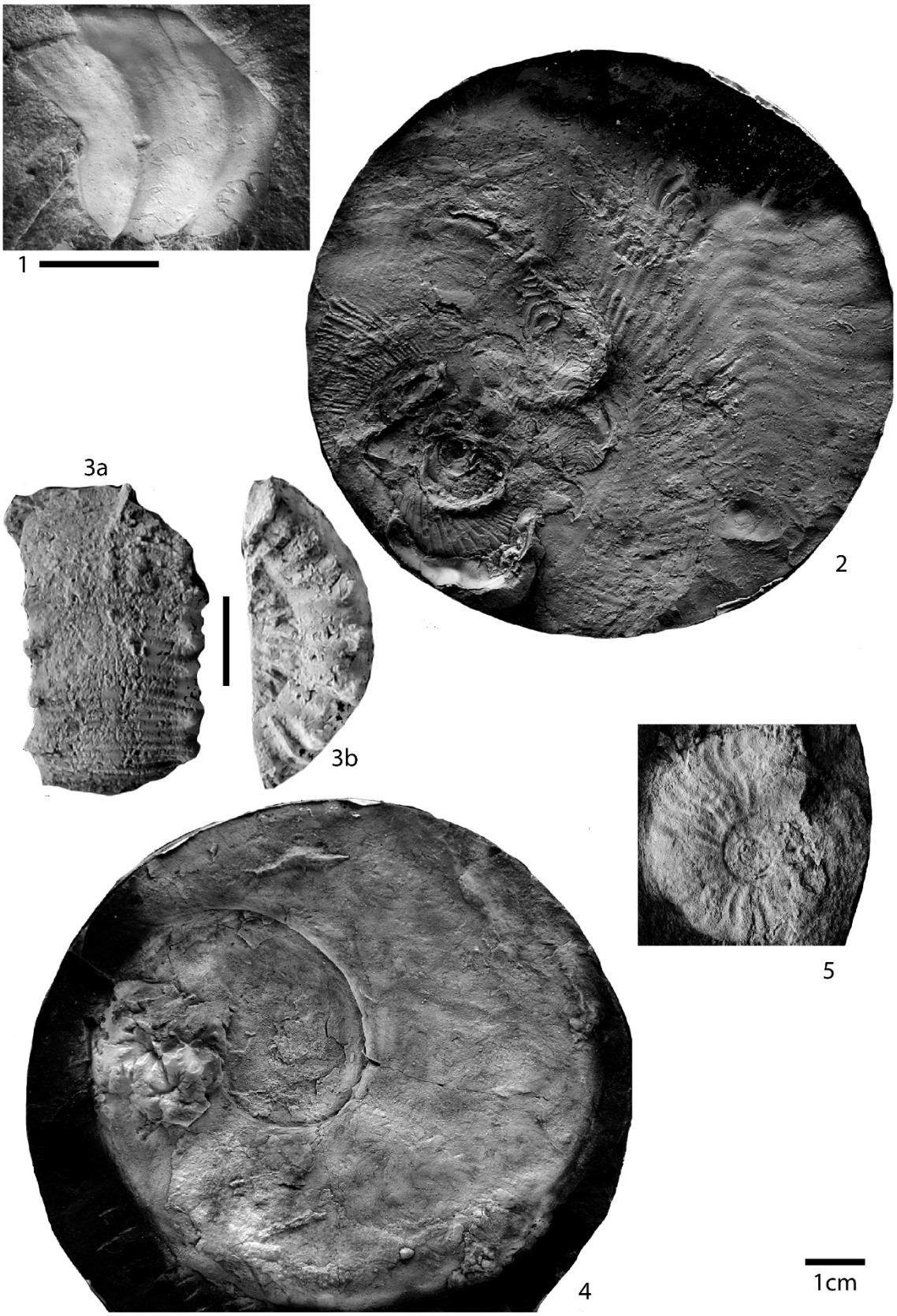

Plate I: BUL1-1 (1'016.77 – 997.17 m)

Plate II BUL1-1 (996.64 – 995.88 m)

Fig. 1: Smaller specimen: *Pleydellia dudelangense* (Maubeuge 1950), larger specimen: *Pleydellia* sp., depth: 996.64 m, Staffelegg Fm. (Gross Wolf Mb.), Aalensis Zone, Aalensis Subzone.

Fig. 2: *Pleydellia* ex gr. *buckmani* (Maubeuge 1947), depth: 996.62 m, Staffelegg Fm. (Gross Wolf Mb.), Aalensis Zone, Torulosum Subzone.

Fig. 3: *Pleydellia* ex gr. *buckmani* (Maubeuge 1947), depth: 996.60 m, Staffelegg Fm. (Gross Wolf Mb.), Aalensis Zone, Torulosum Subzone.

Fig. 4: *Pleydellia misera* (Buckman 1902), depth: 996.29 m, Staffelegg Fm. (Gross Wolf Mb.), Aalensis Zone, Torulosum Subzone.

Fig. 5: *Leioceras*? sp. ex gr. *subglabrum* (Buckman 1902), depth: 995.88 m, Opalinus Clay, Opalinum Zone, Opalinum Subzone.

All figures are illustrated on the original scale; otherwise black bars indicate 1 cm.

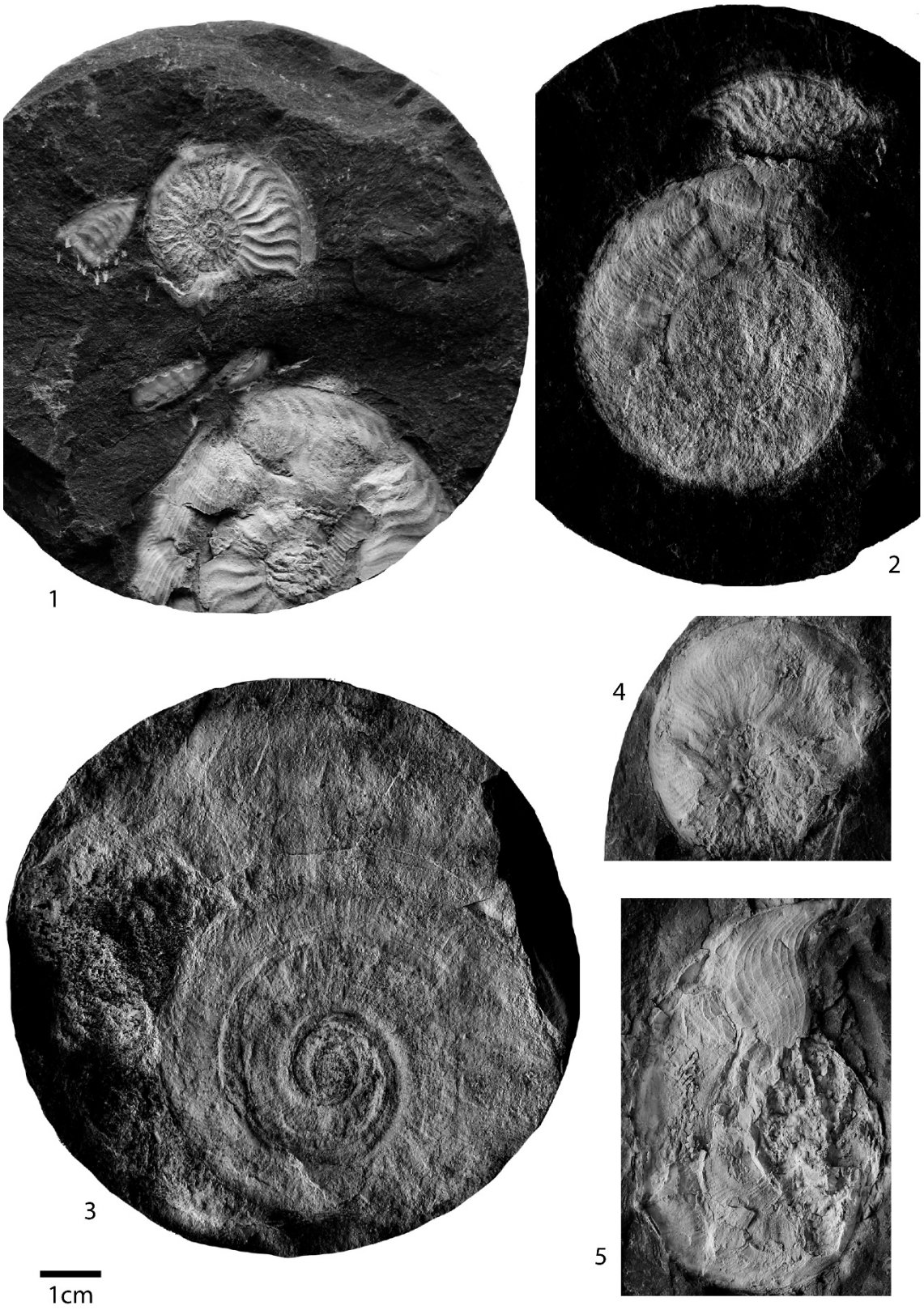

Plate II: BUL1-1 (996.64 – 995.88 m)

Plate III BUL1-1 (995.53 – 812.03 m)

Fig. 1: *Leioceras undatum* (Buckman 1899), depth: 995.53 m, Opalinus Clay, Opalinum Zone, Opalinum Subzone.
Fig. 2: *Leioceras opalinum* (Reinecke 1818) microconch, depth: 969.10 m, Opalinus Clay, Opalinum Zone, Opalinum Subzone.
Fig. 3: *Leioceras opalinum* (Reinecke 1818) microconch, depth: 959.07 m, Opalinus Clay, Opalinum Zone, Opalinum Subzone.
Fig. 4: *Leioceras*? sp., depth: 908.22 m, Opalinus Clay, Opalinum Zone, Opalinum Subzone.
Figs. 5a, b: *Brasilia* ex gr. *bradfordensis*, depth: 891.63 m, «Murchisonae-Oolith Fm.», Bradfordensis Zone, Bradfordensis Subzone.
Figs. 6a, b: Graphoceratidae *Hyperlioceras*? sp., depth: 882.71 m, lower Wedelsandstein Formation, Early Bajocian, Discites Zone? 1a: lateral view, 1b: cross-section.
Fig. 7: *Caenocidaris cucumifera* (Agassiz 1840), depth: 829.82 m, «Herrenwis Unit», Early Bajocian.
Fig. 8: *Pseudogarantiana* sp., depth: 812.03 m, «Parkinsoni-Württembergica-Schichten», Garantiana Zone to early Parkinsoni Zone.

Most of the figures are illustrated on their original scale; otherwise black bars indicate 1 cm.

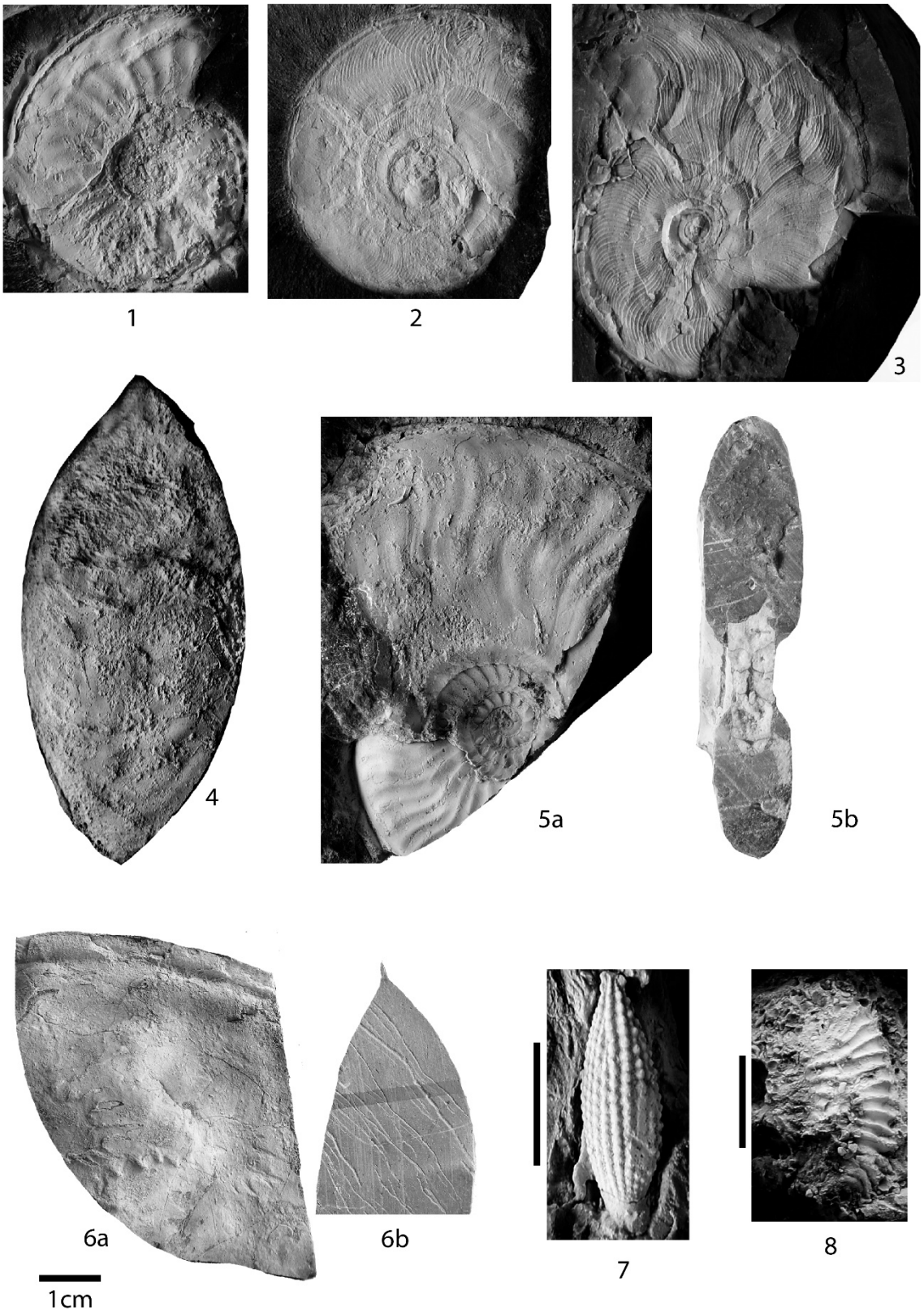

Plate III: BUL1-1 (995.53 – 812.03 m)

Plate IV BUL1-1 (810.58 – 801.65 m)

Figs. 1a, b: *Procerites*? sp., depth: 810.58 m, «Parkinsoni-Württembergica-Schichten», Early Bathonian?
Fig. 2: *Siemiradzkia*? sp., depth: 805.80 m, Wutach Fm., Bathonian?
Fig. 3: *Perisphinctes*? sp., depth: 803.77 m, Wildegg Fm., Transversarium Zone?
Fig. 4: *Glochiceras subclausum* (Oppel 1863), depth: 802.85 m, Wildegg Fm., Transversarium Zone to Bifurcatus Zone, Stenocycloides Subzone. Transversarium Zone?
Fig. 5: *Subdiscosphinctes* sp., depth: 802.61 m, Wildegg Fm., Transversarium Zone, Luciaeformis Subzone to Schilli Subzone according to Gygi (2001).
Fig. 6: *Perisphinctes* sp., depth: 801.65 m, Wildegg Fm., Middle to early Late Oxfordian.

All figures are illustrated on the original scale; otherwise black bars indicate 1 cm.

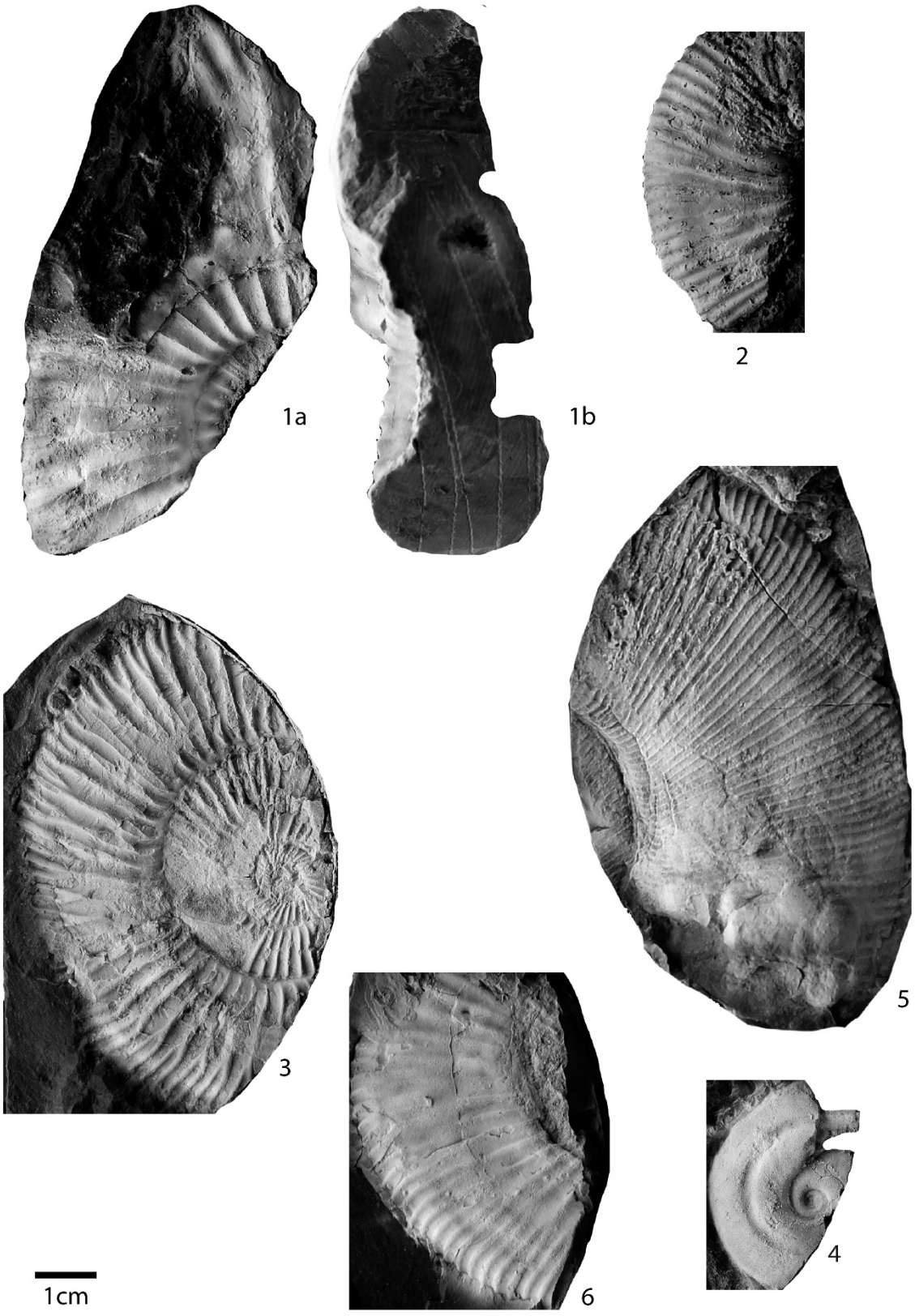

Plate IV: BUL1-1 (810.58 – 801.65 m)

Plate V BUL1-1B (1'005.06 – 997.10 m)

Fig. 1: *Dactylioceras* sp., pathologic specimen, depth: 1'005.06 m, Staffelegg Fm. (Rietheim Mb.), Falcifer Zone?

Fig. 2: *Dactylioceras* ex. gr. *commune*? (Sowerby 1815), depth: 1'004.11 m, Staffelegg Fm (Rietheim Mb). Bifrons Zone, Commune Subzone?

Fig. 3: *Pseudogrammoceras fallaciosum* (Bayle 1878), depth: 999.05 m, Staffelegg Fm. (Gross Wolf Mb.), Thouarsense Zone, Fallaciosum Subzone.

Fig. 4: *Dumortieria* ex gr. *levesquei* (d'Orbigny 1844), depth: 997.63 m, Staffelegg Fm. (Gross Wolf Mb.), Levesquei Zone, Levesquei Subzone.

Fig. 5: *Dumortieria* ex gr. *moorei* (Lycett 1857), depth: 997.36 m, Staffelegg Fm. (Gross Wolf Mb.), Levesquei Zone, Moorei Subzone.

Fig. 6: *Dumortieria* sp., depth: 997.10 m, Staffelegg Fm. (Gross Wolf Mb.), Levesquei Zone.

Most of the figures are illustrated on the original scale; otherwise black bars indicate 1 cm.

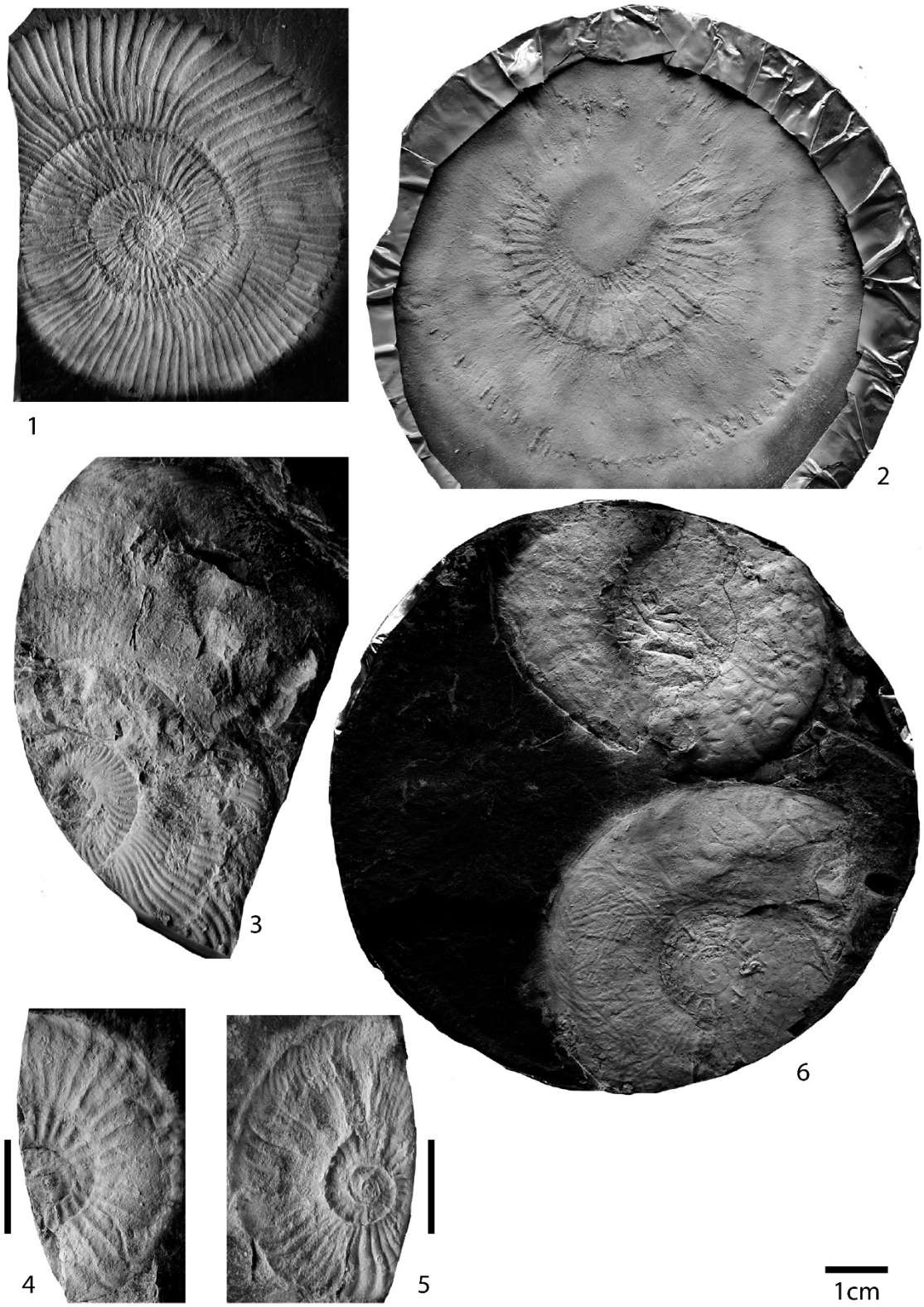

Plate V: BUL1-1B (1'005.06 – 997.10 m)

Appendix D: Palynostratigraphy

Appendix D1: Range Chart: Quantitative stratigraphic distribution of Middle Jurassic palynomorphs in the Bülach-1-1 borehole

Appendix D2: Depth/Age plot

Note: The appendices are only included in the digital version of this report (PDF) and can be found under the paper clip symbol.

Appendix E: Chemostratigraphy

Appendix E1: List of all geochemical samples and results drilled mainly from specific calcareous beds in the Opalinus Clay and its upper confining unit E-2

Appendix E1: List of all geochemical samples and results drilled mainly from specific calcareous beds in the Opalinus Clay and its upper confining unit

Data are plotted and discussed in Section 3.4.

Depth [m]	**Description of sample**	**$\delta^{13}C_{carb}$** [‰ VPDB]	**$\delta^{18}O_{carb}$** [‰ VPDB]	**Carbonate** [wt.-%]
891.53	Limestone bed	-0.85	-4.18	80.1
891.68	Hardground	0.36	-1.56	67.1
904.25	Intraclast, calcareous	-21.98	-1.55	80.1
904.26	Intraclast, calcareous	-17.90	-3.03	72.1
904.27	Intraclast, calcareous	-20.36	-2.95	53.9
904.28	Belemnite	0.23	-4.04	81.5
904.47	Hardground (from thin section)	-3.03	-8.20	16.2
905.50	Septarian nodule	-28.73	-1.17	84.2
908.00	Hardground	-16.15	-0.38	73.9
908.22	Hardground (ammonite sample)	-4.20	-3.96	74.5
908.33	Hardground (from thin section)	-3.40	-2.73	71.7
908.54	Hardground (from thin section)	-3.99	-3.37	67.7
912.44	Hardground (from thin section)	-2.86	-4.06	56.2
967.64	Hardground (from thin section)	-19.52	-4.98	58.2
975.62	Calcareous marl	-8.84	-6.84	52.0
975.67	Calcareous marl	-10.56	-6.12	63.0
981.26	Septarian nodule	-14.80	-1.42	84.8
981.67	Septarian nodule	-30.58	-1.16	79.7